UNIVERSITY OF BIRMINGHAM

Adhesion Strength Testing

– An Improved Approach

Submitted for the degree of

DOCTOR OF PHILOSOPHY

by

Hesham Hassan Elnadif

June 2024

Abstract for the thesis entitled “Adhesion strength testing – an improved approach” submitted by Hesham Mohammed Elnadif for the degree Doctor of Philosophy at the University of Birmingham in June 2024.

Background: Generally, the bonding of one material to another is important for function, and especially with so-called ‘adhesive dentistry’. A test with discriminatory power that mimics the clinical failure mode *i.e.*, the failure of that bond in peel mode, has not emerged.

Objective: Develop and validate a test protocol based on 4-point bending that may be used to examine the bonding of various dental materials to a range of substrates, taking dentine, stainless steel and aluminium alloy as examples.

Methods: An improved approach for static flexural strength of ‘adhesive’ bond to dentine based on 4-point bend was developed. Slices of coronal dentine from extracted molars (larger and more squared teeth) were prepared using a diamond blade. Bonded interface specimens were prepared by shaping the material within the respective manufacturers’ (3M ESPE, Shofu, Ivoclar Vivadent, GC Europe, DE Healthcare, Dentsply DeTrey, Septodont) stated working time using a stainless steel split mould. The support span-depth ratio for the beam was chosen to minimise shear effects and to enable failures to occur in the maximum tension surface due to bending moments only. The new method was used to measure quantitatively the adhesive bond potential of various systems, *i.e.*, zinc phosphate cement, zinc polycarboxylate cement, glass ionomer cement, calcium silicate cement, total-etch resin systems, and a self-adhesive resin cement. Scanning electron microscopy (SEM) and energy dispersive spectroscopy (EDS) were used to examine fracture surfaces, identify failure origins, and confirm failure mode.

Results: Symmetrical 4-point bending was found to be a valid approach, compared with currently employed test methods, for the characterization of ‘adhesive’ and cohesive strengths. The test set up employed a relevant mode of loading with a subsequent failure pattern initiating at the tooth-restoration interface.

Conclusion: With reproducibility, discriminatory power, economy with regard to substrates, and a straightforward robust process, the method is adaptable to many systems.

Declaration

I hereby declare that, with the exception of the assistance acknowledged, all the work described in this thesis is my own original work and no part of it has been included in my thesis, dissertation or report submitted to the University of Birmingham or any other institution for a degree or other qualification.

Signed

_____

_____

ACKNOWLEDGEMENTS

This thesis represents not only my work at the University of Birmingham, it is a milestone in more than one decade of work with my supervisor (and mentor) Professor Brian W. Darvell. I can never be thankful enough for his valuable advice, guidance and continuous support. I am especially indebted to him for inspiring me and encouraging me throughout the course of the project. I acknowledge too, with thanks, his generous help with the statistical data analysis and the systematic re-analysis of the literature.

I would also like to acknowledge, with many thanks, my supervisors Professor William Palin and Dr Mohammed Abdul Hadis for their enthusiasm for the project, encouragement, and for their valuable comments and constructive ideas.

I would like to extend my gratitude to Dr Garry Fleming (external examiner) and Dr Gowsihan Poologasundarampillai (internal examiner) for their detailed and thoughtful feedback, which helped to improve the presentation of the thesis.

The great advice, support, and patience of Dr Jianguo Liu and Dr Helen Wright has been invaluable on the technical side of the project, for which help I am extremely grateful.

Finally, I would like to thank my wife, Naima and my daughters, Rana and Sara for being so understanding and supportive.

Contents

List of figures

List of tables

List of abbreviations

4pb	Four-point bend
10-MDP	10-methacryloyloxydecyl dihydrogen phosphate
AA	Aluminium alloy
AoV	Analysis of Variance
ASA	Adper Scotchbond Multi-Purpose Adhesive
ASP	Adper Scotchbond Multi-Purpose Primer
ASX	Adper Scotchbond 1 XT
BAp	Biologicalapatite
BB	Beautifil bulk-fill
BD	Biodentine
CoV	Coefficient of variation
CS	Calcium silicate
DBA	Dentine bonding agent
DEJ	Dentino-enamel junction
EDS	Energy dispersive spectroscopy
EG	Scotchbond Universal etching gel
FB	Filtek One bulk-fill
FEA	Finite element analysis
FF	Filtek flowable bulk-fill
FR	Filled resin
FS	Flexural strength
FS*	Corrected flexural strength
GIC	Glass ionomer cement
GIC_A	Aquacem
GIC_F	Fuji II
GLM	General linear model
HAp	Hydroxyapatite
HEMA	Hydroxyethyl methacrylate

ISO	International Organization for Standardization
LSR	Log speed range
MTBT	Microtensile bond strength test
PMMA	Poly(methyl methacrylate)
PTF	Pre-test failure
RBC	Resin-based composite
RES	Relative effect size
RH	Relative humidity
RX	RelyX Unicem 2 Automix
se	Standard error
SEM	Scanning electron microscopy
SS	Stainless steel
SSRD	Scaled standard residual deviation
TEC	Tetric Evoceram
T_g	Glass transition temperature
XHD	Cross-head displacement
XHS	Cross-head speed
ZCC	Zinc polycarboxylate cement
ZPC	Zinc phosphate cement

1. Introduction

Enamel, a mineralized tissue, covers the anatomic crown of the tooth and varies in thickness across. The mineral content increases dramatically during enamel maturation and may reach a maximum of ~ 89% by volume at the most mature form [1]. The continuous gain in mineral phase is due to crystal growth in size (using Electron Microscopy and X-ray Diffraction) rather than an increase in the number of crystals [1]. The term hydroxyapatite 'HAp' is most frequently used in the literature to refer to the mineral content of tooth substance. However, failure to recognize the character of 'apatite' as a structure rather than a specific material and the fact that biological apatites 'BAp' are never pure may render HAp to be misleading [2]. The remaining constituents include organic matrix proteins (collagenous and non-collagenous) and water [1]. Dentine is composed of about 50% mineral by volume in the form of BAp; 30% organic matter, which is largely type I collagen; and about 20% fluid similar to blood plasma, (all by volume). [3]. The literature shows that enamel mineralization varies substantially between individuals. A range of mineral concentration of enamel has been reported [1]. Likewise, the mineral and organic content description of dentine is often oversimplistic. Dentine is a highly heterogeneous structure with different types of dentine, reflecting different functions and characterisations.

Wetting ability is the tendency of a liquid to spread on a solid surface, subsequent to intermolecular interactions between the two surfaces when brought together [4]. Thus, wetting ability should be regarded as a prerequisite for adhesive joint formation. To ensure an adhesive bond of resin-based composite (RBC) to tooth structure, adequate wetting ability of the adhesive is essential on both enamel and dentine.

Adhesion refers to the strength of the union between two materials *i.e.,* the adherends. By definition, adhesion involves molecular interactions at the interface between the adherends, implying a chemical interaction stronger than van der Waals forces [4]. This union is facilitated through the employment of a third material in the intervening space and forming the adhesive joint [4]. Adhesives are believed to function through a combination of chemical and micromechanical means of retention. Micromechanical bonding is associated with the retention of an adhesive to a roughened surface. A thickened phosphoric acid solution is the most commonly used to etch the tooth substrate [5], however, there is no systematic laboratory evidence to support the particular conditions used in routine practice. Adhesives then infiltrate the roughened enamel surface. After acid treatment, enamel is easily wettable by the adhesive

monomers forming a relatively durable[1] adhesive joint compared with dentine [4]. On dentine, adhesive monomers permeate in and around collagen matrix fibrils in a process termed hybridization where the two polymers are supposed to be interpenetrating – a different type of mechanical retention to that of the mechanical key of an etched surface [4]. Unfortunately, such simplistic assumptions are considerably undermined by the complexity of the supra-molecular arrangement of the dentine matrix [6]. The complex structure of intrafibrillar collagen, *i.e.*, the staggered arrangement of collagen molecules creates gap zones and overlap zones, coupled with the nanotopographical features of dentine matrix proteins, such as ~ 4 nm surface bumps, have been suggested to hinder resin monomers' infiltration and subsequent complete encapsulation of collagen fibrils, respectively [6] (Figure 1.1). Moreover, the intermolecular spaces of type I collagen were found to be fully occupied by tightly-bound water molecules [6]. This is supported by the observation that much of the exposed (and increased by the etching) collagen network remains uncovered by resin and vulnerable to subsequent attack by enzymes, thus facilitating a pathway for the degradation of the resin-dentine union [7].

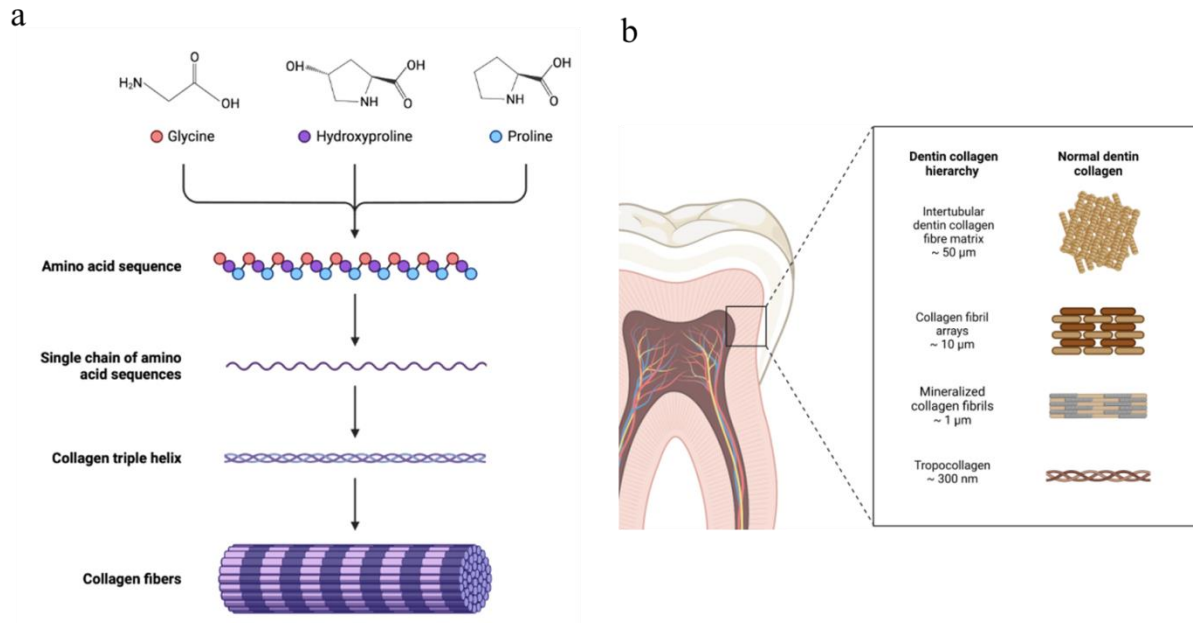

Figure 1.1 Collagen structure. **a**: collagen fibres, **b**: dentin collagen hierarchy [8].

[1] Durability of a bonded component is its ability to perform its required function for long periods of time under normal conditions of use without undertaking excessive repair work [9].

The fracture mechanics approach was originally developed for the study of the cohesive fracture of materials and has aided understanding and analysing the role of flaws in a material's response to an applied load [9]. The extension of fracture mechanics principles to adhesive joints was challenging and unreliable due to the complex stress state at the adhesive joint [10]. It has gained little general popularity, perhaps because it requires a more elaborate procedure. The brittle nature of dental ceramics and resin composite restorations has made energy-expenditure optimization on crack growth during testing difficult, especially as the scale of the critical crack length is approached. This is reflected in the coefficient of variation in the results of fracture toughness studies of adhesive joints (> 25 %) and the consequent discriminatory ability [10, 11].

While strength is the maximum stress a material can withstand before fracture, fracture toughness is the ability of a material to resist crack growth. Fracture toughness quantifies specific energy absorption capacity reflecting material's resistance to crack propagation [11]. Generally, brittle materials have low fracture toughness due to their limited plastic deformation potential upon loading. Unlike strength testing, fractured toughness measuring necessarily involves controlled crack propagation from pre-cracked specimens, estimating the critical crack size at which the crack becomes unstable leading to catastrophic fracture at a certain applied load [11].

Dentine tracer tests (incorrectly termed 'microleakage' tests) are based on the premise that penetration occurs 'only' through interfacial gaps between dentine and RBCs. Multiple factors influence dentine permeability *in vivo*, and these complicate the laboratory simulation of penetration tests. Clinically, the threshold above which a gap is considered pathogenic resulting in symptoms of the involved tooth has not been determined [12]. Gale & Darvell [12] reported that simple sectioning techniques were not adequate to reflect the extent of dye penetration and suggested that full interface mapping is essential. They further showed that dentinal tubule direction controlled dye penetration. That is to say that unless control of tubule orientation to prevent or limit spurious penetration is achieved, the interface might have been stained anyway, thus giving false positive results [12]. Heintze [13] reviewed 30 studies to examine the correlation between bond strength tests and microleakage, and 18 studies for a possible relation between bond strength tests and gap analysis. For both, he found that ~80 % of the studies showed no correlation between the two methods. Heintze also compared the outcome of eleven clinical studies to that predicted with the marginal analysis and found that only two studies matched the clinical expectation based on laboratory tests. He further advised

that microleakage and gap analysis experiments should be abandoned as they have no clinical implication [13].

Tensile and shear (Figure 1.2) are the most frequently used kinds of test to assess the 'adhesive' bond to dentine. However, the clinical relevance of such tests was seriously questioned [14, 15], that is, whether an adhesive interface could fail in pure shear or tension [16]. A major problem with such tests is that failures are initiated due to local stress concentrations and thus subsequent averaging of failure stress by the size of the bonded area is simply inaccurate [15-17].

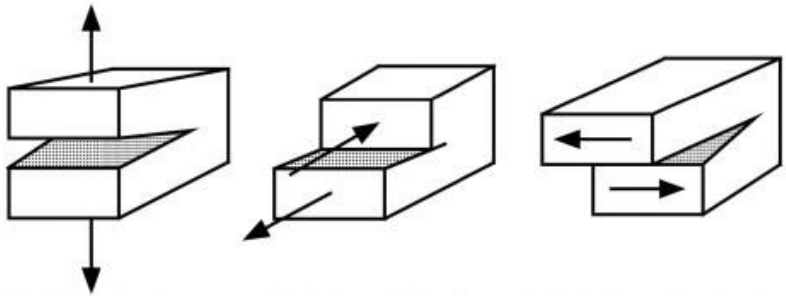

Figure 1.2 The modes of failure. **(I)** Tensile (opening). **(II)** In-plane shear (sliding). **(III)** Out-of-plane shear (tearing) [16].

Despite the well-promoted improvements (with regard to qualities such as strength) that have occurred in nearly all materials used in dentistry, clinical failure rates have not changed very much. The clearest example of this is in ceramics: a 200-fold improvement in strength has not led to an equivalent improvement in clinical serviceability. This clearly reflects the situation that experimental tests used to verify strength improvements cannot be simulating the real-world behaviour of the system under consideration and hence no coincidence is to be expected [16].

2. Literature review

2.1 Strength as a material property

According to Griffith theory, strengths measured using a smaller volume specimen are higher than would be expected from larger-scale tests [18]. Armstrong *et al.* suggested scaling of smaller specimens to the effective volume or surface area to obtain relevant strength data [18]. This could be the case were strength a true intrinsic material property. However, Griffith showed that strength is influenced by many factors, and especially cracks and scratches [19]; therefore strength as commonly understood cannot be an intrinsic material property [20]. Clearly the definition of strength as a material property is quite different from 'measured strength'. In the present context, therefore, whenever 'strength' is mentioned, it is intended to be comprehended as the 'measured nominal strength' rather than a true material property. It is well-said that strength should be dealt with as a conditional material property [20].

Bond strength tests of RBCs to dentine have been used to measure the quality of adhesion ever since the invention of acid etching for dentistry [21]. Theoretically, laboratory bond strength tests should be able to consistently and reliably provide information on the strength of the union between an RBC and tooth tissue. However, due to the extreme difficulties related to the (lack of) purity of the stress field during the measurement procedure, such consistency and theoretical assumptions of a state of pure stress are infeasible. The dental materials field has used static tensile testing as an indicator of the durability of the adhesive joint in the oral environment, with higher bond strength results taken to be indicative of better durability (*i.e.*, expectation of service life) than lower values [21]. Since the actual clinical failure modes involve complex stress states, with pure tension being very unlikely, the relevance of such tests has been questioned [16]. Tagami *et al.* considered that the comparative evaluation of bonding performance through bond strength tests is the primary objective [22]. They argued that adhesive joint strength is determined by the mechanical properties of its components, and thus the weakest component or region is expected to fracture first [22]. However, the generally non-uniform stress field and the occurrence of stress concentrations interfere with actual results in the sense that nominal stress at failure is rarely relevant to the actual event. It has been suggested that the phases susceptible to failure are the components with the highest potential to concentrate stress such as areas of mismatch of modulus of elasticity [20], or those with the lowest endurance limit *e.g.*, a poorly infiltrated hybrid layer exhibits graded mechanical properties [23]. However, de Munck *et al.* (2012) found that the "research group" was the most significant variable affecting the measured bond strength to dentine [24]. That there are so many factors involved in the same test from different laboratories

makes inter-laboratory test result comparison a very difficult task [24]. In the best-case scenario, comparisons between papers (from the same laboratory) are only good – possibly – on rank order, not values. Furthermore, the marked discrepancy between the increased clinical life of RBCs [25] and the rapid degradation of the adhesive interface in laboratory tests [26] suggests only a minor role for 'adhesion' in the retention of RBC restorations, especially over the long term [27]. This observation is in need of further investigation.

However, patient motivation plays an essential role in the success of treatment. Da Rosa Rodolpho *et al.* [25] included well-motivated patients to make sure that they could be followed up long-term, and achieved a minimum of 22 years. They reported annual failure rates for RBCs of 1.5% (midifilled) and 2.2% (minifilled), with filling fracture being the main reason for failure [25]. However, Mjör *et al.* [28] showed that the median age of both amalgam and RBC fillings was 8 and 5.5 years in adults and adolescents, respectively. Despite efforts to improve the adhesive-dentine interface, increased clinical lifetime of amalgam fillings highlights the role of secondary caries in failure, and this applies especially for RBCs. In children aged eight to twelve years the risk of failure due to secondary caries was 3.5 times higher in the RBC group compared with the amalgam group [29]. Thus, with the growing use of RBC, the quality of the adhesion at filling margins is apparently the key for reducing failure rates.

During a monotonic tensile or so-called "shear" test, the movable cross-head usually runs at a constant speed, and the specimen is thereby subjected to a steadily increasing load until a maximum load is recorded, commonly at the point of collapse [24]. With such a force application, resulting in a one-shot event, often with a fast moving crack until fracture, there is no obvious sense of damage accumulation [16]. In the oral cavity, simple axial loading is almost never encountered due to the anatomy of teeth and the three-dimensional nature of jaw mechanics [30]. Besides, the occlusal scheme is different: loading is intermittent inducing variations in the local stress concentration fields that may cause localized cracking [31], and the failure load is usually lower than the recorded maximum load mentioned above. Understandably, failing to simulate potential failure modes will interfere with the clinical implications of laboratory test results [32]. Aside from a few weak relationships, most attempts to examine the correlation between laboratory and clinical data are inconclusive [27]. In principle, the evidence of nature, *i.e.*, clinical trials, is the best way to obtain reliable results as to the service fitness of materials and processes.

2.2 Adhesive bond to the tooth structure

With the advent of materials and techniques designed to create a bond to tooth tissue, the spectrum of possible treatment decisions has changed dramatically. A reliable mechanical bond may be achievable to sound enamel, but that to dentine has difficulties [23]. Various mechanisms contribute to the adhesion condition. For example, with enamel the irregularities created through tooth structure cutting, roughness created through acid etching (Figure 2.1), and the subsequent interlocking of the adhesive with that texture, create mechanical retention [33]. With dentine, due to the much higher organic content, mechanical retention does not seem to be enough (Figure 2.2). Primary (*e.g.*, coordination) and secondary (*e.g.*, hydrogen) chemical bonds are considered necessary to strengthen the joint. This is based on the premise that an adhesive should chemically bond both to the organic components (mainly type I collagen) and the inorganic component of tooth structure, BAp [33].

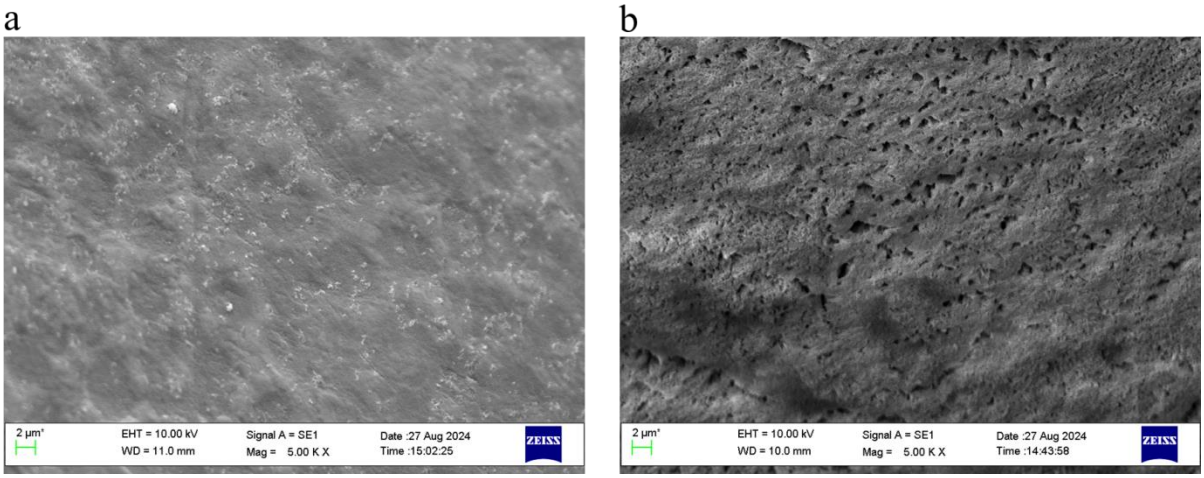

Fig. 2.1 Enamel surface. **(a)** Scanning electron micrograph of unground unetched enamel surface. **(b)** The same enamel surface in (a) etched with 35% phosphoric acid for 15 seconds, creating a porous surface.

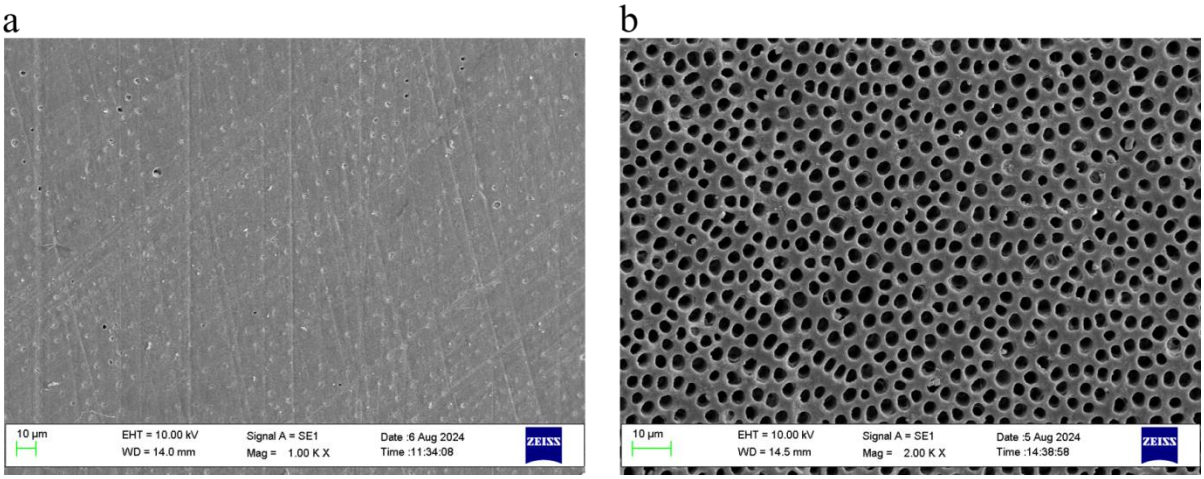

Fig. 2.2 Dentine surface. **(a)** Ground dentine surface. (**b)** Dentine etched with 35% phosphoric acid for 15 s. Acid etching opens dentinal tubules removing the smear layer and, decalcifying peritubular and intertubular dentine.

As discussed above, the long-continued attempts to increase the strength of dental materials have not been matched by an appreciably increased service life for those materials [16, 32]. A remarkable clinical success was noted for Empress 2 (leucite glass-ceramic; Ivoclar Vivadent), with fewer (~0.4%) than predicted actual annual failures (~0.8%), and this was attributed to its amenability to etching, thereby facilitating the mechanical bond to tooth structure [32]. This may reflect an incomplete understanding of the factors determining the clinical lifetime of materials [16] but it also highlights the importance of effective stress transfer across the adhesive joint and the avoidance of stress concentrations. Efforts should be directed towards failure mechanism identification and the production of quality ceramic restorations [32]. Tooth tissue is a composite and complex structure which creates difficulties in understanding its behaviour under mechanical loading. It follows that understanding tooth restoration failure should involve an attempt to simulate the intraoral scenario [32].

For the first time, Nakabayashi *et al.* characterized the monomer-infiltrated and ‘polymerized’ layer in the acid-etched dentine [34], *i.e.*, the transitional hybrid layer [35]. They further suggested that the penetration of monomers into intra- and intertubular dentine, followed by polymerization, reinforces the tooth substance and avoids stress concentration [34]. At the dentine-adhesive interface, stress distribution and stress concentration are affected by the elastic moduli of the various phases, taking into account micro-scale structure [36].

Using finite element analysis, Misra *et al.* showed that the affected area of stress concentration increases as the hybrid layer gets wider [37]. Significantly greater stress concentrations were associated with wider intertubular dentine and the surrounding narrower peritubular dentine. This reflects the effect of mismatch of Young's modulus of elasticity (E), and that of microstructure on stress distribution at the adhesive-dentine interface [37]. A dentine-adhesive interface with a thin hybrid layer, showing less anisotropy of mechanical properties, had a longer fatigue life [38]. If the bond between the adhesive resin and peritubular dentine is defective, the highest stress concentrations probably form within the hybrid layer and acid-treated dentine [36]. Thus, the anisotropy of the hybrid layer (whether bonded or not) is reflected in the stress-strain distributions and subsequent probable failure initiation sites [36]. Analysis of fracture surfaces provides valuable information, the most important is the identification of the size and location of the fracture-initiating crack [39].

Tooth is a unique biological structure, having a complex hierarchical damage-resistant structural organization. Enamel is the hardest substance in the human body. The hardness of enamel decreases gradually inward. being lowest at the dentino-enamel junction (DEJ). Dentine hardness averages one fifth that of enamel and also decreases gradually towards the pulp. The ability of the enamel to withstand occlusal loads is highly-dependent on the critical union to dentine through the dentino-enamel junction (DEJ) [40]. Enamel rods that lack a dentine base are easily chipped away [33].

2.2.1 Chemical bond to tooth structure

Chemical bonds are formed at the atomic level, and such interactions are commonly dependent on their relative electronegativity as well as other factors including steric hindrance, abundance, *etc*. Surface forces that work to hold two bodies in contact, through a third medium, are called adhesive forces. This interplay of forces includes possibilities for covalent, ionic, metallic and chelation bonding [4]. Chemical bonding is strong but also quite challenging to produce with sufficient density across an adhesive joint [4]. Micromechanical retention remains the most effective means of creating a strong joint to tooth structure [4]. However, the distinction between the quantitative contribution of the mechanical retention compared with the chemical bonding in the effectiveness of the joint has never been assessed. This creates a gap between the observed development of various adhesive systems and the criteria for such development to be assessed objectively.

The chemical bonding of RBCs to tooth structure occurs through interactions with the inorganic component (BAp) or organic components (mainly collagen) using their respective dentine bonding agents (DBAs) [41]. The three-step etch and rinse systems consist of (so-called) conditioners, primers and sealers. Primers (coupling agents) are bifunctional molecules, consisting of three groups: polymerizable methacrylate, spacer and reactive groups. The methacrylate group has the ability to bond covalently to the composite resin, whereas the spacer group provide the necessary flexibility to enhance the potential for interfacial coupling of the reactive group with the tooth structure. The reactive groups are polar-pendant or end-groups that can combine with similar polar molecules in dentine [41]. Alcohols, amines, carboxylic acids and aldehydes are frequently employed as reactive groups, with hydroxyethyl methacrylate (HEMA) [42] being a more popular choice for manufacturers. HEMA is a colourless liquid that easily polymerizes, and is miscible with both water and ethanol [43]. Thus, reactive or polar groups can combine with similar groups on the dentine surface: hydroxyl groups on BAp crystals, or amino groups on collagen [41]. Although some micromechanical retention is established through sealer penetration into open dentinal tubules, it is the primer that establishes the base to enhance the quality of the final bond [41].

2.3 Why do we need mechanical tests?

Laboratory bond strength measurements are performed with the presumption that under well-controlled conditions they will produce valuable information on the adhesion between materials [44]. There is growing importance for obtaining an adhesive bond to dentine, as that would enable improvement in the quality of and prognosis for RBC restorations, as well as enhancing the conservation of tooth tissue. Accordingly, the need for a relevant adhesive bond test is insistent and urgent, one that has the potential to judge the durability and performance of the adhesive joint intra-orally.

Although the actual bond strength values may have little meaning in themselves, current adhesive bond tests, as well as morphological and spectroscopic characterization techniques, are used as comparative evaluation tools for the constantly emerging new products in the dental market. Despite the inherent constraints in the embodiment of theoretical assumptions, laboratory methods served as a useful screening tests of new products under various conditions of storage and ageing [18]. It is possible to study one variable while keeping others controlled, which makes it possible confidently to identify relationships and make comparisons between different systems [44], and thus potentially detect problems. For example, the simplified

approach through combining etching, priming, and bonding in a single clinical step, *i.e.*, one-step self-etch adhesives, have shown inferior clinical performance, confirming the less favourable laboratory findings in comparison with multistep systems [45]. This lower bonding potential was ascribed to inferior mechanical properties due to a lesser polymerization conversion, and subsequent enhanced water sorption and phase separation [45]. However, the persistence of the disparity between the hoped-for progress and the current situation highlights the need for an improved laboratory test [16] and not to remain stuck.

Obviously, it is important to enhance the clinical value of laboratory tests. However, progress in the development of laboratory methods predictive of clinical behaviour is slow [46]. For a laboratory bond test to be useful in clinical terms, a clear understanding of the stress state that causes failure in service must be made (1). An assessment then service failures, and recognition of the usual gradual damage accumulation in actual service [16, 32]. Such detailed, complex experiments are likely to be long and expensive; however, the value added for dental applications would be undoubtable [16, 32].

2.4 Adhesive bond tests methods commonly employed

The primary objective of mechanical testing is to inform the selection of materials for specific tasks under specific load conditions without ignoring other factors that are strongly relevant at the same time (7). The forces of mastication may generate complex stress states involving compression, tension and shear, and so may have a significant effect on all dental restorations. The reproduction of such dynamic and complex stresses in the laboratory is likely to be difficult with regard to both method and cost (7). Consequently, various static load-to-failure (LtF) strength tests *i.e.*, compressive (diametral and axial), tensile, flexure, and shear, have been used to investigate the mechanical properties of dental materials (7). Different types of strength test are used to assess the effectiveness of the bond to dentine, the most frequently used being tensile and shear tests (both macro- and micro-scale).

2.4.1 Macro- versus microscale bond tests

Despite the increased popularity of “micro-scale” bond tests (both shear and tensile), macro-scale bond tests are also used with significant contributions to the field of adhesive dentistry [18]. The inclination towards conventional tensile and shear strength tests is possibly explained by the minimal demand in equipment and specimen preparation [18], also the fact

that the specimen size is more representative of actual restorations. Depending on the size of the bonding area, bond strength tests are classified arbitrarily as macro- or micro-scale. Bond tests with a bonding area larger than 3 mm^2 are said to be macro-scale [45], which renders the term 'micro-scale' somewhat misleading as it is largely involves bonded areas on a millimeter scale, and to a much lesser extent a micrometer scale. The fact that reports of the favourable long-term performance and reliability of the three-step etch and rinse technique appear to have been consistent has been taken to justify the assumed clinical relevance of the tests [5, 31]. There is also some evidence that the use of self-etch adhesives containing a monomer such as 10-methacryloyloxydecyl dihydrogen phosphate (10-MDP) is effective for bonding RBCs [45].

2.4.2 Shear tests

The apparently relatively uncomplicated set up of shear tests is probably the main reason for their continued use. They have easier specimen alignment in the test machine compared with tensile strength tests, thus avoiding the stress inhomogeneities associated with misalignment [47]. Shear is the essence of flow displacement, or plastic deformation (6). Pure shear modes loads can be in-plane (Mode II) or out-of-plane (Mode III) (Fig. 1). However, there is no realisation of a simple shear test in either mode in the dental context. All current tests have parasitic stresses and stress concentrations that destroy that assumption of a pure shear mode. Pure shear can naturally be resolved into equivalent tensile and compression forces, and *vice versa*. Aside from the rare uniform axial loading (Poisson ratio = 0), simple axial tension or compression necessarily involves shear stress *i.e.*, as part of the ordinary state of a body under tension or compression (7). So-called shear tests are the most frequently used to measure the bond of RBCs to dentine [48]. Both macro- and microscale "shear tests" have the following problems: [1] failures occur as a result of tensile stresses on the external surface opposing the loaded area; [2] nominal "shear stresses" are severely underestimated; and [3] most failures do not occur at or involve the adhesive interface [49]. The lack and difficulty of standardization is the main problem with all adhesive strength bond tests to dentine, and this leads to wide variation of reported mean bond strength values, and with large scatter, even for the same dentine bonding system [18, 44, 50]. This variation is attributed to the nature of the specimens and the lack of detailed control over experimental conditions [31]. Strength data results arise from an extremely complex interplay of multiple factors, however, the presence of control groups in factorial design may facilitate the establishment of trends and lessen the

influence of interlaboratory variation. Leloup *et al.* attempted to quantify the contribution of the most important parameters through a meta-analysis [31]. They drew some sensible conclusions: for example, a positive correlation (Pearson Correlation Coefficient = 0.64) between mean bond strength and mode of failure – higher bond strength was associated with a higher rate of cohesive dentine failures. It becomes complicated because the classification of failure modes as adhesive, cohesive or mixed (*i.e.*, a combination of the two) is based on subjective evaluation [51], but the latter two have no real value anyway in the sense that only the adhesive bond is of interest, and failure elsewhere means that the data are censored and inaccessible. In some failures the demarcation between adhesive and cohesive is difficult as there is no clear criterion to make the distinction [51]. In fact, cohesive failure in brittle materials could be explained by the mechanics of the test rather than an indication of a strong union [51]. Leloup *et al.* also found that shear strength values were significantly higher than tensile test values. The stiffness of the test set-up was identified as an important factor [31]. RBCs with a high (Young) modulus of elasticity (E) will give a greater bond strength than those of low E [31]. Indeed, Meerbeek *et al.* similarly questioned the conclusions made regarding brands of dentine bonding agents since the rigidity of their respective RBC has an important role [45]. Also, application of the bonding agent outside the bonding area was suggested to direct the shear load to the RBC-adhesive interface rather than to the adhesive-tooth interface, *i.e.*, shear stress caused the specimen to debond over a much larger area compared with that to which the RBC cylinder nominally was bonded [45]. However, fractures must occur along the path of least resistance, *i.e.*, minimum internal work.

With the (simplistic) assumption that stress and strain fields are generally homogeneous, the area of bonding has a significant influence on the 'calculated' bond strength values [31] simply due to the fact that "strength" is calculated by dividing the applied load by the initial cross-sectional area of the specimen [31], while the Griffith theory says that local stress concentration is always the cause of crack initiation [19]. Thus, Sultan *et al.* questioned the relation of shear bond loading to the bonded interface and suggested that failures due to shear loading were directly related to contact stresses: they found that failure loads did not scale with the bonded area but instead scaled with the circumference of the loaded cylinder [17]. The inability to approach the theoretical strength of materials despite the known bond strength at molecular level was explained by Griffith based on understanding the role of flaws in limiting the measured strength compared with the scaled theoretical value [16]. This may be further complicated by the structural inhomogeneities of quasi-brittle materials [52] and the difficulties with the supposed 'shear' testing [17], rendering the scaling of strength values less

predictable. Shear tests frequently result in cohesive dentine failures. This was attributed to the brittle nature of tooth structure and the observation that contact stresses produce compression on the RBC and tension on the tooth structure [53]. This leads to cracks deviating towards the tooth tissue [53].

"Shear bond tests" have complex stress states, with uncontrolled tension as a possible cause of failure [44]. Various configurations are employed to apply a "shear" load, the most frequently used are blade and wire-loop designs. A wire-loop was suggested to be better than a blade because it has a less severe stress concentration [44]. For both, the knife-edge chisel and the wire-loop methods, near the interface tensile stresses are actually higher than those of shear. However, "shear strength" values from both designs, based on the nominal assumed stress at failure, will be grossly underestimated due to failure to accommodate the stress concentrations near the loading site [44].

Current "shear test" designs are faulty due the high local stresses exerted *i.e.,* in stress concentrations [16], causing failure more quickly under highly nonlinear compressive and tensile stress states [17, 54]. However, while "shear tests" are said to be especially useful for substrates such Glass Ionomer Cement (GIC) and enamel, the properties of these materials render them particularly susceptible to specimen preparation effects, and likewise for the test conditions for tensile bond testing [18], especially those related to the test machine grips. Fowler *et al.* [55] reported that all Scotchbond 2 - enamel tensile specimens failed cohesively; thus the values obtained did not represent the interfacial bond to enamel. They further recommended shear over tensile tests for the tooth-adhesive interfacial bond as shear tests supposedly had the advantage of producing an increased number of adhesive failures [55].

2.4.3 Tensile tests

It is generally agreed that the testing of devices under the most demanding mechanical service situation would be the most informative way to provide a safety margin under operational conditions. This would help to avoid catastrophic and premature failures and thus improve the selection of appropriate materials [30]. Possibly, this is the reason that tensile testing is typically considered most appropriate [30].

2.4.3.1 Macroscale tensile tests

The majority of 'macro' specimens in the dental literature have a bonded area between three and four mm in diameter [51]. In ordinary speech, the term 'macro' is used to describe

the scale of working, although the term is not absolute in any sense and cannot be relied on to describe usefully that scale.

Using finite element analysis (FEA), van Noort *et al*. investigated the effect of changes in specimen geometry on the interfacial tensile peel stress [56]. They found that if the RBC blocks are kept above 3 mm in height, peak stresses are at the surface where failure might occur. To ensure a uniform load application across the adhesive joint, the RBC block must be increased in height to approximately four or five mm [56].

The strength of the union of dissimilar materials depends not only on the composition of the materials but also on the quality of the adhesive joint set-up as depicted through idealized test designs [16]. In any test, purity of the stress field is very hard to attain because of the geometrical requirements for the specimen and grips. Ensuring that the applied load axis remains perfectly aligned with respect to the test interface is difficult when the specimen is not uniform and especially with very small specimens [16], and as the applied force grows larger the system may become impossible to control. Also, parasitic stresses from the irregularities introduced during specimen preparation can influence test findings*, e.g.,* use of abrasive papers to simulate clinically prepared dentinal surfaces [16]. The smear layer*, i.e.,* the adherent layer of tooth debris resulting from grinding the tooth surface, impairs the bonding strength as it is (relatively) weakly attached to the underlying dentine. SEM (scanning electron microscopy) examination of early studies of dentine bonding agents (DBA) revealed that the failure was not adhesive, instead the smear layer failed cohesively*, i.e.,* both fracture ends of the interfacial joint were covered by the smear layer components [57]. Removal of the smear layer through phosphoric acid etching led to significant improvement in the bond strength to dentine [58]. As the bond of RBC to dentine become relatively stronger the need for a more controlled test set-up becomes evident [57].

2.4.3.2 Microscale tensile tests

Pashley *et al.* [57] noticed that bond strengths to dentine were often higher than those to acid etched enamel. It was explained as follows: the ‘higher’ bond to dentine created non-uniform stress distributions in the dentine leading to cohesive failures in the adherents rather than adhesively. Consequently, they suggested that conventional (macro) laboratory testing should be replaced with new test methods capable of detecting further improvements in bond strength to dentine [57].

Microtensile bond strength tests (MTBTs) were originally developed to avoid the cohesive fracture of dentine and to enable measurements of regional differences in bond strength to dentine [59]. The coefficient of variation (CoV) for such tests is of the order of 10 ~ 25%, compared with 30 ~ 50% for conventional tensile tests; this is explained by improved stress distribution during testing [59]. However, Roylance [60] suggested that the CoV for tensile strength is commonly in the range of 1 – 10% with values much higher than that indicating substantial inconsistency in specimen preparation or even experimental errors. However, Scherrer *et al.* [50] did not report a smaller CoV for microtensile compared with tensile tests for any adhesive except Scotchbond Multi-Purpose. Other factors also influence test results: demineralized dentine matrix tensile strength was said to be influenced by the proportion (cross-sectional fraction) of collagen fibres rather than the total cross-sectional area of the interface [57]; the tooth type and condition (human or other animal, carious or sound, young or adult, erupted or unerupted); pretreatment (storage medium and time, temperature); handling during and after testing; depth and location of interface [57]; and the mechanical characteristics of the restorative material used [61]. Stress rate [62] and test temperature also matter [11]. The cross-sectional area of MTBT specimens has a strong effect on test results (*i.e.,* there is a size effect). An ultrafine diamond bur was used to reduce the bonded area to an hour-glass shape, at the waist of which failures are expected to occur. Consistent bur grinding was technically challenging. A non-trimming technique markedly minimized this effect through elimination of the need to use to the bur to locate the weak interface [57]. However, Staninec *et al.* [63] questioned the meaning of strength measurement in dentine in the light of the observation that a preexisting population of flaws controls the fracture. They suggested that inherent flaws or flaws introduced during cavity preparation will significantly influence the durability of bond to dentine. Therefore, Staninec *et al.* [63] recommended that study designs should identify these flaws and determine their distribution in various dentine types and sites so as to minimise the potential influence.

Statistical problems associated with MTBTs were first related to limited or small sample sizes (some five to eight specimens per tooth) [59]. Development of the non-trimming technique (yielding ~ 25-30 specimens tooth) [59] may have resolved the problems of small samples from one aspect, but they are all from a single tooth thereby creating concerns about the lack of statistical independence of the results. Results from specimens from a single tooth are necessarily correlated. Using these values as if they were independent, and thus assuming that each contributes a degree of freedom to the statistical analysis, inflates the presumed power

of the test results. Eckert & Platt [64] concluded that correlations between beams from the same tooth should be accounted for to avoid over-stating the statistical significance of the study results. Thus, the effects of variation between teeth, between materials, and between treatment details may have been spuriously reported as important (*i.e.* statistically-significant) when in fact they were not due to other than chance.

For example, it has been reported that there are differences in the intrinsic strength of dentine in different regions of a tooth (*e.g.,* superficial *vs*. deep) [59, 65], while luting resins with different chemical formulations and applications are said to yield significantly different bond strengths to different regions in human dentine [66]. With multiple correlated specimens from the same tooth (or region of a single tooth), such conclusions may be unsound. When only few teeth are involved overall, the effective degrees of freedom for the analysis may be unacceptably low. Thus, generalizations based on these results are likely to be less than representative of real-world behaviour. On the other hand, if the bond to the dentine is varying systematically across the exposed region, the scatter observed will be greater, further weakening statistical comparisons.

In some research centres procurement of extracted teeth is difficult, so MTBTs using few teeth may be the only approach available in practice, but the statistical problems cannot be ignored. Given the volume of interest in bonding, and its importance to dentistry, sound conclusions based on valid data properly analysed is crucial. Dentine is an heterogeneous structure even within the same tooth, and definitely so between teeth. Assuming that the dentine, or the bond to dentine, is uniform between teeth is unjustified.

2.4.3.3 Pre-test failures

Pre-test or premature failures (PTFs) (*i.e.,* before being deliberately loaded) are rarely recorded. Such failures in fact are not uncommon; this may be because of the small size of the specimens. Some studies consider PTFs as yielding test values of zero while others simply delete them and consider them as missing data [67]. PTFs may reflect the non-uniformity or absence of the adhesive bond to the tooth substrate – which condition is itself plainly of importance – or just rough handling (although the implication is that the bond was weak anyway). Ignoring such failures, as if technical errors, interferes with the interpretation of the actual clinical scenario. An RBC restoration is bonded to dentine through a hybrid layer which results from the demineralization of the dentine and its subsequent infiltration by resin

monomers to varying depth. The formation of the hybrid layer is affected by many factors, *e.g.*, type of acid used, duration, composition of the resin, *etc.* This is reflected through variation in the thickness and quality of the 'hybridization' which in turn controls the quality of the adhesive bond.

It is clear that microscale bond tests simply assume that the adhesive layer has sufficient uniformity. Ferracane *et al*. [68] suggested that constant thickness of the adhesive layer and optimized load configurations in microshear bond tests have the potential to control the overall stress distribution due to the lower elastic modulus of the adhesive layer [68]. Over a prepared tooth surface there will be inevitable variation in the substrate; such variations and their influence on the bond will not be reflected through micro-scale bond tests that ignore location. A different approach that relates the results to the state of the adhesive may be more informative.

As mentioned at the end of the previous section, dentine has a heterogeneous structure, both within and between teeth. This fact undermines the assumption that the dentine, or the bond to dentine, is uniform between teeth, and which is therefore unjustified. The use of four-point bend (4pb) testing would allow relatively better specimen dimensions that can reflect the non-uniformity of adhesive bond to tooth structure. Relevant specimen size enables appropriate flaw populations and strain-energy content [69].

There is a statistical problem that is apparently never addressed: quality attainable might be indicated by the maximum value in a series, while all that is ever used is the mean. But, 'mean' behaviour is not real world, the worst case is what matters – how poor can the union be when all effort has been made? The risk of failure in service has to do with the lower-tail density: low values fail early. What is the lower bound? Raising that is of greater importance, that is to say, improve the reliability of the bond.

2.5 Importance of adhesive joint design

Joint design is a critical factor to bear in mind during specimen preparation, since the strength of an adhesive joint is greatly affected by the geometry of the joint and choice of the adherents [9]. That is to say, the soundness of a measured mechanical property is influenced by the underlying stress distribution in the joint. For example, a flash of an adhesive outside the boundaries of the bonding area of a butt joint is said to create an overlap on the substrates

that results in the imposed load within the adhesive layer manifesting as shear stresses rather than tensile or peel stresses [9]. Such overlap often goes unnoticed and results in an apparently simple joint design having complex stress distributions due to off-axis loading, thus emphasizing the importance of the exact details of the joint [9].

Testing a material under the most challenging possible mechanical situation is said to be the best way to ensure adequate strength and avoid premature failures under complex occlusal loading [30]. A joint geometry that enables stress concentration to coincide with the interfacial region focuses on joint durability [9]. A peel test has been said to be a good example of a method to enable inter-laboratory comparisons and to assess the performance of an adhesive joint under the stresses likely to be experienced in service [9]

2.6 Service failures

Failure for brittle materials occur at the point of fracture [9]. Fracture points are easy to define for a uniaxial stress state, such as four-point bend test where fracture occurs when the stress reaches the ultimate strength [9]. However, service conditions (masticatory forces) could represent a complex triaxial stress state [70] and failure prediction becomes very difficult. Instead, failure predictions are suggested by assessing and comparing the more reliable and relatively easy to measure mechanical properties and then attempt to establish a relationship with clinical failures [9]. Interfacial bond strength is possibly the most important piece of information in static tests. Generally, failure prediction should be consistent with clinical observation [15].

2.7 Immediate *vs.* aged dentine bond strength

Multiple factors influence the bond strength to dentine over time, *e.g.,* nature of the adhesive system, material degradation, whether sound or caries-affected dentine, *etc*. However, the immediate bond to dentine is of interest since RBC restorations are placed in functional use immediately after the restorative procedure, and in some cases while performing the occlusal adjustments in the finishing stage. However, since the oral cavity is a wet environment, water exposure matters. Evaluation of hydrolytic degradation on bond strength after 24 h is convenient, but only part of the story – how does it change with time, in the long run, on a scale of hours, days, months, years? No one time is enough.

It gets more complicated when properties vary with time, *e.g.*, improvement with continued setting reaction, softening by water sorption, damage by dissolution and hydrolysis. That is to say, the details are too complex to be captured at only one or two times, which are entirely arbitrary and cannot be justified as such unless for process quality control. Understanding the behaviour of a system needs more. However, evaluation of immediate bond strength can be viewed as a way to validate a test set up and to establish a reference point that is of direct interest in itself, that is, investigating the immediate challenges experienced by a bonding system on their own.

2.8 Thermal cycling

The use of thermal cycling to evaluate restoration materials is based on the premise that thermal changes break or exacerbate the inadequacy of the seal to the cavity wall. Thermal stresses affect mechanical stresses at the interface and thus increase the potential for crack propagation. Thermal stresses may also change the gap dimensions and hence facilitate cyclic fluid flow at the interface [71, 72].

Thermal cycling has been frequently used as an ageing method in tracer penetration studies. However, penetration depth measurements and gap sizes have been inconsistent and even contradictory. This was partially explained by the lack of a standard test protocol. Gale and Darvell [72] highlighted the importance of water sorption as a confounding factor. A trend was observed for increasing the depth of penetration with increasing the number of thermal cycles. They suggested that with an increased number of cycles there is more time for the tracer to go deeper on a simply diffusive basis, but increased temperature also aids hydrolytic reactions for bond breakage within the adhesive.

Marginal gap formation occurs gradually over time allowing for fluid seepage around the filling. Stress, whether mechanically or thermally implemented, accelerates a catastrophic failure that does not reflect failures in practice *i.e.*, unrealistic failure rate. Gale and Darvell [72] suggested standardized test conditions, proposing a much less severe thermal cycling regimen than is usual. Tests using excessive stresses will have relatively less discriminatory power and would not provide grounds for a decision [72].

Assuming test conditions that are derived from a clinically-relevant failure mode were chosen, and in the absence of predictive pathogenic gap criteria, the presence of an adequate

seal at the interface is the only clinically-interpretable outcome, *e.g.*, the bond of adhesive resin to etched enamel can be stressed until the beginning of leakage is noted. Conversely, dentine as a bonding substrate has difficulties that negatively affect the adhesive joint as a complete seal [12]. That is to say that there is no point in thermally stressing the bond to dentine as it will leak anyway [12]. However, if used for extended periods (weeks), less severe thermal cycling may prove to be useful in investigating weak and susceptible aspects of the joint that could lead to the formation of possible crack initiation sites. This might possibly be verified through the investigation of the rates of various hydrolytic reactions, and these can be further influenced through variations in pH.

2.9 Strain rate effects

It became apparent in reviewing the relevant literature that the conditions under which bonding tests were conducted were far from standardized. In particular, the strain rate – as represented by cross-head speed (XHS) in the mechanical testing machine – was essentially arbitrary (between 0.01 and 200 mm/min). However, since it is known that polymeric systems are strain-rate sensitive, it can be expected that the results obtained for mechanical properties in general will depend on that arbitrary choice. From a review of those papers that examined strain rate effects no clear conclusion was apparent. Accordingly, in order to inform future work, it was decided to examine more closely the data in those few papers with a view to better understanding of both the experimental circumstances used and the results obtained. The analysis is set out in Chapter 6.

2.10 Study significance

Reliable bonding and perfect marginal sealing at the RBC-dentine interface are of paramount importance to achieve a satisfactory prognosis. Despite the considerable improvement of dental adhesives over the last decade, it is still quite challenging to establish a durable joint to dentine owing to its structural heterogeneity [73]. However, an improved adhesion to dentine has been reported with the advent of mild self-etch adhesives, despite a thin hybrid layer and the absence of resin tags compared with total-etch systems, said to be explained by an additional chemical interaction between resin monomers and residual BAp [5]. Furthermore, it was also reported that exposed BAp on enamel surface is expected to enable

intimate chemical bonding with the functional monomers, *e.g.*, 10-MDP, of some mild self-etch adhesives, which may delay the progress of marginal leakage [5]. Still, when bonding to enamel, strong self-etch adhesives perform better than the mild, highlighting the importance of micromechanical retention and questioning the contribution of chemical bonding [5].

A combination of mechanical and chemical means of retention would be logical to augment the adhesive joint to enable it to survive being stressed. Key questions are how much more strength does the chemical bond add and, possibly of greater relevance, what are the consequences of having only mechanical retention, *i.e.*, does micromechanical retention provide a satisfactory effective bond? Generally, without sufficient intimate molecular contact across the interface, interatomic and intermolecular forces cannot be established between the surfaces of the adhesive and adherend [9]. Secondary and primary interfacial bonds are important in initiating extensive energy dissipative deformations and increasing the resistance to environmental attack adhesively. Bonding to rough surface also improves the extent of interfacial contact [9]. However, the demarcation between mechanical and chemical contributions on a rough surface can be very difficult to identify.

Besides, etching using phosphoric acid demineralizes dentine over a depth of ~3-5 μm, exposing a scaffold of collagen fibrils. Enzymatic degradation of collagen fibrils and hydrolysis of polymers at the hybrid layer are the two main factors involved in the destabilization of the resin-dentine interface [74]. In experimental work, bonding to a flat surface would minimize the effect of mechanical retention, and better to evaluate the interfacial molecular interactions on the strength of the adhesive joint.

The literature is replete with studies discussing adhesive strength testing. The diversity of results from the various tests may be caused by faulty set-ups and inappropriate sample geometry, as well as several relevant factors that cannot easily be standardized. This clearly undermines conclusions based on comparison of such reports [50]. It is clear that detailed control of specimen preparation and identification of potential modes of failure during service conditions are needed. This may be achieved through a better understanding of the relevant factors in attempting to simulate oral service conditions. Thus, in practice, loading systems are never ‘pure’ and the concept of service-condition simulation may be more applicable than in presumed ‘idealized’ test conditions [75]. In other words, the test system or experiment should be set up to reproduce or mimic the actual mode of failure of the material in service (13,14).

Marginal chipping of RBCs can be visualized as follows: after placement of an RBC restoration, degradation will ensue, starting most obviously at the restoration margins, leading to varying extents of bond loss *i.e.*, loss of 'intimate' support. This leads to a margin more susceptible to fracture or chipping. Marginal deterioration is probably caused by the continued flexure of the RBC fillings due to compressive loads leading to gradual loss of strength of the adhesive joint. In the proposal set out in this thesis, dentine slices bonded on both sides to an RBC, placed in a suitable intra-oral mimic environment, are then subjected to a symmetrical four-point bend (4pb) test as proposed by Mutluay *et al.* [21][2] and Sanli *et al.* [75][3]. Adhesive bonds may fail in a manner similar to peeling in that crack initiation (bond separation) commonly begins at the free edge, where there is a stress concentration, and progresses inward relatively slowly. Four-point bending might be a means of addressing the study of such failure, even though not an exact mimic of the service stress system.

For strength data to be meaningfully scaled to specimen size, simulation of environmental factors, crack growth rates, and stress distributions should be well characterized. In symmetrical four-point bend (4pb), the stress field to which the specimen is subjected can be calculated, and this is nominally uniform over the length of the central region.

2.11 Aims of the study

Given the above review of the literature, the motivation was the inadequacy and deficiencies of common existing test approaches, with the goal of developing a method that will ensure that routine interfacial strength testing can be performed in an accurate, reproducible and reliable manner, but most importantly one that will provide discriminatory power within and between systems. Without a sound 'bonding' test method, uncertainty will remain as a critical issue limiting progress in 'adhesive' dentistry and related procedures as well as in other dental systems where bonded interfaces are involved. The aim is to permit the examination of developments in techniques for improving adhesive bonds and variations in multifactorial systems such as to optimize choices more efficiently.

[2] Mutluay MM, Yahyazadehfar M, Ryou H, Majd H, Do D, Arola D. Fatigue of the resin–dentin interface: A new approach for evaluating the durability of dentin bonds. Dental Materials. 2013; 29(4):437-449.

[3] Şanlı S, Çömlekoğlu MD, Çömlekoğlu E, Sonugelen M, Pamir T, Darvell BW. Influence of surface treatment on the resin-bonding of zirconia. Dental Materials. 2015; 31(6):657-668.

The primary purpose was to develop and validate a protocol for bond testing that is applicable to the diverse systems relevant to dentistry, based on a symmetrical four-point bend (4pb) test.

In the process, a secondary aim was to investigate the 'chemical bond potential' between dentine and a variety of allegedly 'adhesive' systems employed in the dental field. This was to be evaluated through the use of relatively flat and smooth test surfaces to minimize mechanical retention ("key")[4]. In the process, for consistent results, the development of an appropriate technique for specimen preparation was seen as vital, minimising specimen defects and creating a reproducible method as a proof of principle. The development of a robust test method is a prerequisite such that it may be transferred reliably between laboratories and contexts, even if protocol adjustments to suit some systems better may be required.

Thirdly, the role of mechanical key, by way of contrast with any chemical bonding, was to be examined, noting that in several systems they may not be entirely separated, *i.e.*, acidic components may etch to some extent anyway even when direct etching in a separate step is not used.

In addition, some claims as to the effectiveness of some kinds of alleged bonding may be tested in the course of the above work.

[4] key: interlocking roughness of two materials conferring resistance to shear and, if undercuts are present, to tension [120].

3: Materials and Methods

List of materials and conditions

The following provides a key to the various conditions and materials tested in this section, and an outline of the experimental scheme is given in the following figure (3.1).

1. Monolithic bars 3.2.2
    a. High viscosity 3.2.2.1
        i. Filtek One bulk-fill (FB) 3.2.2.1
        ii. Beautifil bulk-fill (BB) 3.2.2.1
            1. Hand pressed 3.2.2.1
            2. Constant load 3.2.2.1
        iii. Tetric Evoceram (TEC) 3.2.2.1
    b. Low viscosity 3.2.2.2
        i. Filtek flowable bulk-fill (FF) 3.2.2.2
            1. 50 mm specimens 3.2.2.2
            2. 28 mm specimens 3.2.2.2
2. Repair bond strength 3.2.3
        i. Monolithic Filtek bulk-fill (FB) 3.2.2.1
        ii. Repair Filtek bulk-fill (FB) 3.2.3
3. Dentine coupons - room humidity 3.2.4
        i. Conventional cements 3.2.4
            1. Smooth surface 3.2.4
                a. Zinc phosphate cement (ZPC) 3.2.4.1
                b. Zinc polycarboxylate (ZCC) 3.2.4.2
                    i. Stainless steel (SS) 3.2.4.2
                    ii. Aluminium alloy (AA) 3.2.4.2
                c. Glass ionomer cement (GIC) (Fuji II, Aquacem) .3.2.4.3
                    i. Stainless steel (SS) 3.2.4.3
                    ii. Aluminium alloy (AA) 3.2.4.3
                d. Calcium silicate cement (Biodentine, BD) 3.4.3.5
            2. 120-grit abrasive paper 3.2.4
                a. Zinc phosphate cement (ZPC) 3.2.4.1
                b. Zinc polycarboxylate (ZCC) 3.2.4.2
                    i. Stainless steel (SS) 3.2.4.2
                    ii. Aluminium alloy (AA) 3.2.4.2

The general plan of this work was to investigate the various effects of surface treatments to demonstrate the effectiveness of the method:

1. Initially, monolithic specimens were examined.
2. Then the repair bond strength of RBC was investigated.
3. Investigation of the potential adhesion of various materials to human dentine, namely resin and conventional cements.
4. Lastly the potential adhesive bond to zirconia was also examined.

The list of the method development steps is shown in Figure 3.1.

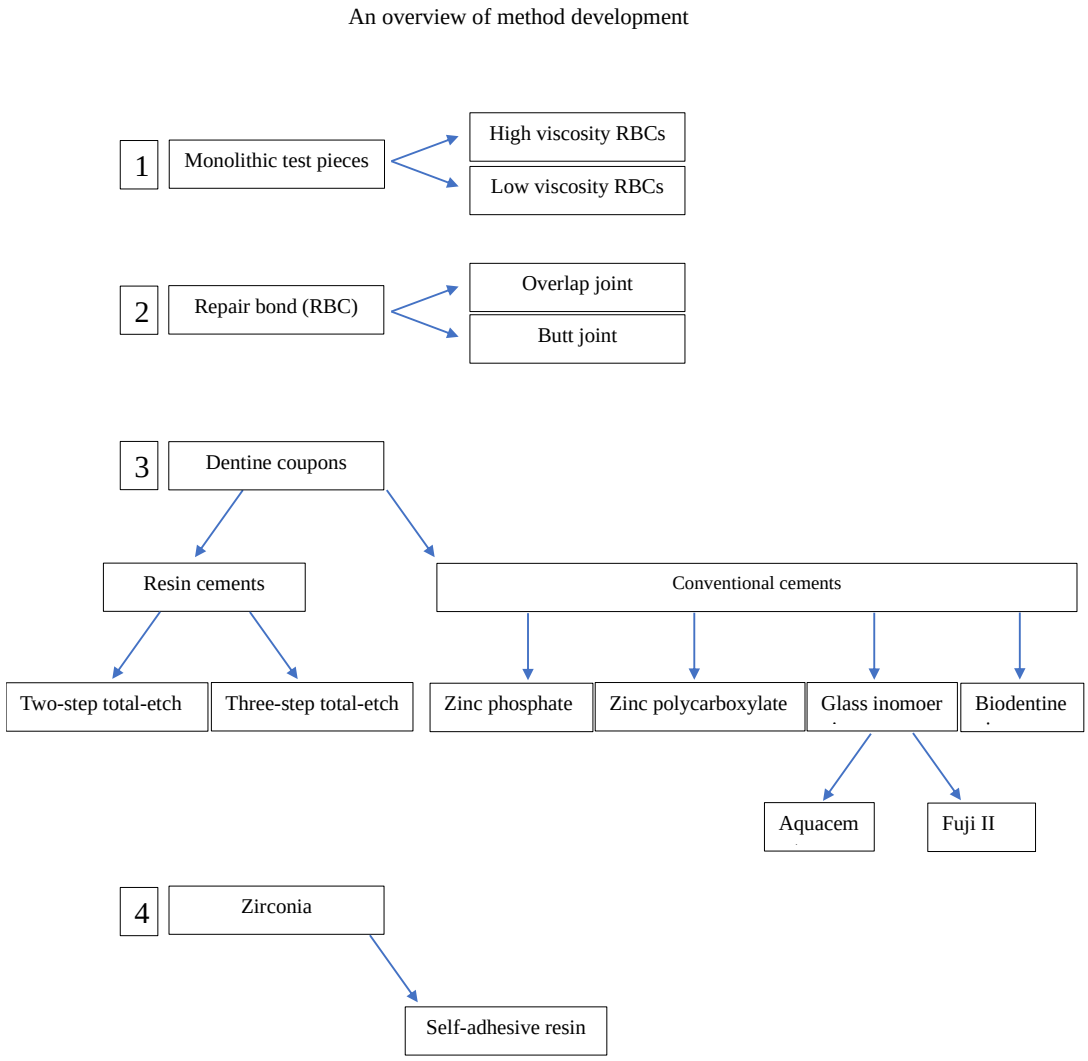

Figure 3.1 Method development steps (optimization of four-point loading system). **(1)** Monolithic long specimens to specify a load span half of the support span. **(2)** Establishment of the butt joint geometry. **(3)** Use of a number of adhesive systems in dental field with dentine coupons. **(4)** Due to the

potential self-etching effect of the adhesive systems on the dentine coupons in (3), zirconia-zirconia bond was investigated.

3.1 Four-point bend (4pb) test

Specimens were placed symmetrically on two supporting rods which were 5 mm in diameter and placed 40 mm apart (centre to centre). Specimens were loaded centrally under compression (crosshead speed of 0.5 mm/min) on the upper surface, applied using a Universal Testing Machine (Criterion Universal Test System; MTS System Corporation, Eden Prairie, MN, USA) with a moving cross-head which had an attachment with an additional two rods (5 mm diameter) placed 20 mm apart (centre to centre) (Figure 3.2). The load at fracture was recorded, and four-point flexural strength, σ_4 [11], was calculated from:

$$\sigma_4 = \frac{3F(L-L_1)}{2wh^2} \quad [1]$$

where F is the load at failure (N), L is the distance between the (lower) supports (40 mm), L_1 is the distance between the (upper) loading rods (20 mm), and *w* is the width and *h* the thickness of the specimen (mm). The beam pieces were retrieved after fracture; *w* and *h* were measured at the fracture using a calliper gauge (reading to 0.03 mm) (Duratool, digital vernier 150MM D00352; Farnell, Leeds, UK).

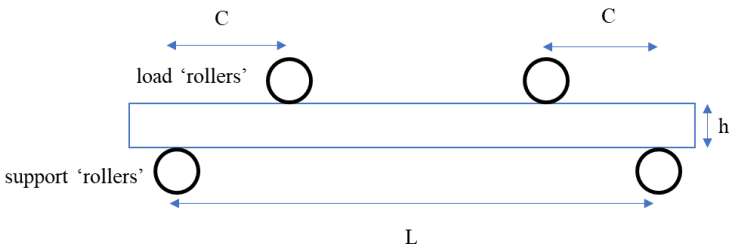

Figure 3.2 Four-point bend test set-up (long specimens).

A correction factor was included in the equation for 4pb strength [76] which corrects for large deflections and consequent departure from simple beam theory [77].

$$\sigma_4^* = \frac{3F(L-L_1)}{2wh^2}\left(1 - \left(\frac{10.91Dw}{L^2}\right)\right) \quad [2]$$

where *D* is the specimen displacement (the derivation of *D* is discussed in 3.3). Values for flexural strength were calculated with and without the correction factor. Beam theory is based

on the assumption that beam geometry remains unchanged during bending [78]. This is the case at relatively small deflections, however, thin beams show large deflections and subsequently the theoretical basis of linear beam theory becomes less satisfied [76]. An approximate correction factor has to be applied to flexural strength formula to account for the deflection [76].

Table 3.1 shows the brands and main chemical compositions (from manufacturers' product data sheets) of the cements and other materials used.

Code	Material	Shade	Composition (filler loading: mass, volume) %	Manufacturer	Batch No
FB	Filtek One, Bulk Fill Posterior Restorative	A2	AFM, aromatic UDMA, UDMA, DDDMA. (76.5, 58.5)%.: 20 nm silica, 4-11 nm zirconia, zirconia/silica cluster, 100 nm agglomerated ytterbium trifluoride,	A	NA20550
BB	Beautifil Bulk (Bulk-Fill)	Universal	Bis-GMA, UDMA, MPEPP, TEGDMA. (83, 74.5)%.: S-PRG filler based on F-B-Al-silicate glass.	B	091618
TEC	Tetric EvoCeram (Nanohybrid)	A2	Dimethacrylates (17-18%), copolymers, (83, 54)%: barium glass, ytterbium trifluoride, mixed oxide, (40 nm–3 µm).	C	Z01435
FF	Filtek Flowable Bulk-Fill	A3	Bis-GMA, bis-EMA (6), Procrylat resins. (64.5, 42.5) %: ytterbium trifluoride (0.1-5.0 µm), silica/zirconia 0.01-3.5 µm).	A	NA91826
Z250	Filtek Z250 Restorative	A2	TEGDMA 1–5%, bis-GMA 1–10%, bis-EMA 1–10%, UDMA 1–10%. (75- 85)%: silica/zirconia.	A	N721517
EG	Scotchbond Universal Etching Gel	--	Water 50-60%, phosphoric acid 32%, silica 5-10%, polyglycol 1-5%, aluminium oxide < 2%.	A	8407293
ASP	Adper Scotchbond Multi-Purpose Primer	--	HEMA 35-45%, water 40-50%, copolymer of acrylic and itaconic acids 10-20%	A	NE23236
ASA	Adper Scotchbond Multi-Purpose Adhesive	--	Bis-GMA 60-70%, HEMA 30-40 %.	A	NC53204
ASX	Adper Scotchbond 1 XT	--	Bisphenol A glycerolate dimethacrylate, 2-HEMA, UDMA	A	NE89265
GIC_F	Fuji II Glass Ionomer	22 yellow brown	Powder: calcium fluoroaluminosilicate [79] Liquid: polyacrylic acid, tartaric acid 10-20%	D	2109021
GIC_A	Aquacem Glass Ionomer	-Luting-	Powder: calcium-sodium-fluoro-phosphoro-aluminium-silicate, polyacrylic acid, tartaric acid, iron oxide pigments. Liquid: deionized water	E	2202000372
ZCC	Zinc Polycarboxylate Cement	--	Powder zinc oxide 70-80%, stannous fluoride 1-10 Liquid: acrylic acid copolymer 1-10%	E	052124-4
ZPC	Zinc Phosphate Cement	Dentine shade	Powder: zinc oxide 50-100%, magnesium oxide 2.5 ~ 10% Liquid: phosphoric acid 50-100%	F	2108001128
CS	Calcium Silicate Cement, Biodentine	Light grey white	Powder: tricalcium silicate, dicalcium silicate, calcium carbonate and oxide, iron oxide, zirconium oxide Liquid: calcium chloride, hydrosoluble polymer	G	31245121
RX	RelyX Unicem 2 Automix	A2	Bifunctional methacrylate inorganic fillers 50 – 70%	A	8756096
SS	Stainless Steel Strip	--	Grade A2. Cr 18.5%, C 1.2%, Ni 8%	H	A136208
ZrO_2	Zirconia blocks	B1	Zirconium oxide 88-95.5%, yttrium oxide > 4.5- ≤ 6%, hafnium oxide ≤ 5%, aluminium oxide ≤ 1%, other oxides for colouring ≤ 1% [80]	C	Z03ZNC

Table 3.1 Manufacturers' information on products used. It is important to draw the distinction between mass and volume fractions of the filler content as sometimes the difference can be high. This is particularly important when heavy elements with high density are included. Subsequently, advertised figures need to be interpreted cautiously.

Key to Table 3.1

AFM: addition-fragmentation monomer (= DDDMA).

bis-EMA: ethoxylated bisphenol A dimethacrylate.

bis-GMA: bisphenol A diglycidyl ether dimethacrylate.

bis-MPEPP: 2,2-bis[(4-methacryloxy polyethoxy)phenyl]propane.

MPEPP: 4-methacryloxy polyethoxy(pheny1)propane

DDDMA: 1,12-dodecane dimethacrylate

TEGDMA: triethylene glycol dimethacrylate.

UDMA: urethane dimethacrylate.

Manufacturers

A 3M ESPE, St Paul, MN, USA.

B Shofu, Kyoto, Japan

C Ivoclar Vivadent, Schaan, Liechtenstein

D GC Europe, Leuven, Belgium

E DE Healthcare, Northampton, UK.

F Dentsply DeTrey, Konstanz, Germany

G Septodont, St Maur des Fosses, France

H Manutan UK, Verwood, Dorset, UK

3.2 Specimen preparation

3.2.1 Moulds

3.2.1.1 Stainless steel

A knife-edged split stainless steel mould (50 mm length × 5.0 mm width × 2.0 mm thickness) was used to prepare resin specimens (Figure 3.3). The design and dimensions were adapted from previous work [75, 81]. The purposes of the design were:

1. Multi-part split-mould for easy retrieval with minimal stress (no bending).
2. Knife-edge margin for easy separation of the excess (‘flash’) [81].
3. Open and flared ends allow material flow, adaptation to the mould slot and moulding stress relaxation, minimizing air entrapment [81].

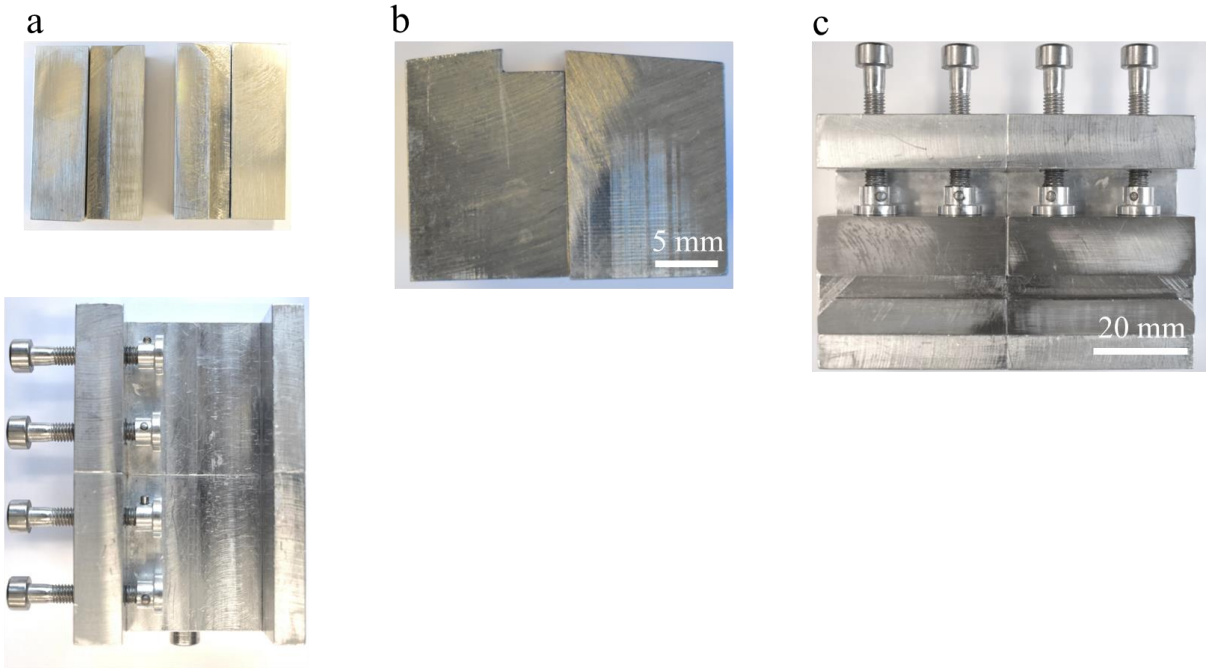

Figure 3.3 Knife-edge split stainless steel mould. **(a)** Parts of the split mould and clamping block with cap screws (top view). **(b)** End view showing knife edges. **(c)** Assembled, showing mould slot (top view).

3.2.1.2 Acrylic

An acrylic mould (30 mm length × 2.0 mm width × 2.0 mm thickness) (Figure 3.4) with similar design features as the stainless steel mould, except for the different length and width was used for preparation of the conventional cement specimens.

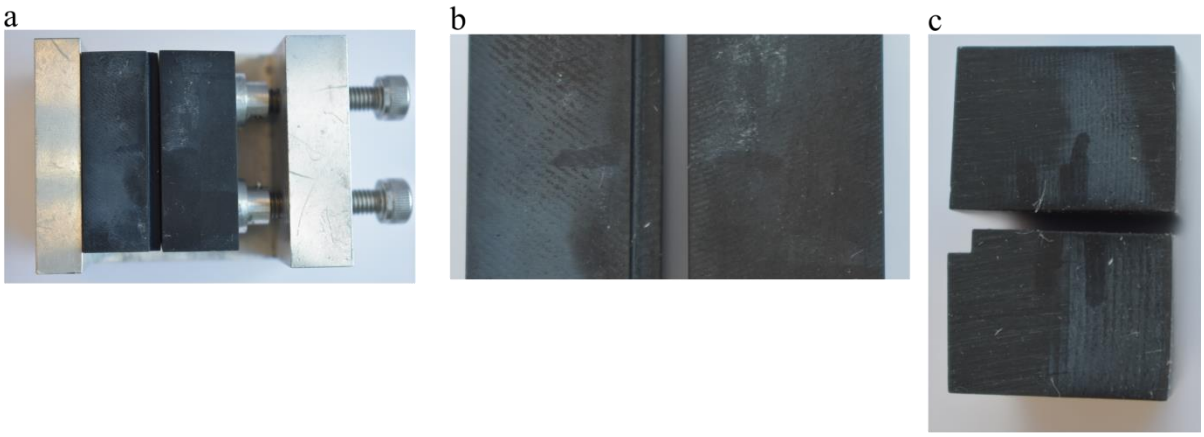

Figure 3.4 Acrylic mould [30 mm length × 2.0 mm width × 2.0 mm thickness]. **(a)** Parts of the mould and clamping block with cap screws (top view). **(b)** Close top view showing mould slot. **(c)** End view showing knife edges.

3.2.2 Monolithic bars

Three types of material were studied: one 'nanohybrid' (TEC), two high-viscosity bulk-fill restoratives (BB, FB), and one low-viscosity (flowable) material (FF) (Table 3.1) (Figure 3.1). Nanohybrids contain the smallest size of filler particles (5 - 100 nm to 0.6 - 1 µm) [82, 83], however it is generally difficult to distinguish between nanohybrids and microhybrids [83]. The smaller filler size was said to improve mechanical as well as appearance [82].

3.2.2.1 High-viscosity RBCs

Monolithic bar-shaped specimens were fabricated by extruding material from the supply syringe into a stainless steel mould. The top surface of the specimens was prepared against a transparent acetate strip (Cephalometric Tracing Acetate, DB Orthodontics, Silsden,

England) to provide a smooth glassy surface. A bench-top hand press, using index, middle, and ring finger pressure, for 60 s at ~70 N on an interposed glass microscope slide, was used to press the slide down to contact the knife edges of the mould. Specimens were then cured by placing the tip (diameter 10 mm) of the light emitting diode (LED) light curing unit (Elipar S10; 3M ESPE, St Paul, MN, USA) in direct contact with the acetate strip, irradiating each specimen at eight slightly overlapping spots, 20 s per spot. A plastic mould was used to guide the overlapping spots. The output of the light curing unit (LCU) was checked using a calibrated spectrophotometer (USB4000; Ocean Optics, London, England) at the beginning of the experiment, the output was "nominally 2500 mW/cm² (Appendix 1) [84]. The top acetate strip was removed, and the mould disassembled, enabling free retrieval of the specimen. Excess flash at the upper surface periphery was removed using a sharp blade and wet 1000-grit abrasive paper (CarbiMet papers; Buehler, Cleveland, OH, USA). All specimens were preliminarily inspected under light microscopy (magnification 0.63×, 1.6×, 2.5×, 4×) (stereomicroscope, MST 130 3945; Polymer Optics, Wolston, Coventry, UK) for visible defects, however, none were found and all specimens were used, with none were discarded (Figure 3.5). The specimens were then stored ‘dry’ in a transparent container on the bench *i.e.*, were not protected from light, for 24 h at room temperature (~18 - 19 ºC). The flexural strength was then measured in four-point bend as described in Section 3.2 and shown in Figure 3.2.

Figure 3.5 Monolithic specimens examined under light microscopy for visible defects.

The experimental sequence of steps performed to optimize the monolithic specimens design is shown in Figure 3.6. The high viscosity RBC yielded improved and consistent surface finish under constant load compared with hand pressure. Also illustrated is the repair joint development to the correct joint design *i.e.*, butt joint. Low viscosity flowable RBC was too flexible to fracture with 50 mm specimens, so the length was reduced to 28 mm.

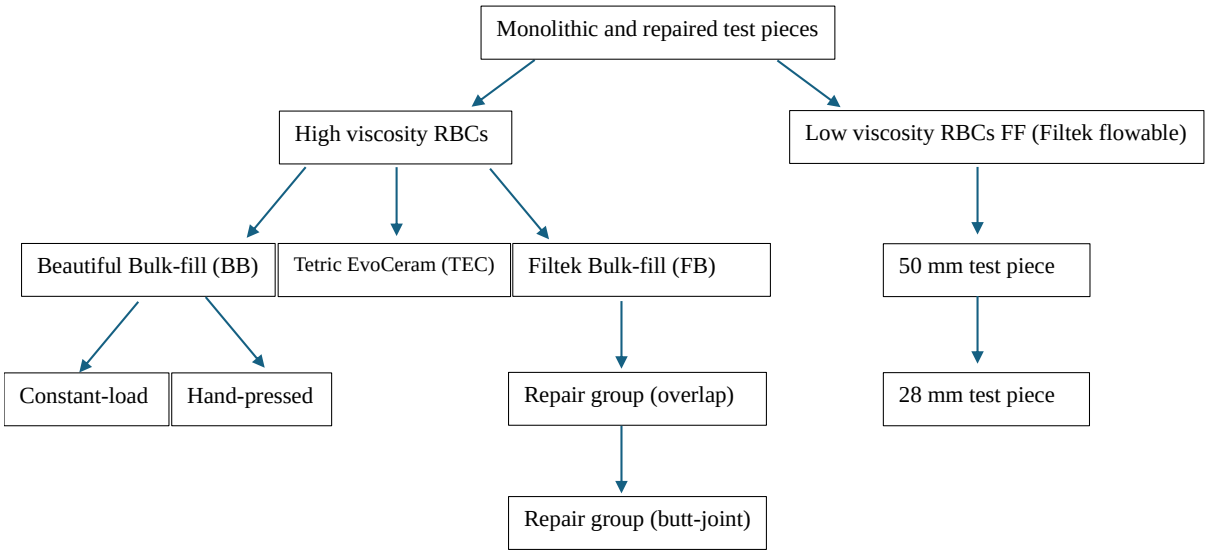

Figure 3.6 Schematic of the experimental sequence of monolithic and repaired specimens.

3.2.2.2 Low-viscosity RBC

Specimens of FF were prepared as described in Section 3.2.2.1. The pressure was applied for 10 s instead of 60 s for the high viscosity RBCs. However, the material was too flexible to fracture with 50 mm beams due to their relatively higher resin volume fraction than the other materials. Thus, reduction of the span length was used to enable fracture through decreasing the deflection of the beam. However, the shorter span length also means that a different volume is under test, *i.e.* fewer flaws, and therefore expected to raise the calculated failure stress, on average, by reducing the risk of large flaws initiating failure. The reduced span length involved two changes: the upper and lower rods were repositioned (for the already made specimens) so that L_1 = 13 mm and L_2 = 26 mm, and new shorter specimens (28 L × 5.0 W × 2.0 T mm) were also prepared.

3.2.3 Repair bond strength

After testing the monolithic beams (Filtek Bulk-fill), eight specimens were selected at random, the fracture ends were ground flat and polished successively using silicon carbide papers (1000, 1200, and 2000 grit), under continuous water flow, back to undamaged material which was verified using the light microscope (Figure 3.7). Specimens were kept at close to

90º to the paper while grinding and polishing using a test-piece holder (Figure 3.8, a and b). Specimens were placed in the 'V' of this grinding jig against the two opposing walls and held in position using a cap screw. Grinding was then initiated against abrasive papers using gentle pressure, 1 mm was ground away from each fracture end. The specimens were then ultrasonically cleaned (Vitasonic II; Vita, Bad Säckingen, Germany) in deionized water (E-Pod, ZRXSP0D01; Merck, Darmstadt, Germany) for 10 mins, and stored at 37 ± 1°C in an oven (Hybaid Shake 'n' Stack, Knutsford, Akribis Scientific, Knutsford, England) for two days to dry. Specimens were returned to the mould and repaired by adding a new layer of RBC (without the use of adhesive or other treatment). An RBC beam, 2 mm thick was placed in the mould to control the thickness of the added material (Figure 3.8c). The specimens were then approximated to the beam thickness (2.0 mm) and bonded using fresh RBC. A metal spatula was used to insert the RBC into the repair cavity. An acetate slip and glass slide were then placed onto the specimens upper surface before being hand pressed flat, down to contact with the knife edges. The 'repair' material was then light-cured for 20 s with the tip of the light-curing unit in contact with the acetate slip. The resulting specimen was then stored dry in a transparent container *i.e.,* not protected from light, for 24 h at room temperature (18 ~ 19 ºC).

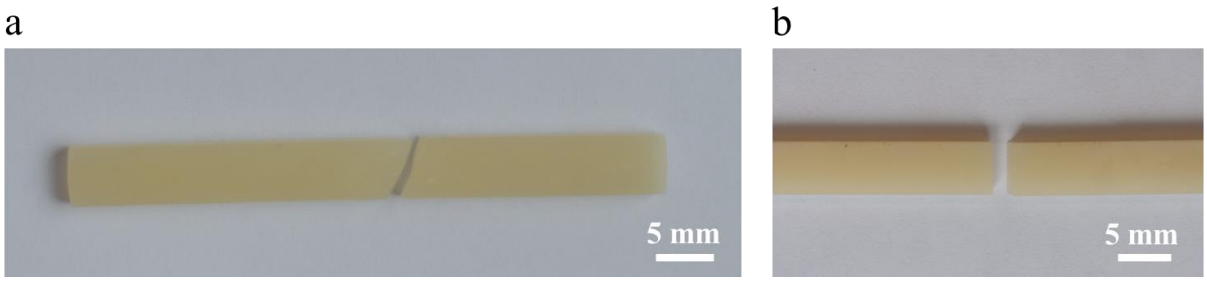

Figure 3.7 Repair process. **(a)** Fractured specimen. **(b)** Following successive grinding to remove damaged material and establish correct repair joint outline.

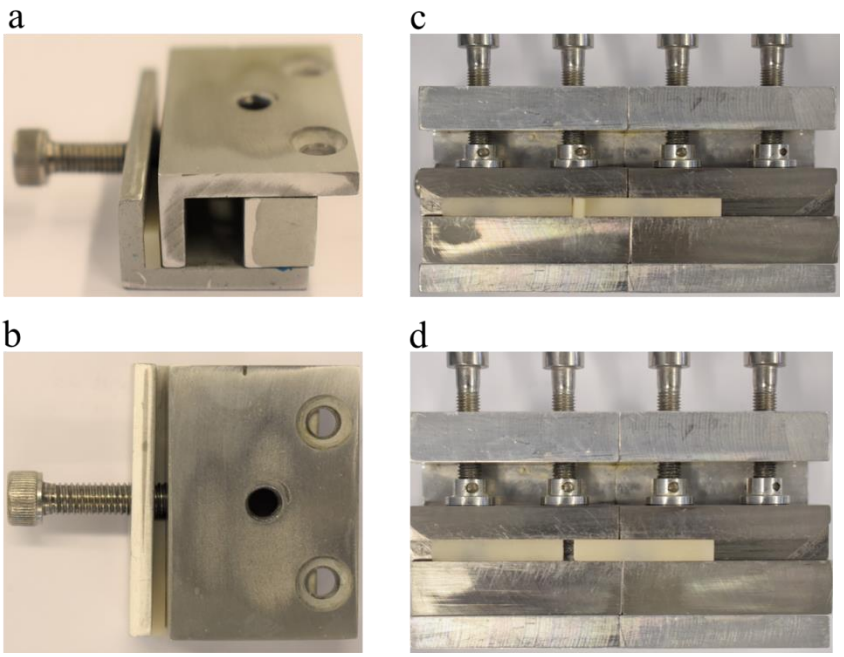

Figure 3.8 Test beam repair process. **(a)** Top view and **(b)** Lateral view of a grinding jig. **(c)** After a monolithic RBC beam had been tested, the fractured beams were returned to the mould with an interposed beam segment as a spacer to control the thickness of the joint. (**d)** After removal of the spacer, repair cavity ready for insertion of fresh RBC.

When the initial group of repaired specimens was examined under the light microscope, an overlap joint was noticed rather than an end-to-end interface (Figure 3.9a) (Primostar binocular, Zeiss group, Jena, Germany). The overlap was mainly on the top surface (tension surface) since the bottom surface was inside the mould slot. In order to remove the overlap and create an abut joint, the top surface was gently ground using silicon carbide papers (1000, 1200, and 2000 grit), under continuous water flow (Figure 3.9b).

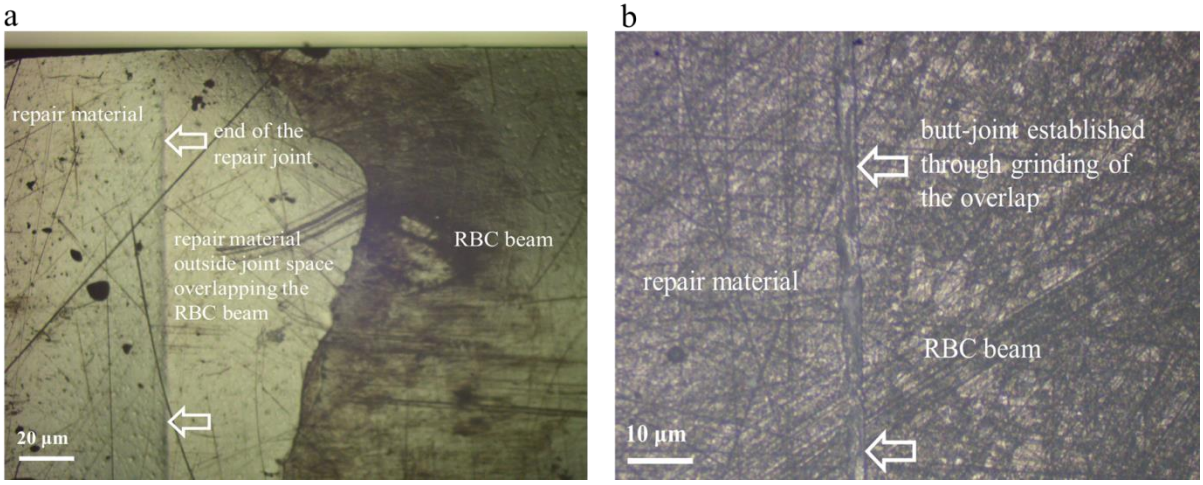

Figure 3.9 Correction of the overlap joint. **(a)** Overlap joint on the top surface (the tension surface). **(b)** Corrected joint geometry following successive grinding.

3.2.4 Preparation of dentine coupons

The proposed method of evaluation was also used to assess the static flexural strength of the dentine interface at an adhesive joint. Dentine slices bonded on either side to one of five 'adhesive' systems commonly employed were subjected to a symmetrical four-point bend (4pb) test as proposed by Mutluay *et al.* (2013) [21] and Sanli *et al.* (2015) [75]. Specimens were prepared from coronal dentine from human second and third molars. This study protocol was approved by the Ethics Committee for Research at the University of Birmingham. Teeth were donated anonymously under verbal consent to retain waste tissue (19/SW/0198 ethics code); those from individuals with known infective risks were not accepted. Teeth were collected into tubs containing a bacteriostatic solution (aqueous sodium azide, 15 mmol/L) (SKU: SBL-40-1999-01; Thistle Scientific, Uddingston, Glasgow). After collection from the clinic the teeth were washed in a circulating tap water bath for approximately 5 h, then stored at ~ -20 ºC until selected for use. The molar teeth were then mounted on clear epoxy resin discs (Epofix kit, Cat. No. 40200029, Struers) using green stick impression compound (Kerr Impression Compound; Spofadental, Jičín, Czech Republic). Teeth were sectioned transversely to obtain a slice around 3.0 mm thickness using a low-speed water-cooled blade (Isomet; Buehler, Lake Bluff, IL, USA). Secondary cuts were made mesiodistally and buccolingually followed by successive face grinding to obtain rectangular coupons from the mid-coronal dentine with nominal dimensions of 2.0 × 5.0 × 5 mm^3 (Figure 3.10). A device (Figure 3.11)

was used to hold the dentine coupons during grinding to aid in coplanarity of the two test surfaces. The dentine coupon was stuck to the sliding rod using a double-sided tape (Tesa 4946, 0.39 mm thick, 25 mm × 50 m, RS components, Corby, UK). Both the occlusal and pulpal surfaces were ground and polished, one at a time. Grinding was initiated by firmly holding on a rotating water lubricated disk (Grinder-polisher, Phoenix Beta, Buehler) using abrasive papers in the order of 1000, 1200, 2000 and 4000 grit. To avoid abrasive particles being carried over, coupons were washed and swabbed under running water using a cotton gauze at each stage. The coupons were then manually polished with a polishing paste (1 μm particle diameter, active oxide polishing suspension, DiaDuo-2; Struers), and again ultrasonically cleaned in deionized water for 10 mins. The coupons were stored in deionized water for no more than 48 h at room temperature and used at random. Figure 3.12 shows the various test groups investigated in the present study.

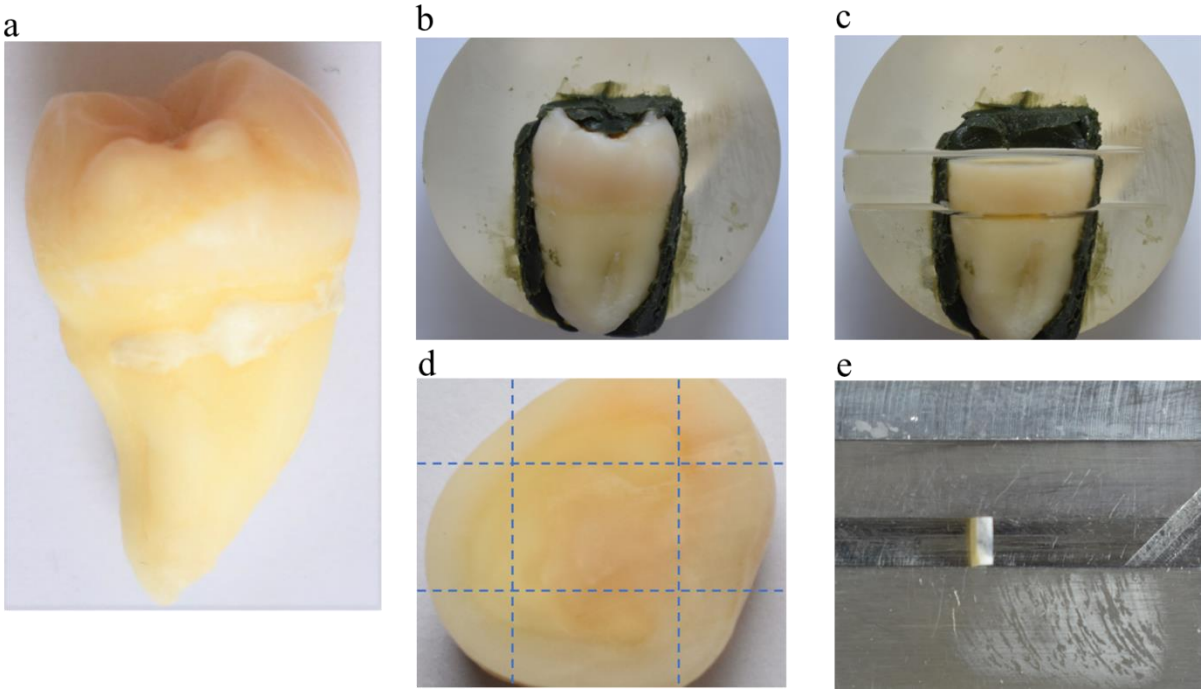

Figure 3.10 Preparation of dentine coupon. **(a)** Molar tooth. **(b)** Using impression compound the tooth was mounted on an epoxy resin disc. **(c)** Tooth slice. **(d)** Secondary cuts in buccolingual and mesiodistal directions. **(e)** Coupon in place in the mould.

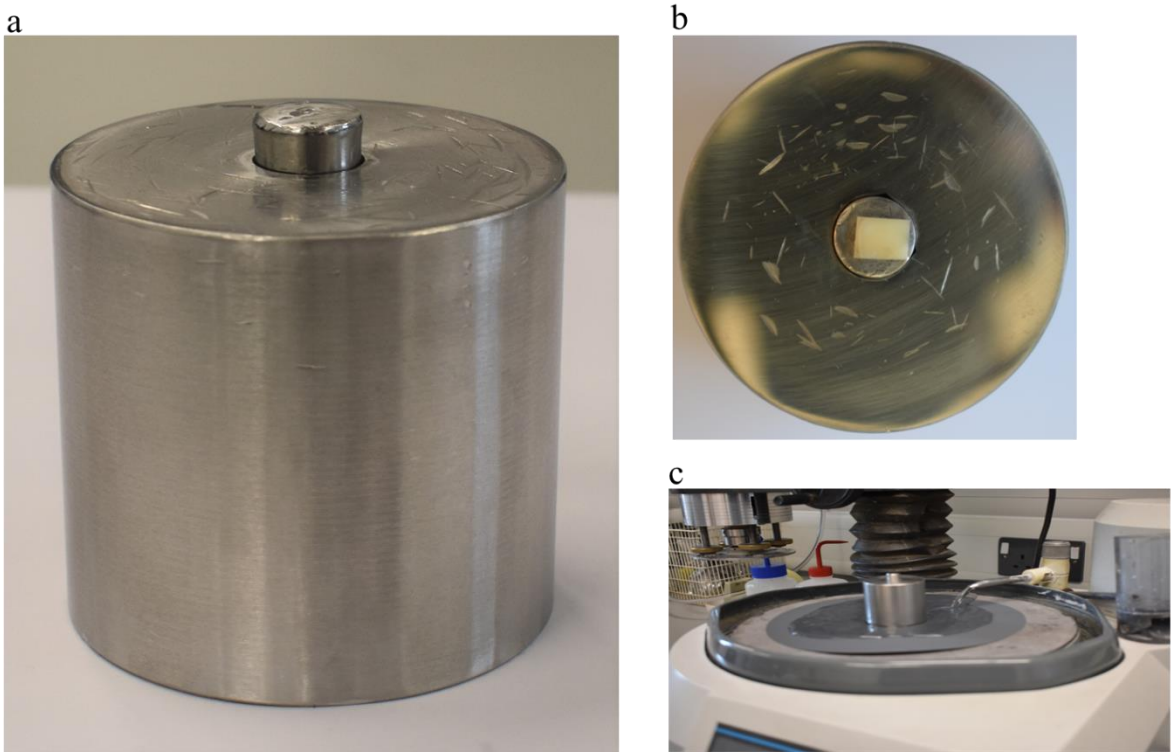

Figure 3.11 Dentine coupon grinding and surface finishing equipment. **(a)** Large metal cylinder with an inner sliding rod (bottom view). **(b)** Dentine coupon attached to the sliding rod (bottom view). **(c)** Grinder-polisher, showing assembly (b) in place.

Versatility of the method being taken as key to having many uses or applications, a range of adhesive systems that were investigated to assess that applicability as a matter of principle (Figure 3.12).

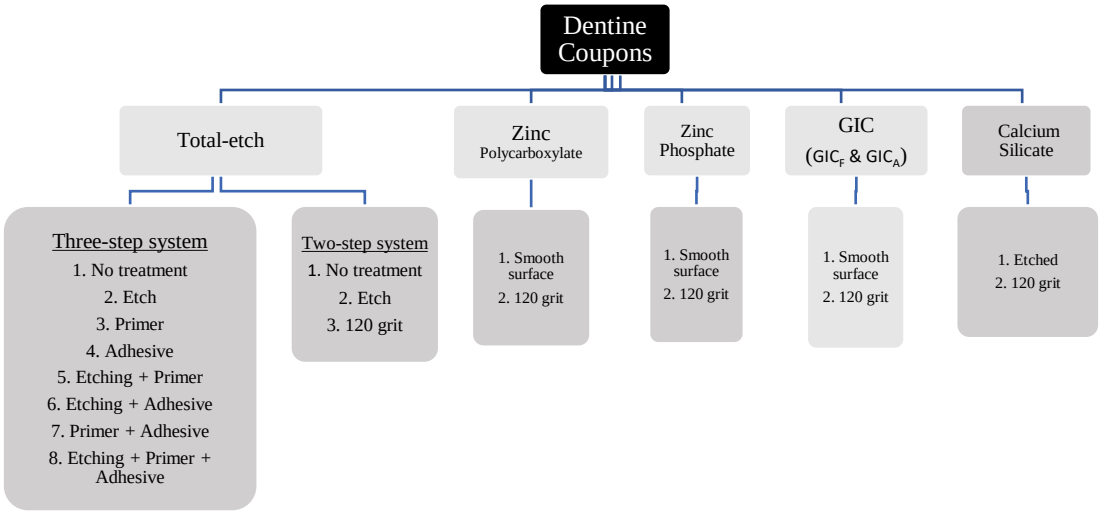

Figure 3.12 Test groups using the dentine coupons. To minimise the influence of mechanical retention, each system used a smooth and flat dentine surface (*i.e.*, no treatment) as a control group.

Bonded interface specimens were prepared by shaping the material within the manufacturers' stated working time using the stainless steel mould. A dentine coupon was placed in the mould slot and fixed in place with cap screws. The relevant test material was applied to the two opposing surfaces of each beam according to the manufacturer's recommendations. After filling the mould slot, an acetate strip was placed on the mould, a slight pressure was applied using glass microscope slide to make sure the surface was perfectly flat to aid in load distribution (Figure 3.13).

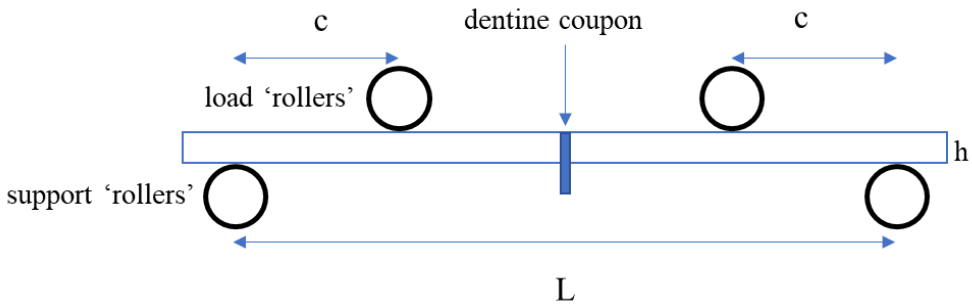

Figure 3.13 Test arrangement for bonded dentine coupon, centrally placed in pure bending region.

3.2.4.1 Zinc Phosphate Cement (ZPC)

The zinc phosphate powder was fluffed by shaking the bottle every time before use. Powder and liquid ratio was 5.6 g powder: 1.0 g liquid. To ensure the correct weight of the powder and liquid a cooled glass slab was placed on a scale (Fisherbrand analytical balances, 15987490, Fisher Scientific, Loughborough, UK). Then the powder and liquid were dispensed at the exact amount onto the glass slab. The powder was divided into three increments which were added to the liquid one by one at 30 s intervals and spatulated thoroughly (mixing time 90 s) ensuring that all the powder was incorporated into the liquid. The cement was then immediately applied to the mould slot on both sides of the dentine beam (working time 60 s).

3.2.4.2 Zinc Polycarboxylate Cement (ZCC)

As in 3.2.3.1, the powder and liquid (4.3 g powder: 1.4 g liquid) were dispensed onto a cooled glass slab which was placed on the scale. The powder was incorporated into the liquid in three increments at 10 s intervals and spatulated thoroughly using a stainless steel spatula (mixing time 30 s). The cement was then immediately applied to the mould slot on both bonding sides of the dentine beam (working time 60 s).

ZCC and ZPC specimens were stored for 60 min in a sealed container with a wet tissue alongside (not in contact) at room temperature (18 ~ 19 ºC) before testing.

3.2.4.3. Glass Ionomer Cement (GIC)

Two brands of GIC (powder and liquid, and anhydrous) were tested:

i. Fuji II Glass Ionomer (GIC_F)

The powder bottle was shaken three times before use each time. The powder and liquid, standard ratio 2.7 g: 1.0 g (1 level scoop of powder to 1 drop of liquid); were dispensed onto the pad which was placed on the scale to ensure the correct weight. The powder was divided into two halves. The first portion was mixed with the liquid for 10 s, then the remaining portion was incorporated and mixed for 20 s. The cement was transferred to mould slot using a plastic spatula. Specimens with visible voids or defects were discarded.

ii. Aquacem Glass Ionomer (GIC_A)

The powder bottle was inverted twice to counteract any settling of the powder every time before use. The scoop was overfilled with powder and the excess removed with the bottle insert leaving a flat surface level with the edge of the scoop (powder 3.4 g: 0.3 g liquid). The powder and liquid were dispensed onto the pad which was placed on the scale to ensure the correct weight. The powder was divided into two halves. Two drops of water were dispensed by holding the bottle vertically and squeezing gently. One half was added to the water and mixed for 15 s. Then the second half was incorporated, then mixed thoroughly for 15 s. The mix was transferred to mould slot using a plastic spatula (working time 2 min 30 s from the start of mixing).

Specimens for GIC were stored for 24 h in a sealed container with a wet tissue alongside (not in contact) at room temperature (18 ~ 19 ºC) before testing.

3.2.4.4. Calcium Silicate Cement

Biodentine (BD) was prepared according to manufacturer's instructions. A capsule was gently tapped on a hard surface to loosen the powder (powder 0.75 g: 0.2 g liquid). The capsule was kept upright on a capsule-stand, then the capsule was removed. Holding vertically, a pipette was squeezed and pressure maintained until five drops were dispensed into the capsule. Then the capsule cap was replaced and placed on the mixing device (Septodont, St Maur des Fosses, France) for 30 s (4000 - 4200 rpm). The mix was then transferred to the mould using a plastic spatula on each side of the dentine coupon.

BD specimens were left for 60 min to develop initial strength, then were stored in a sealed container with a wet tissue at room temperature (18 ~ 19 ºC) for 1 wk.

3.2.4.5 Total-etch bonding systems

i. Three-step total-etch system - Scotchbond Multi-Purpose (ASP)

Specimen preparation

A smooth dentine surface (1 μm finish, section 3.2.4) was created as described in Section 3.2.4 An adhesive tape was used to define the boundaries of the bonding area. In order to strictly control the size of bonding area the tape was used to expose the exact height of the

dentine coupon, *i.e.*, specimen thickness of 2.0 mm, and prevent the involvement of distant areas in the adhesive joint. The calliper gauge was used to measure 2 mm of the height of the dentine coupon, then a pencil was used to lightly mark the measurement. A transparent polypropylene tape (25 mm × 66 m clear general purpose packaging tape; Kite Packaging, Coventry, England) was applied just off the mark. Due to the transparency of the tape, its application before the pencil mark was easier to control along the boundary line. Two quick coats of a separating agent (Very Special Separator Pen, 15 mL, Dental Ventures of America, Corona, CA, USA) was applied to the mould slot around the adhesive joint location, and left to set for 2-3 mins. Dentine coupons were then placed in the mould slot and fixed in using cap screws. Specimens were fabricated by extruding the RBC material (Z250) from the supply syringe into the stainless steel mould. Z250 was used because as it is compatible with the three-step total-etch multi-purpose system (same manufacturer), and it is widely used in dental literature and in many instances as a control group. The top surface of the specimens was prepared against a transparent acetate strip to avoid preparation surface defects that might influence the crack nucleation sites. A bench-top hand press was used to press the samples for 60 s under moderate pressure. Specimens were then light-cured and immediately retrieved from the SS mould, then carried on a glass-slide to be placed onto the flexure jig (Figure 3.14 c). The specimen was then stressed up to measure the force required to fracture the beam (Figure 3.14 d) which was used to calculate the flexural strength using Equation [2] (Section 3.1). This process was common to all test groups following the treatments described below. Three-step total-etch multi-purpose was used, a three-factor experiment was designed resulting in eight groups as follows:

a. No treatment (N): nothing further was done in the preparation of the dentine coupon (Section 3.2.4), and RBC was then applied as described above.
b. Etching (alone) (Scotchbond Universal Etching Gel) (E): Prior to the application of the RBC, the EG was applied to the exposed dentine surface on both sides simultaneously and allowed to react for 15 s. Since the etchant was not easy to wash off, it was rinsed thoroughly for 15 s under running tap water, then washed with DiW water for 5 s. Excess water was removed leaving the surface moist using paper towels, *i.e.*, avoiding excessive drying. RBC was then applied.
c. ASP (Adper Scotchbond Multi-Purpose Primer) (P) only: The dentine coupon was held using metallic tweezers from the sides (Figure 3.15). Prior to the application of the RBC, the primer was applied using a brush to both sides of the dentine and gently dried

with air for 5 s, *i.e.*, until the surface appeared shiny. Excess material (due to primer flowing beyond the boundary and also being spread by air-thinning) around the borders, *i.e.*, on sides and bottom surfaces, was removed using small disposable brushes.

d. ASA (Adper Scotchbond Multi-Purpose Adhesive) (A) only: Prior to the application of the RBC, the adhesive was applied using a brush and gently thinned with air for 5 s. Excess material (due to adhesive flowing beyond the boundary and also being spread by air-thinning) around the borders, i.e., on sides and bottom surfaces, was removed using small disposable brushes. The adhesive was then light cured for 10 s.

e. Etching + Primer (E+P): The etching was applied first as in (b) and then followed by the primer as in (c), in that order.
f. Etching + Adhesive (E+A): The etching was applied first as in (b) and then followed by the adhesive as in (d), in that order.
g. Primer + Adhesive (P+A): The primer was applied first as in as in (c) and then followed by the adhesive as in (d), in that order.
h. Etching + Primer + Adhesive (E+P+A): The etching was applied first as in (b), then the primer as in (c), and followed by the adhesive as in (d), in that order.

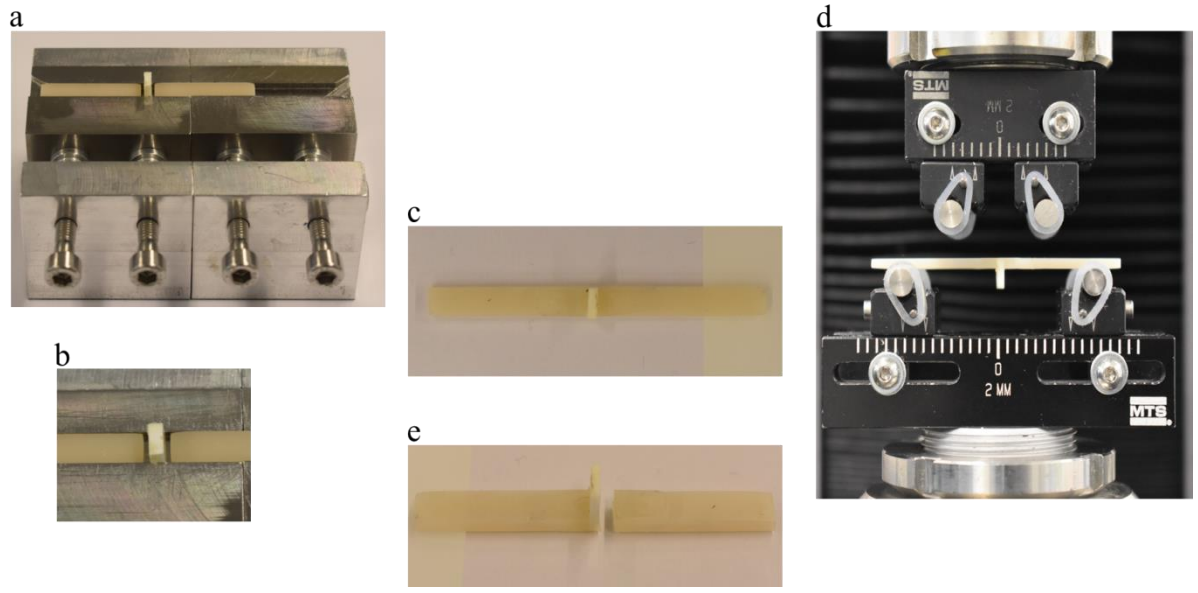

Figure 3.14 Test procedure for bonded dentine coupons. **(a)** Dentine coupon in place between RBC beams before fresh RBC is added. **(b)** Close-up of (a). **(c)** Specimen carried on a glass slide to be placed on the flexure test jig. **(d)** Specimen in place for testing. **(e)** Specimen after fracture.

One pair of RBC beams was used throughout the preparation of three-step total-etch system specimens. The aim was to conserve materials and reduce expense as well as to improve the efficiency of the method. After specimen fracture, both beams were ground using 1000 grit silicon carbide papers to remove the damaged part, then create an oblique surface with greater surface area (thus a relatively thicker and stronger repair joint) (Figure 3.16), and then replaced in the mould. Fresh RBC was then added to establish interfacial joint of the next specimen (Figure 3.16, a and b).

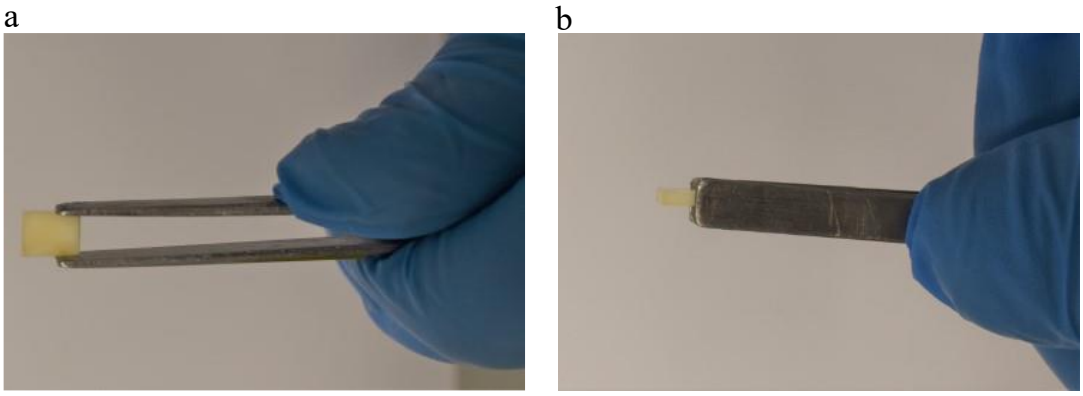

Figure 3.15 Dentine coupon held during the application of total-etch bonding systems. **(a)** top view. **(b)** side view.

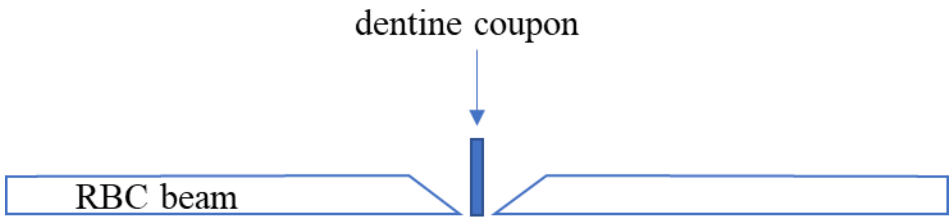

Figure 3.16 Positioning of RBC beams with respect to the dentine coupon after grinding prior to repair material being added.

The excess protrusion of the dentine coupon helped in preventing overlap at the adhesive joint, *i.e.*, making sure that it was a butt joint and that the interfacial bonding surface

area was well defined. The key to a square-cut quality butt joint was to stop the seepage of Etching, Primer, and Adhesive outside the joint boundary, and also to control the application of RBC within the markings. The polypropylene tape limited the fluid seepage and dentine protrusion stopped RBC spread over dentine which might happen if a similar height to the adjacent RBC beams was employed. The projection was then on the bottom (tension side) during the bending test. There was minimal excess (flash) at the upper surface periphery which was carefully removed while the specimens were still tightened in the mould.

ii. Two-step total-etch Adper Scotchbond 1 XT (ASX)

Two-step total-etch multi-purpose (Adper Scotchbond 1 XT, 3M ESPE) was tested. Three groups were prepared:

a. Adhesive only (A)
b. Etching + Adhesive (E+A)
c. 120-grit abrasive paper (G) + Adhesive

Procedures otherwise similar to those above.

3.2.5 Zirconia (ZrO_2)

ZrO_2 blocks (IPS e.max ZirCAD; Ivoclar Vivadent, for inLab, Bridge B 65, Schaan Liechtenstein) were cut with a low-speed diamond blade under water cooling (Isomet 1000; Buehler) to give bars with the dimensions of 26.20 L × 6.35 W × 2.60 H mm.

Sintering was done according to the manufacturer's standard program for IPS e.max ZirCAD up to 14 units [85] (Table 3.2)**.** The flexural strength of ZrO_2 bodies is significantly influenced by the various sintering temperatures and holding times [86]. Raising sintering temperature and prolonging the holding time can improve the microstructure by increasing densification, and by reduction of defects at grain boundaries [86].

Table 3.2 Standard sintering program for IPS e.max ZirCAD, according to the manufacturer (Ivoclar-Vivadent) [85].

	Temperature 1 / °C	**Temperature 2 / °C**	**Heating or Cooling rate / °C.min^{-1}**	**Holding time / min**
Heating phase	20	900	10	88
Holding phase	900	900	–	30
Heating phase	900	1500	3.3	182
Holding phase	1500	1500	--	120
Cooling phase	1500	900	–10	60
Cooling phase	900	300	–8.3	60
--Switch off--				

The final dimensions after sintering shrinkage were exactly 20.0 L × 5.0 W × 2.0 T mm. The ZrO_2 bars were then ultrasonically cleaned (Vitasonic II; Vita) for 15 min each in 96% ethanol and deionized water to remove particulate debris immediately before surface treatment.

The effect of mechanical *versus* chemical surface roughening on the bonding of luting resin cements to zirconia was investigated in a three-way design; where the independent variables were: adhesive material × grit blasting (alumina particle air abrasion) × etching (Figure 3.17).

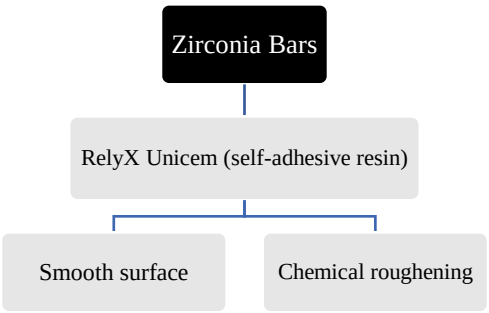

Figure 3.17 Zirconia test groups.

The etching process was as follows [87]. Potassium hydrogen fluoride, KHF_2 (455830-25G; Sigma-Aldrich, Missouri, USA) was ground to fine powder in an agate mortar. A 40 mg of the powder was mixed with deionized water (10 mL) to a viscous slurry (~4.0 mg/mL), and then applied to bonding surfaces. The specimens with KHF_2 slurry were placed on an aluminium foil (REO-FL-000114; GoodFellow Cambridge, Huntingdon, England) and placed in a preheated furnace at a temperature of 280 °C for 10 min. The aluminium foil with the specimens was then removed from the oven and bench-cooled. Specimens were ultrasonically rinsed in for 15 min each in ethanol then in DiW, and dried in air [87].

The ZrO_2 bars were luted end-to-end on the prepared surfaces with one of self-adhesive luting resin (RelyX Unicem 2 Automix, 3M ESPE). A custom-made stainless steel mould was used to standardise the luting material thickness to ~0.10 mm [75]. Specimens were placed in the mould end-to-end having applied the cement to one end of each using a dispenser syringe, the mould's screws were tightened to approximate the pieces and decrease the cement gap thickness to the target value, as indicated by the separation of the mould faces. A 4 mm gap between the mould's approximating faces was left to allow for the removal of excess cement. The gap enabled the excess cement removal from the sides, top and bottom surfaces of the beams before light curing to avoid the formation of overlap joint.

3.3 Test system compliance calibration

To determine the displacement of the specimen, the contribution due to the compliance of the load train (which includes the load frame) and flexure test rig was subtracted from the measured cross-head displacement (XHD) [88].

Displacement of the load train was recorded in a compression test. Compression platens were cleaned and well aligned, and then loaded against each other (Figure 3.18) up to around 4000 N.

Figure 3.18 Arrangement for determining the machine compliance: compression loading of flat platens. **(A and F)** standard Clevis adaptors (has female inside). **(B and G)** Clevis pin (male). **(C)** universal grip joint**. (D and E)** Bionex stainless steel compression platens [89].

Displacement of the flexure test jig was measured through aligning the load and support rollers in parallel. A dummy hardened steel disc, assuming its compliance was negligible, was installed (Figure 3.19) on the flexure test jig and loaded to 470 N.

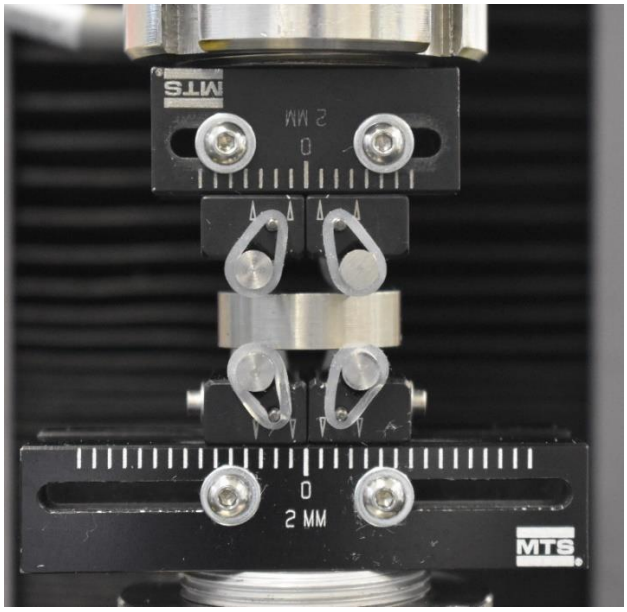

Figure 3.19 Arrangement for determining the flexure test rig compliance: compression loading of dummy steel specimen with rollers vertically aligned.

$D_{\text{rig displacement}} = \text{Slope}_{\text{rig}} \times \text{Load at fracture}$

$D_{\text{specimen displacement}} = D_{\text{total displacement}} - D_{\text{rig displacement}}$

3.4 Fractography

Fractographic analyses were carried out on surface-treated adherends and adhesive fracture surfaces. The fracture surfaces were initially examined using a light microscope to identify the fracture origin and fracture features such as hackle and curl, allowing the mapping of the direction of crack propagation. Both failure surfaces were examined; this was carried out randomly on half of the specimens used in the above bond strength tests (three-step total-etch group). Fracture origins and flaws in ceramics and glasses can often be detected with the stereoptical microscope, but higher magnifications are often needed to see the flaw more clearly.

If the specimen being analysed was nonconductive (*e.g.,* RBCs and dentine surfaces), a gold coating (5 - 20 nm) was applied to the surface of the specimen by means of a sputter coater (Emitech K550X, LabTech, London, England).

3.4.1 Scanning electron microscopy (SEM)

3.4.1.1 Three-step total-etch

SEM specimens should be dry. Fracture surfaces (dentine coupon and RBC beams) were kept in a desiccator (DES0004, 240 × 330 mm, Nottingham, England) for a minimum of 24 h. The desiccator contained a desiccant substance *i.e.,* silica gel, and an inert gas (Argon) that was introduced as soon as the cover was placed. Fractured surfaces were viewed to see the whole fracture surface and also to obtain a detailed high magnification image.

Conductive carbon adhesive (8 mm × 20 m double-sided tape, Nisshin EM, Sakaiminato, Japan) was used to bond specimens onto aluminium stubs. The dentine coupon size enabled mounting on the aluminium stubs without further cutting, however, RBC beams were ground to within 10 mm of the fracture surface. Specimens were mounted such that the fracture surface was approximately perpendicular to the incident beam. The scanning electron microscope (EVO MA10-1592; Carl Zeiss, Cambridge, UK), operated using the secondary electron mode, at an accelerating voltage of 10 kV, was used to obtain micrographs of the fracture surfaces at various magnifications (working distance of 35 - 33 mm for the whole fracture surface and 7 – 8 mm for the high magnification).

3.4.2 Energy-Dispersive Spectroscopy (EDS)

3.4.2.1 Glass ionomer *vs.* Zinc polycarboxylate cements

The EDS analysis was used to investigate the chemical bonding potential of GICs and ZCC to smooth surface stainless steel. SEM-EDX was used to identify the elemental composition of the fracture surface, followed by quantitative analysis to determine how much of each was present.

The stainless steel strip was ultrasonically cleaned for ten min in 96% ethanol and then in deionized water for 15 min to remove contaminants, then left over the bench for 60 min to dry. Firstly, the chemical composition of the stainless steel was analyzed by EDX before applying the cements. The SS surface (smooth finish) was not subject to any treatment. GIC and ZCC were applied to the SS surface and left for 60 min at room temperature. The cements were then gently debonded at the cement margin using a surgical blade. This aided in the

confirmation of a visually-assessed failure, *e.g.*, whether cohesive in the adhesive or interfacial fracture [90].

3.5 Statistical analysis

Raw data of flexural strength was subjected to checks for normality (Shapiro-Wilk) and homogeneity of variance (Brown-Forsythe). Bond strengths were subjected to three-way analysis of variance (three-way AoV), one-way analysis of variance (one-way AoV) and Student's *t*-test (SigmaPlot 15, Systat Software, San Jose, CA, USA), as appropriate. Log transformation was used to stabilize the variance between materials and groups. The critical value was set at $\alpha = 0.05$.

4. Results

4.1 Flexural strength (4pb)

The corrected flexural strength values (Section 3.1) were used for all graphical and statistical work; the uncorrected values are shown in graphs for comparison.

4.1.1 Monolithic bars

4.1.1.1 High viscosity RBCs

The flexural strength results of the four-point bend specimens are given in Table 4.1 and Figure 4.1. The raw data are given in Appendix 2, Tables 1, 2 and 4. The log-transformed data were analysed using one-way analysis of variance (1×AoV). The flexural strengths differed significantly ($P = 1.22 \times 10^{-11}$) (Table 4.2).

Table 4.1 Flexural strengths by four-point bend of monolithic RBC bars; FS: simple, FS*: corrected (Equation 2, Section 3.1), sd: standard deviation, CoV: coefficient of variation. (FB: Filtek One Bulk-Fill, BB: Beautifil Bulk, TEC: Tetric Evoceram, hp: hand-pressed. Section 3.2.2.1)

RBC type	Flexural Strength / MPa (mean ± sd)		CoV%		Number of specimens
	FS	FS*	FS	FS*	
FB	77.70 ± 4.47	74.49 ± 3.25	5.75	4.37	14
BB_{hp}	53.33 ± 7.88	52.16 ± 7.80	14.78	14.95	11
TEC	61.78 ± 4.18	60.67 ± 4.01	6.76	6.61	9

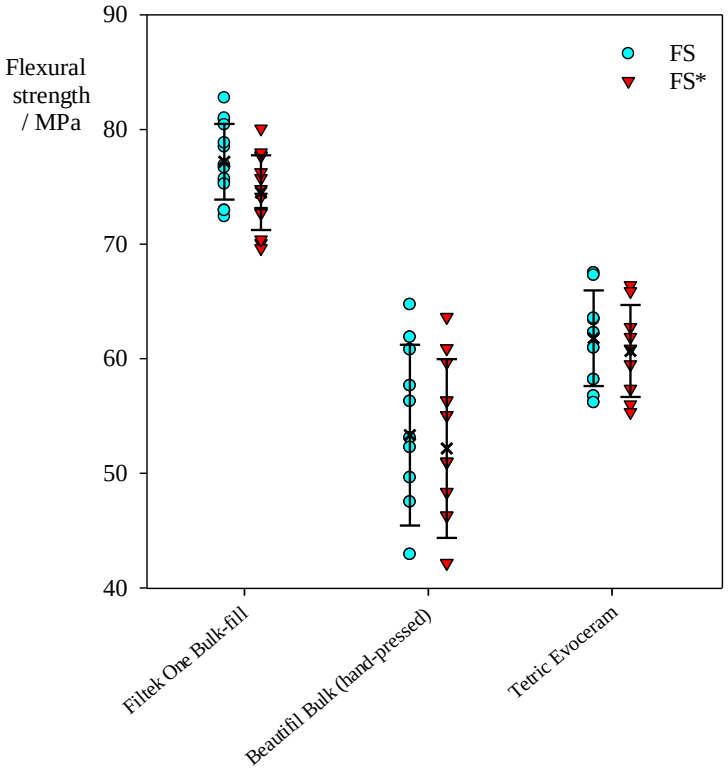

Figure 4.1 Flexural strength of high-viscosity RBCs. Error bars indicate mean and standard deviation. In each set, the left-hand array is for the simple calculation (FS), the right-hand is corrected (FS*).

Table 4.2 One-way analysis of variance of four-point bend strength: monolithic bars. df: degrees of freedom, SS: sum of squares, MS: mean sum of squares, *F*: *F* ratio, P: *F*-ratio significance probability.

Source of Variation	SS	df	MS	F	P	F_{crit}
Between Groups	3666.542	2	1833.271	62.92969	1.22×10^{-11}	3.305
Within Groups	903.094	31	29.132			
Total	4569.636	33				

4.1.1.2 Filtek Flowable Bulk-Fill (FF)

The specimens were hand pressed for only 10 s (high viscosity for 60 s) due to ease of flow. The results for the modified specimen length and test span yielded a better (smaller)

spread of data (CoV = 3.57 MPa), suggesting either that the ≈100% additional material of the 50 mm specimens beyond the supports on each side influenced the failure stress, or alternatively – and more likely – that the shorter span was intrinsically more reliable. The results of the four-point bend test are given in Table 4.3 and Figure 4.2. The raw data are given in Appendix 2, Tables 5 and 6. The log-transformed data (FS*) were analysed through a *t*-test. The difference was non-significant ($t = -1.67$, df = 19; P = 0.12).

Table 4.3 Flexural strengths by four-point bend of monolithic RBC bars; FS: simple, FS*: corrected (Equation 2, Section 3.1), sd: standard deviation, CoV: coefficient of variation. (FF: Filtek Flowable Bulk-Fill).

Specimen length / mm	Flexural Strength / MPa (mean ± sd)		CoV%		Number of specimens
	FS	FS*	FS	FS*	
50	134.79 ± 19.92	127.32 ± 18.13	14.78	14.24	10
28	145.19 ± 5.18	137.26 ± 4.88	3.57	3.55	11

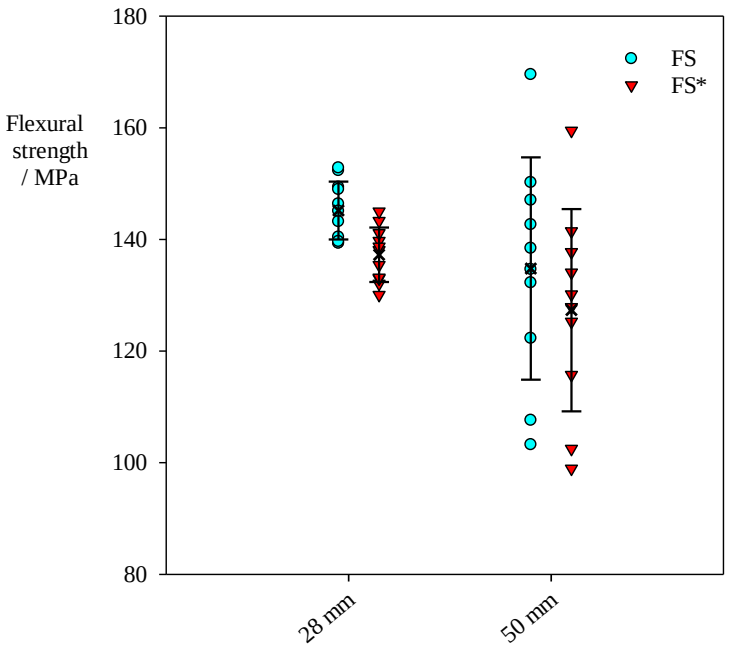

Figure 4.2 Flexural strength of low-viscosity RBC.

4.1.1.3 Hand pressed (hp) *vs.* constant load (cl) preparation (BB)

The flexural bond strength results for Beautifil bulk-fill (BB) bars prepared using the two mould-packing techniques are shown in Table 4.4 and Figure 4.3. The raw data are given in Appendix 2 Tables 2 and 3. The log-transformed data (FS*) were analysed through a *t*-test; this showed that during specimen preparation the application of constant load had a significant effect enhancing resin flow (before curing) and the subsequent adaptation causing a significant improvement on the flexural bond strength ($P = 2.25 \times 10^{-6}$) (Table 4.4).

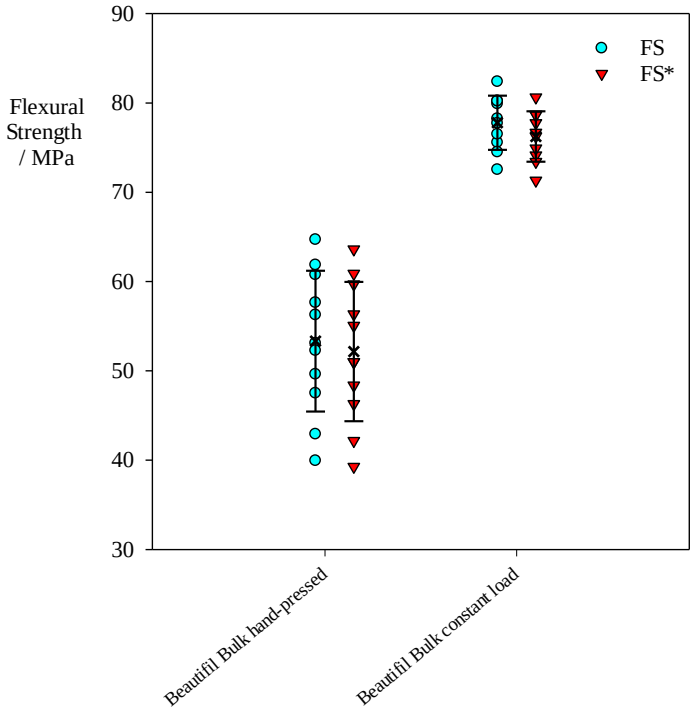

Figure 4.3 Flexural strength (MPa) of hand-pressed (hp) *vs.* constant load (cl) BB bars.

Table 4.4 Flexural strengths by four-point bend of hand-pressed (hp) *vs.* constant load (cl) preparation for BB bars; FS: simple, FS*: corrected (Equation 2, Section 3.1), sd: standard deviation, CoV: coefficient of variation. (BB: Beautifil Bulk-Fill).

Method	Flexural Strength / MPa (mean ± sd)		CoV%		Number of specimens
	FS	FS*	FS	FS*	
Hand-pressed	53.33 ± 7.88	52.16 ± 7.80	14.78	14.94	11
Constant load	77.79 ± 3.03	76.25 ± 2.83	3.89	3.71	10

4.1.2 Monolithic *vs*. repaired (Filtek One bulk-fill) (FB)

The mean flexural bond strength of monolithic bars was around seven times the value of the repaired bond strength. The results for the flexural bond strength of monolithic bars and after their repair are shown in Table 4.5 and Figure 4.4. The raw data are given in Appendix 3, Table 1 and 2. The log-transformed data were analysed using one-way×AoV. The flexural strengths of the overlap- and butt- joints differed significantly ($P = 1.4 \times 10^{-3}$), implying that joint geometry is an important parameter.

Table 4.5 Flexural strengths by four-point bend by four-point bend of monolithic *vs*. repaired FB bars; FS: simple, FS*: corrected (Equation 2, Section 3.1), sd: standard deviation, CoV: coefficient of variation. (FB: Filtek One Bulk-Fill).

Condition	Flexural Strength / MPa (mean ± sd)		CoV%		Number of specimens
	FS	FS*	FS	FS*	
Monolithic	77.70 ± 4.47	76.24 ± 3.02	5.75	3.96	14
Overlap joint	22.53 ± 3.55	22.06 ± 3.47	15.53	15.50	8
Butt joint	11.11 ± 3.64	10.85 ± 3.57	32.75	32.90	11

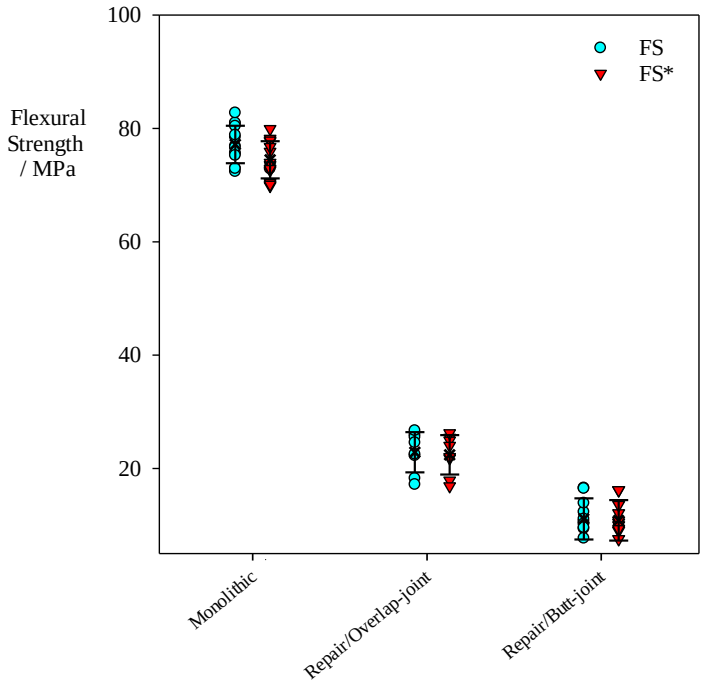

Figure 4.4 Flexural strength of monolithic *vs*. repaired Filtek One Bulk-fill bars.

4.1.3 Bond to dentine coupons

4.1.3.1 Conventional cements

i. Zinc Phosphate Cement (ZPC)

For a smooth dentine surface (1 µm finish, section 3.2.4), specimens could not be retrieved from the mould without breakage, all due to adhesive failures, *i.e.*, the adhesive joint was too weak to be tested. When the dentine surface was roughened using 120 grit abrasive paper (120 grit is ~120 µm particle size, therefore, the expected scratch would be of the order of ≤ 50 µm), ZPC showed both cohesive and adhesive failures but no flexural strength data could be obtained, *i.e.*, the 4pb could not be performed. Some specimens still broke adhesively upon attempted retrieval from the mould (Figure 4.5a), while the others could successively be retrieved (Figure 4.5b) but broke adhesively/cohesively upon flash removal. Table 4.6 and Figure 4.6 show the cohesive bond strength data for monolithic ZPC bars. The raw data are given in Appendix 4 Table 1.

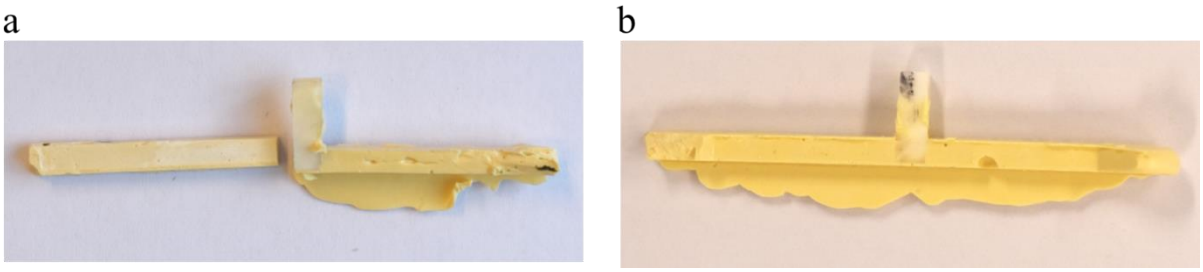

Figure 4.5 ZPC specimens. **a:** specimen broke adhesively upon retrieval from the mould. **b:** specimen was successively retrieved from the mould but broke cohesively/adhesively upon removal of the excess flash.

Table 4.6 Cohesive strengths of monolithic ZPC bars, FS: simple, FS*: corrected (Equation 2, Section 3.1), sd: standard deviation, CoV: coefficient of variation. (ZPC: Zinc Phosphate Cement).

Cement	Flexural Strength / MPa (mean ± sd)		CoV%		Number of specimens
	FS	FS*	FS	FS*	
ZPC	2.03 ± 0.49	2.00 ± 0.48	24.21	24.01	5

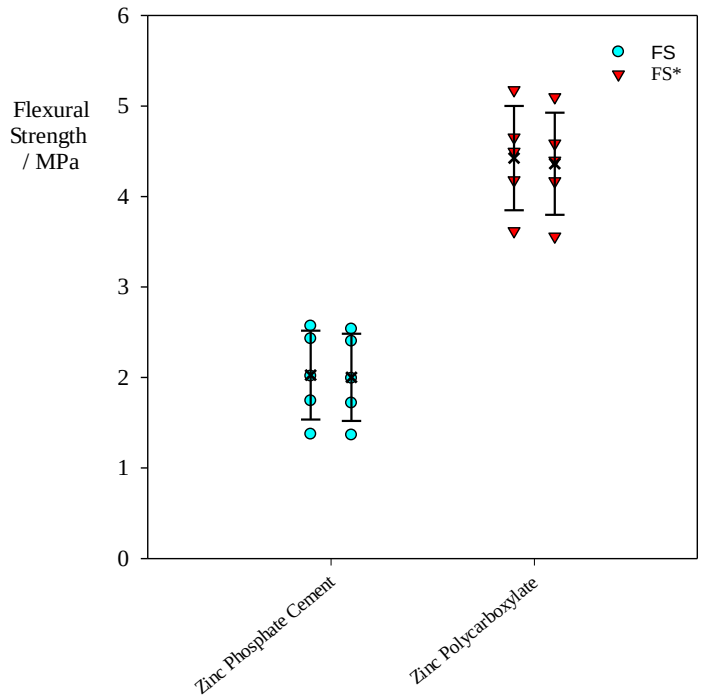

Figure 4.6 Cohesive strength of ZPC and ZCC.

ii. Zinc Polycarboxylate (ZCC)

The adhesive bond to dentine survived (after 60 min at ~18 - 19 ºC) to be tested, the fracture being cohesive (Table 4.7, Figure 4.6). In other words, the interfacial bond formed between the ZCC and dentine, both smooth (1 µm finish, section 3.2.4) and rough (120 grit is ~120 µm particle size, therefore, the expected scratch would be of the order of ≤ 50 µm), was stronger than the cohesive strength of the cement. Similar results were obtained when bonding ZCC to stainless steel (SS) (smooth and rough). The raw data are given in Appendix 4, Table 2.

Table 4.7 Cohesive strengths of monolithic ZCC bars, FS: simple, FS*: corrected (Equation 2, Section 3.1), sd: standard deviation, CoV: coefficient of variation. (ZPC: Zinc Polycarboxylate Cement).

Cement	Flexural Strength / MPa (mean ± sd)		CoV%		Number of specimens
	FS	FS*	FS	FS*	
ZCC	4.42 ± 0.58	4.36 ± 0.56	12.94	12.32	5

iii. Glass Ionomer Cement (GIC)

a. Fuji II (GIC_F)

When GIC_F was applied to the various substrates (dentine, stainless steel (SS), aluminium alloy (AA)), whether with smooth or rough surfaces, the specimens fractured adhesively upon attempted retrieval from the mould, *i.e.*, the interfacial bond strength was very low. No test values could be obtained. Figure 4.7 shows that GIC_F left almost no residual material on smooth surface SS in a visual check.

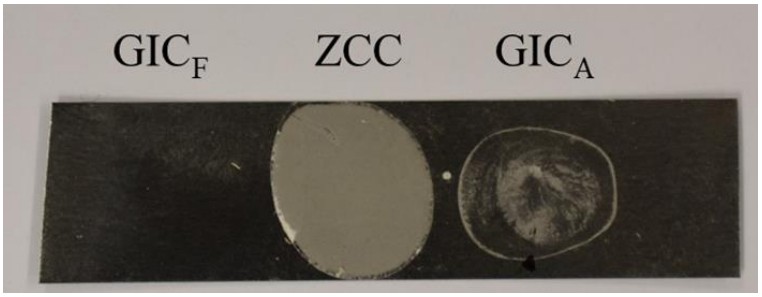

Figure 4.7 Residual of Glass Ionomer Cement (Fuji II), Zinc polycarboxylate and Glass Ionomer Cement (Aquacem) on smooth surface stainless steel (SS) (after 60 min at ~18 - 19 ºC). While GIC$_F$ had almost no residuals on SS, (GIC$_A$) had less homogeneous residuum compared with ZCC.

b. Aquacem (GIC$_A$)

Table 4.8 and Figure 4.8 show the adhesive bond strength of GIC$_F$ (Fuji II) to the dentine coupon and smooth stainless steel (SS). A *t*-test showed a significant difference between the bond strengths to dentine and stainless steel (P = 0.0057). The raw data are given in Appendix 5, Tables 1 and 2.

Table 4.8 Adhesive strength of GIC$_A$, FS: simple, FS*: corrected (Equation 2, Section 3.1), sd: standard deviation, CoV: coefficient of variation. (GIC$_A$: Aquacem, SS: stainless steel).

Cement	Flexural Strength / MPa (mean ± sd)		CoV%		Number of specimens
	FS	FS*	FS	FS*	
Dentine	0.18 ± 0.05	0.17 ± 0.04	25.92	24.92	5
SS	0.37 ± 0.10	0.37 ± 0.10	28.17	27.95	5

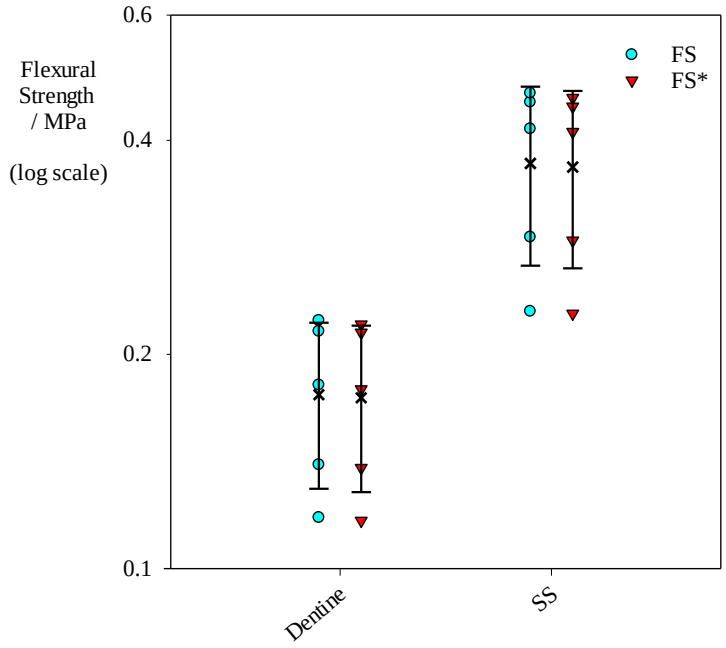

Figure 4.8 Adhesive strength of Glass Ionomer Cement (Aquacem) to smooth surface dentine and stainless steel.

iv. Calcium Silicate

When Biodentine (BD) was bonded to dentine coupons, whether with smooth (1 µm finish, section 3.2.4) or rough (acid-etched or 120 grit) surfaces (120 grit is ~120 µm particle size, therefore, the expected scratch would be of the order of ≤ 50 µm), the specimens fractured adhesively upon attempted retrieval from the mould (60 min, n = 3; 1 wk, n = 3) (~18 – 19 °C, ~90% RH). No test results were obtained.

4.1.3.2 Total-etch bonding systems

i. Three-step total-etch (Adper Scotchbond Multi-purpose)

The flexural strength results are given in Table 4.9 and Figure 4.9. The raw data are given in Appendix 7. For the three-way AoV, although the data passed the normality test (P = 0.14), they failed the equal variance ($p < 0.05$). This is a common finding associated with strength measurements [75]. In consequence, the data were transformed by taking logarithms and the analysis was repeated. Both normality (P = 0.14) and homogeneity of variance (P =

0.07) tests were then passed. The raw results of the statistical analysis (three-way AoV) is given in Appendix 7.

All two-way ($P < 10^{-5}$) and the three-way interaction ($P = 0.037$) between the effects of Etch, Primer and Adhesive (Table 4.10) were statistically-significant. This means that the effect of one factor is not consistent at all combinations of the two other factors, that is, the effects are not additive, and therefore an unambiguous interpretation of the main effects is not possible.

The flexural strengths of all subgroups were significantly different from each other (Table 4.10). The raw data are given in Appendix 7 Table 1-8. It can be observed that all treatments were significantly better than untreated smooth surface, suggesting a combination of mechanical and chemical means of retention. When the adhesive was added to an etched and primed dentine coupon, the difference in flexural strength was statistically insignificant ($P = 0.859$). Also, there was a statistically insignificant difference ($P = 0.696$) between the flexural strength of etched only and primed only groups.

A total of four premature failures were encountered in the N group only, these were not included in the analysis.

Table 4.9 Flexural strengths for three-step total-etch, FS: simple, FS*: corrected (Equation 2, Section 3.1), sd: standard deviation, CoV: coefficient of variation.

Adper Scotchbond Multipurpose	Flexural Strength / MPa (mean ± sd)		CoV%		Number of specimens
	FS	FS*	FS	FS*	
N	1.38 ± 0.56	1.38 ± 0.56	48.00	40.96	5
E	9.48 ± 1.82	9.39 ± 1.78	19.20	18.99	8
P	9.82 ± 0.89	9.73 ± 0.88	9.03	9.07	5
A	5.10 ± 0.73	5.06 ± 0.73	14.34	14.36	5
E+P	21.24 ± 2.63	21.03 ± 2.63	12.37	12.51	7
E+A	12.89 ± 1.56	12.80 ± 1.53	12.10	11.98	5
P+A	17.57 ± 3.12	17.16 ± 3.03	17.75	17.63	11
E+P+A	21.31 ± 3.96	20.84 ± 3.93	18.57	18.84	10

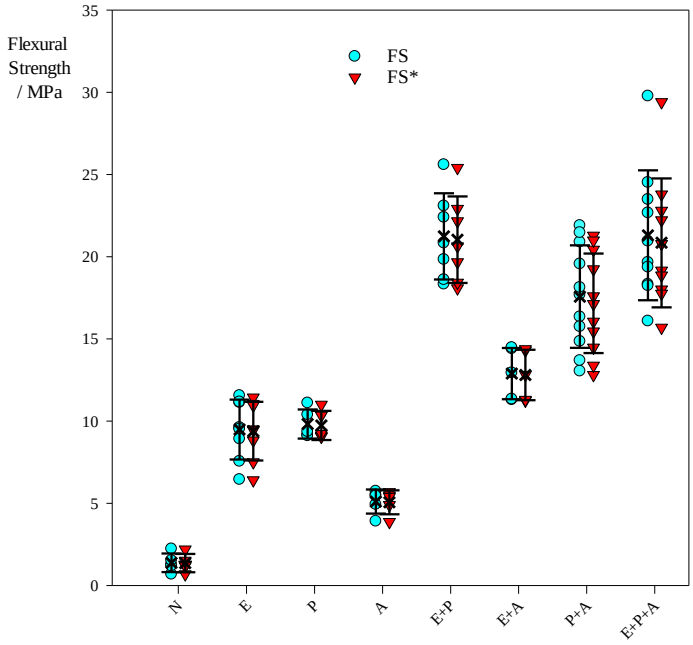

Figure 4.9 Adhesive flexural strength of three-step total-etch to dentine.

Table 4.10 Three-way analysis of variance of flexural strength: three-step total-etch (log-transformed). df: degrees of freedom, SS: sum of squares, MS: mean sum of squares, *F*: *F* ratio, P: *F*-ratio significance probability.

Source of Variation	df	SS	MS	F	P
Etch	1	2.252	2.252	300.054	$<10\times10^{-16}$
Primer	1	3.140	3.140	418.247	$<10\times10^{-16}$
Adhesive	1	0.766	0.766	101.980	2.54×10^{-13}
Etch × Primer	1	0.572	0.572	76.235	1.67×10^{-11}
Etch × Adhesive	1	0.400	0.400	53.257	2.77×10^{-9}
Primer × Adhesive	1	0.191	0.191	25.444	4.32×10^{-6}
Etch × Primer ×Adhesive	1	0.035	0.0348	4.632	0.037
Residual	48	0.360	0.00751		
Total	55	7.151	0.130		

ii. Two-step total-etch adhesive (ASX: Adper Scotchbond 1 XT)

The results of the four-point bend test are shown in Table 4.11 and Figure 4.10. The flexural strength of etching + adhesive was double that of the 120 grit + adhesive, highlighting the difference between chemical- and mechanical-roughening patterns. One-way AoV showed that the flexural strengths of all groups were significantly different from each other ($P = 0.67 \times 10^{-5}$). Pairwise comparisons are set out at Table 4.12. The raw data are given in Appendix 6, Table 1, 2, and 3.

Table 4.11 Flexural strength of two-step total-etch ASX, FS: simple, FS*: corrected (Equation 2, Section 3.1), sd: standard deviation, CoV: coefficient of variation.

ScotchBond XT 1	Flexural Strength / MPa (mean ± sd)		CoV%		Number of specimens
	FS	FS*	FS	FS*	
Adhesive	5.03 ± 0.96	4.99 ± 0.96	19.11	19.23	5
Etching + Adhesive	21.98 ± 2.7	20.06 ± 2.31	12.27	15.5	6
120 Grit + Adhesive	11.58 ± 2.18	10.83± 2.17	18.81	20.06	5

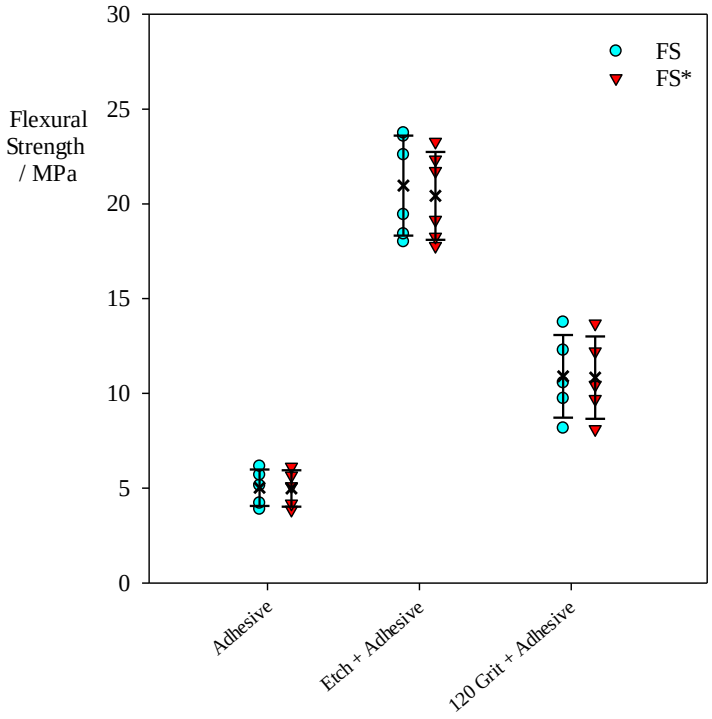

Figure 4.10 Adhesive flexural strength of Adper ScotchBond XT1 to dentine.

Table 4.12 One-way analysis of variance of flexural strength: two-step total-etch (log-transformed). df: degrees of freedom, SS: sum of squares, MS: mean sum of squares, *F*: *F* ratio, P: *F*-ratio significance probability.

Source of Variation	df	SS	MS	F	P
Between subjects	5	0.020	4.089×10^{-3}		
Between treatments	2	0.968	0.484	74.604	0.67×10^{-5}
Residual	8	0.052	6.487×10^{-3}		
Total	15	1.109	7.391×10^{-2}		

4.1.4 Zirconia

The results of the four-point bend test are given in Table 4.13 and Figure 4.11. The raw data are given in Appendix 8, Tables 4.13. The log-transformed data (FS*) were analysed through a *t*-test. The difference was non-significant ($t = -1.15$, df = 8; P = 0.28).

Table 4.13 Flexural strength of self-adhesive resin cement RX, FS: simple, FS*: corrected (Equation 2, Section 3.1), sd: standard deviation, CoV: coefficient of variation.

RelyX Unicem	Flexural Strength / MPa (mean ± sd)		CoV%		Number of specimens
	FS	FS*	FS	FS*	
Adhesive	15.63 ± 2.08	15.51 ± 2.05	13.33	13.24	5
Etching + Adhesive	18.34 ± 4.89	18.21 ± 4.86	26.64	26.67	5

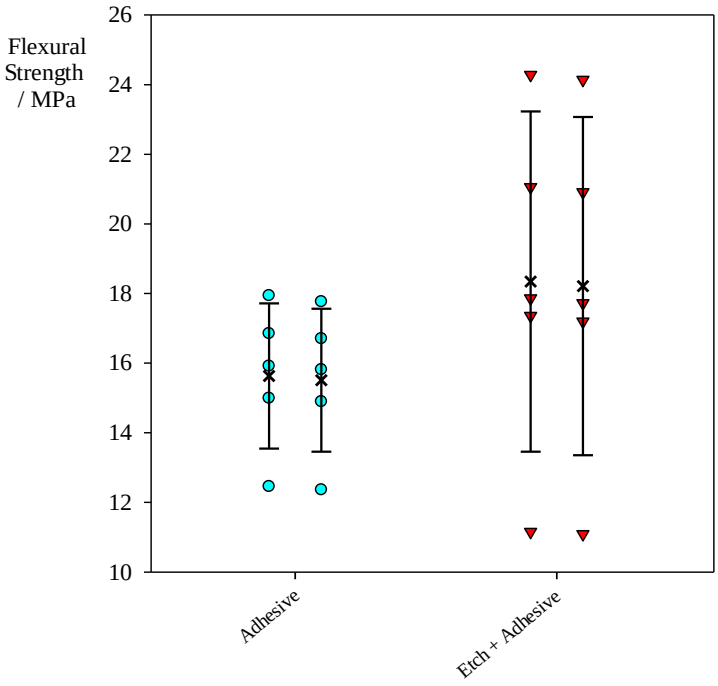

Figure 4.11 Adhesive flexural strength of self-adhesive resin cement to zirconia.

4.2 Test system compliance calibration

The raw data used to draw the (cross-head displacement) XHD/load curve of the load train and flexure jig is given in Figure 4.12 and 4.13, respectively. The load train yielded a relatively linear response function over a certain range; beyond this region, the calibration curve was less linear. It is therefore important to choose the correct region of the curve (~500 – 2900 N for the machine and 90 – 290 N for the flexure jig) to avoid the relatively nonelastic behaviour.

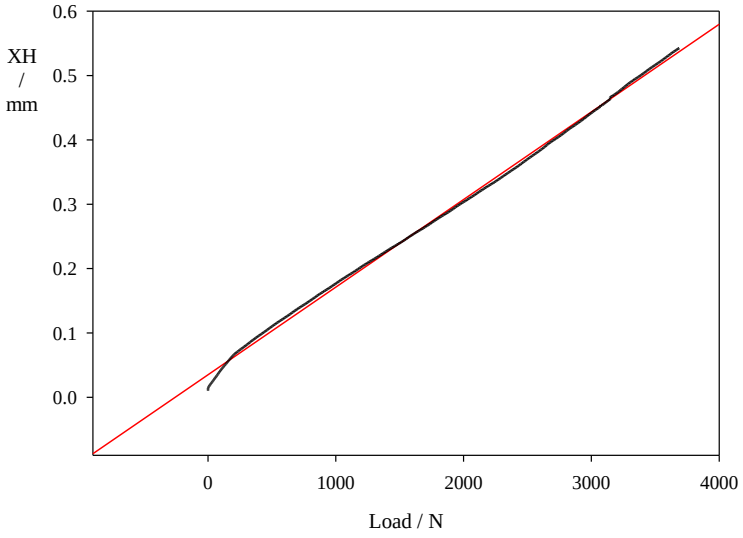

Figure 4.12 Compliance of the machine

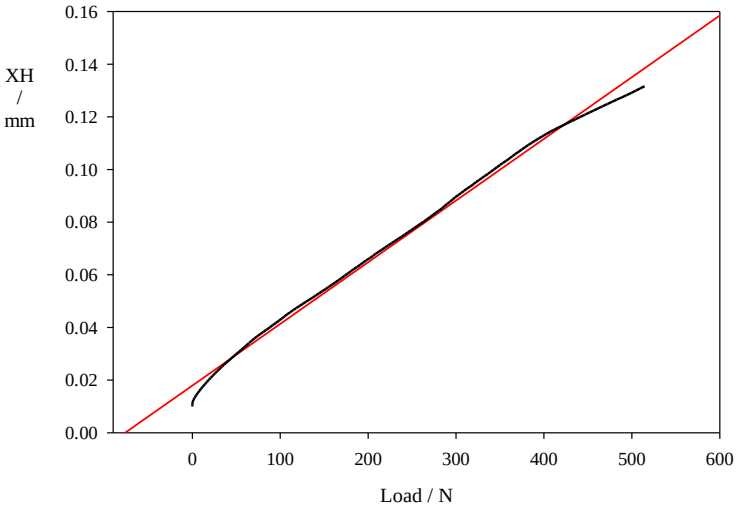

Figure 4.13 Flexure testing rig with dummy specimen

4.3 Fractographic analysis

4.3.1 SEM analysis

4.3.1.1 Three-step total etch (Adper Scotchbond Multi-purpose)

The crack path started consistently at the tension (bottom) surface of the beam at different parts of the adhesive joint. The mirror region surrounding the fracture initiation was not easily identified, especially with weak joints, however, as the joint became stronger the mirror and secondary crack markings, *i.e.* hackle, and a compression curl region were recognized (Figure 4.14). Figures 4.15 - 22 show examples of the fracture surfaces of the various groups; the tension surface is at the bottom.

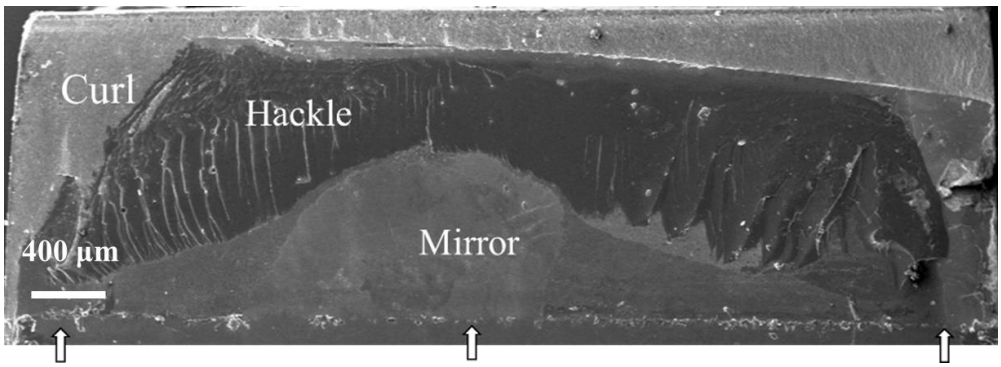

Figure 4.14 Example of the fracture surface bonding area of a dentine coupon (Etching + Primer + Adhesive group). White arrows indicate crack initiation border (tension surface). A fracture mirror is a smooth region surrounding failure origin. Hackle is the region of secondary cracks created when sufficient energy is available. Curl is a horizontal ridge created as the crack approaches the compression zone on the 'upper' surface [91].

In broad terms, SEM showed that the surface topography of the interfacial joint of the N (untreated) group was largely unaffected (Figure 4.15), *i.e.*, a weak interface. The E (etch only) group showed a different mode of failure compared with the P (primer only) group which showed largely cohesive RBC crack propagation (Figures 4.17 and 4.21). Although with lower intensity, the same features were noted with E+A (etch plus adhesive) (Figure 4.19) and P+A (Figure 4.20), with the E+A group showing less distinctive features, perhaps indicating lower intrinsic adhesion forces.

For the No treatment group (N), Figure 4.15a shows a smooth dentine surface lacking the roughness and pores generally recognized as necessary for mechanical adhesion – the tubules appear to be largely blocked (Figure 4.15c). Figure 4.15b shows a more-or-less featureless RBC surface, with no sign of tags (Figure 4.15d). However, even those apparently smooth surfaces are still rough at the sub-microscopic level, suggesting some very slight mechanical retention role for the dentine smear layer (Figures 4.15c and d) since some very weak retention was apparent, although about half of the specimens still fell apart before testing, despite care being taken to avoid that.

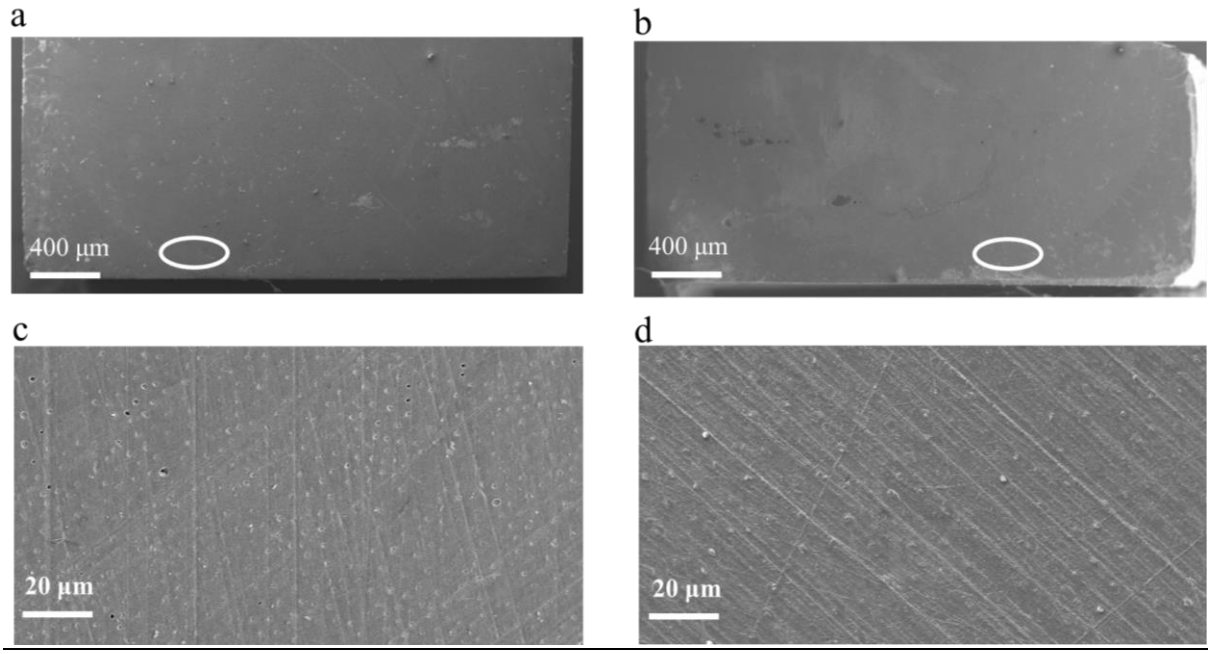

Figure 4.15 No treatment group (N): at low magnification both **(a)** dentine and **(b)** RBC show a smooth featureless appearance. **(c)** A high-power view of (a) shows the smear layer blocking the orifices of the dentinal tubules and preventing the penetration of RBC, thus limiting the mechanical key. **(d)** There is little sign of resin penetration of those blocked tubules. (The regions for the high-magnification images are shown by the ovals, here and subsequently.)

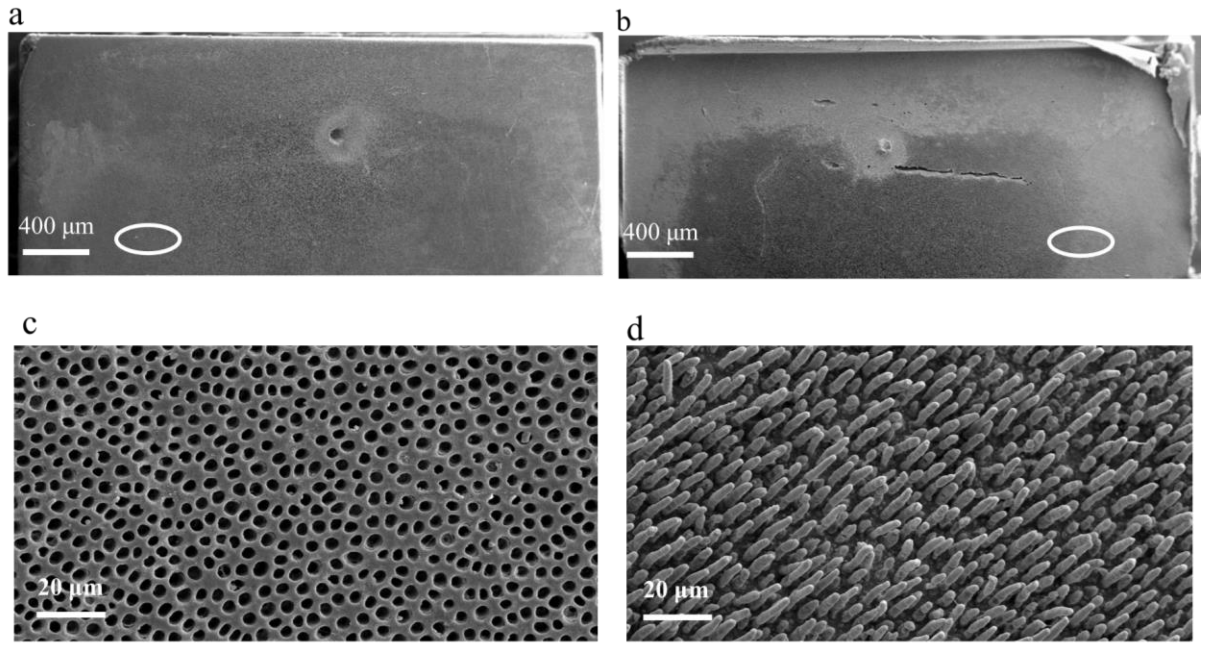

Figure 4.16 Etching-only group (E). **(a and b)** Under low magnification only a relatively-featureless fracture surface was found. **(c)** Under higher magnification the etched dentine surface showed patent tubules. **(d)** Composite resin protrusions (tags) that had been pulled from the tubular lumina were found. These do not appear to be broken

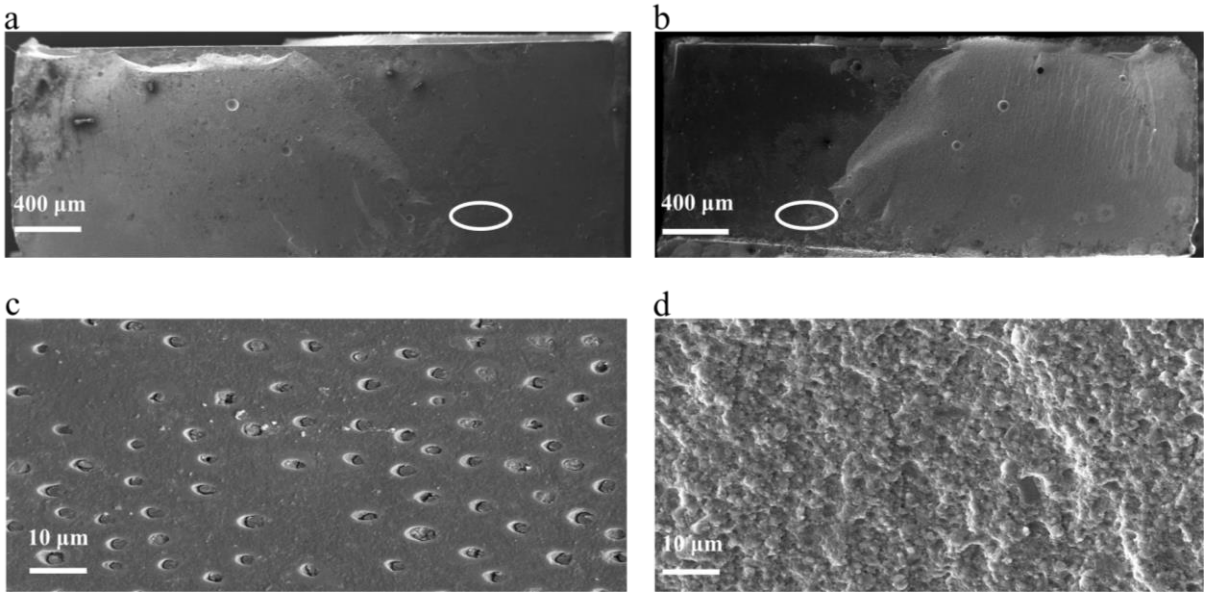

Figure 4.17 Primer-only group (P). **(a and b)** Failure partially occurred with a large cohesive fracture through the RBC material; this suggests a different retention figure compared with Etching only and possibly enhancement of adhesion. **(c)** Shows fractured RBC protrusions inside the dentinal tubules. **(d)** Shows cohesive fracture in the RBC substance. Parts of the RBC at the interface shattered into small pieces that could not be recovered.

The failure pattern for etching only (E) (Figure 4.16) differed from that for primer only (P) (Figure 4.17), where cohesive fracture initiation was observed, compared with the relatively featureless surface for etching only (E). That the tags pulled out of that etched surface without fracture (Figure 4.16d) suggests little or no actual adhesion (*i.e.*, chemically) the etched surface, as would be expected for the resin alone, but the fact that the tags had fractured with primer (Figure 4.17c) indicates some form of retention in the depths of the tubules. Despite the different modes of failure, both groups (E only and P only) had comparable and significant improvements in bond strength compared with the N group. It is also noted that the effect of primer was not consistent across the bonding area, unlike the effect of the etchant.

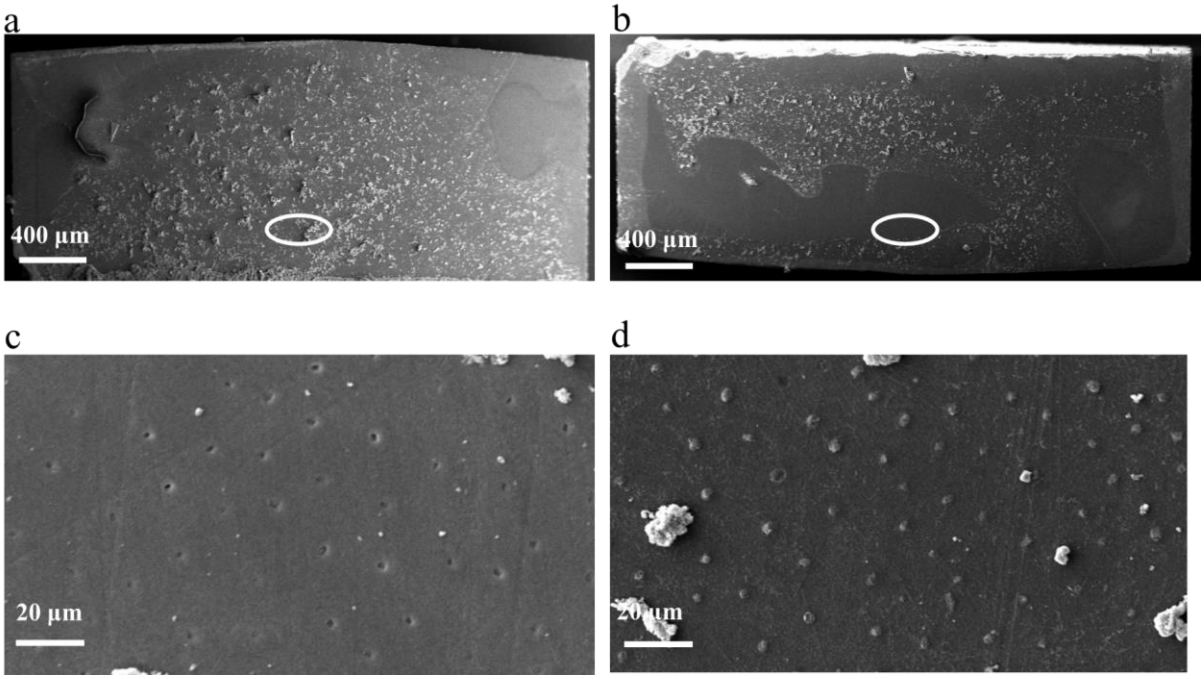

Figure 4.18 Adhesive-only group (A). **(a & b)** Some kind of interaction between dentine and the adhesive seems to have occurred as there is much debris. **(c)** The dentine surface again shows largely blocked dentinal tubules. **(d)** Relatively short resin protrusions are apparent, corresponding to the shallow depressions of the blocked dentinal tubules. The adhesive appears to have remained attached to the RBC such that the fracture was at the interface with the dentine.

Adhesive only (A) (Figure 4.18) resulted in significantly less improvement in bond strength compared with Primer only and Etch only. This highlights the importance of mechanical retention compared with chemical bonding, but again, with the tubules being blocked, no tags were formed. Further work would be needed to understand better the dentine-adhesive interaction.

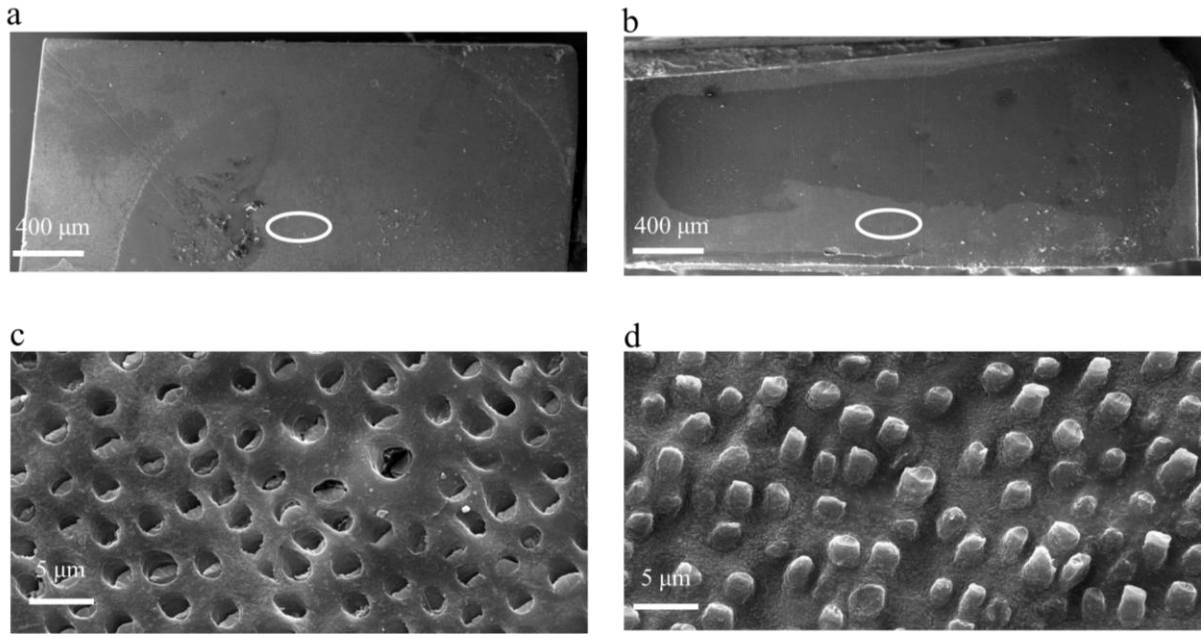

Figure 4.19 Etching + Adhesive (E+A). **(a and b)** Low magnification shows similar appearance to that of the E only group in that the surfaces are largely featureless. **(c)** Widened tubules at least partially obliterated by fractured resin tags, formed by penetration into the acid-etched dentine, are clear. **(d)** Fractured resin tags on the RBC side.

The use of adhesive on the etched surface (E+A) improved the adaptation to the etched surface, presumably due to the greater fluidity of the adhesive, and this was reflected in the bond strength compared with E only (Table 3.1). While there were no notable macroscopic features (Figure 4.19a and b) the tags formed were clearly broken (Figure 4.19d), leaving remnants in the tubules (Figure 4.19c), suggesting improved penetration and adaptation to the etched surface, again with retentive effect inside the tubules. The bond of the Adhesive to the RBC appeared to be largely intact suggesting that interface with the dentine was the weak link (Figure 4.19d).

The fracture for primer + adhesive (P+A), that is, on untreated dentine, was apparently cohesive in the Adhesive with a small area of cohesive failure through the RBC substance (Figure 4.20) – no dentine surface was exposed. Similar observations were made for E+P+A (Figure 4.22), where the fracture largely occurred through the adhesive layer. E+P (Figure 4.21) was similar to P, where fracture of the resin protrusions occurred just inside dentinal tubules, however, in E+P the tubules were wider and obliterated by the RBC protrusions.

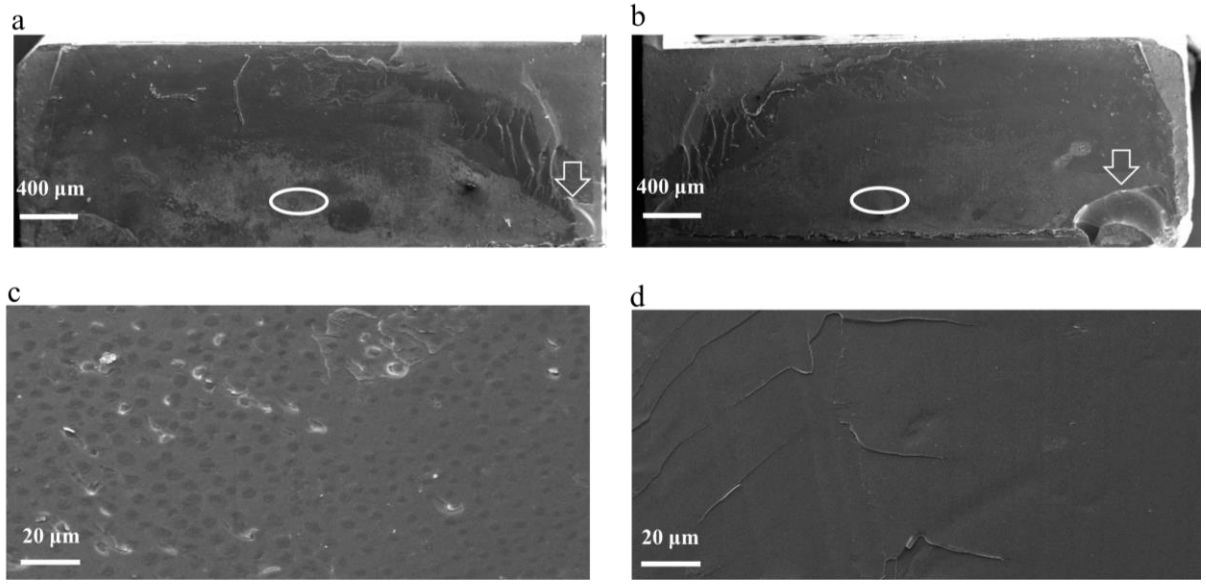

Figure 4.20 Primer + Adhesive (P+A). **(a and b)** Richer fracture markings are apparent compared with Etching + Adhesive (E+A) (Figure 4.19), suggesting more stored energy. **(c & d)** The adhesive layer appears to be homogeneous on both sides of the interface, quite different from the appearance in Figures 4.19c and d, suggesting treatment of the smear layer, compared with the complete removal evident in Figure 4.16c. The arrow indicates a small cohesive fracture through the RBC which remained covered with the adhesive.

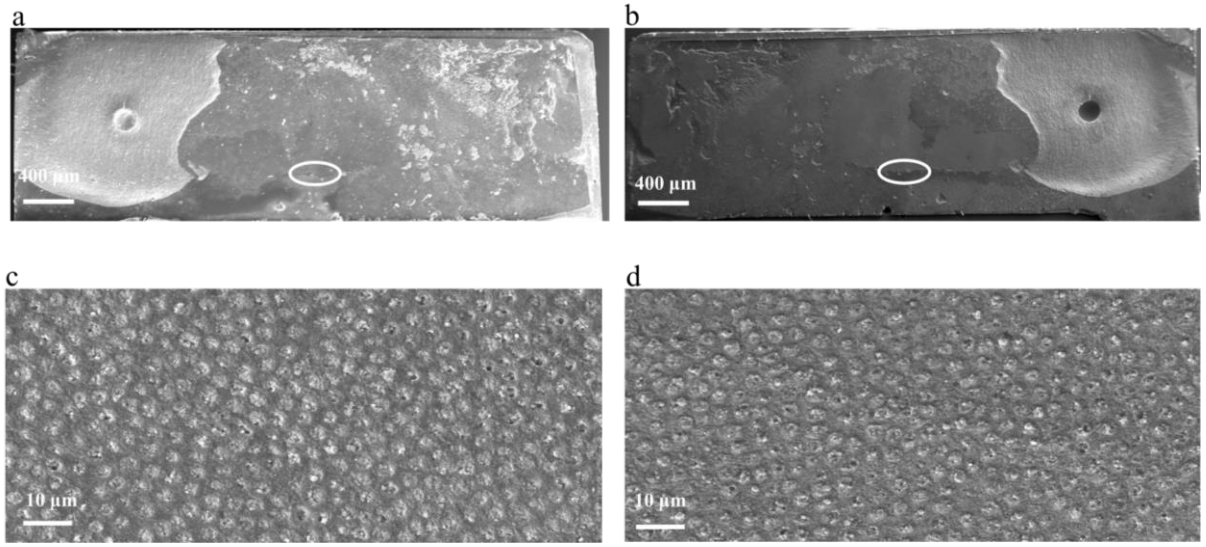

Figure 4.21 Etching + Primer (E+P). **(a and b)** Cohesive fracture in the RBC substance has occurred. **(c and d)** The two images are similar (complementarily) suggesting a failure at the RBC-dentine interface.

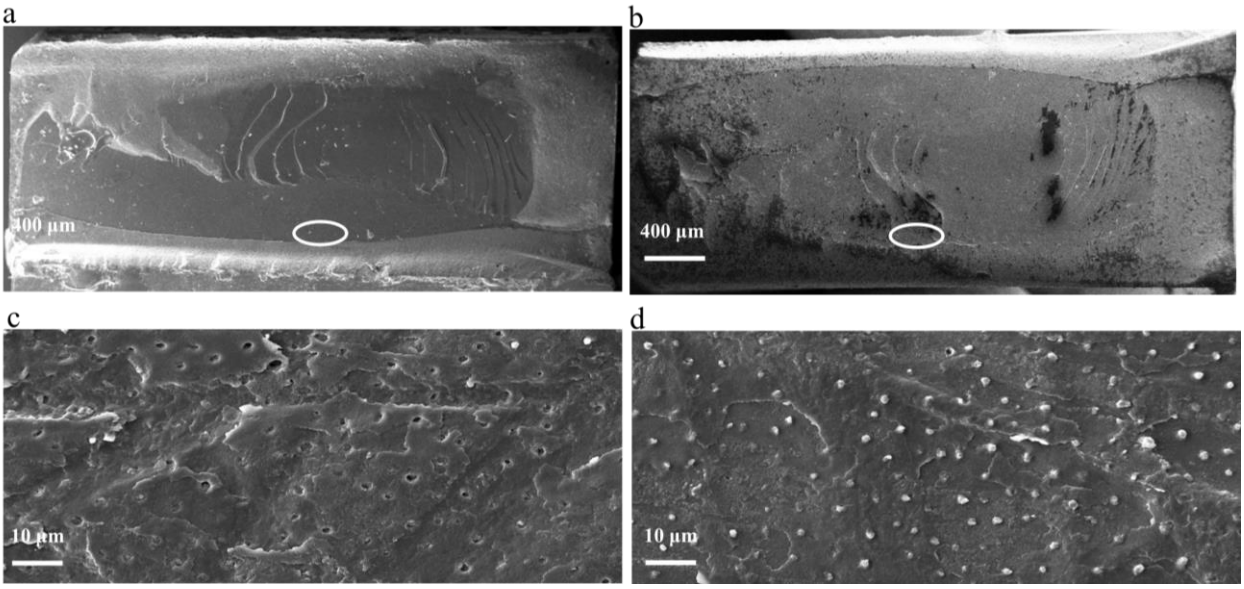

Figure 4.22 Etching + Primer + Adhesive (E+P+A). **(a & b)** Intact dentine and RBC fracture surfaces showing richer fracture surface suggesting relatively increased stored energy. **(c)** The openings of dentinal tubules are less demarcated compared with Figure 4.19c. **(d)** As observed earlier, the adhesive appears to have remained bonded to the RBC indicating a cohesive fracture in the adhesive.

4.3.1.2 Zirconia

A clear interfacial fracture initiation was evident between the self-adhesive cement and ZrO_2 in both groups (Figure 4.23 and 4.24), suggesting limited chemical and micromechanical interaction. Surface changes produced by KHF_2 etching were minimal to be observed at 1000× magnification (Figure 4.25).

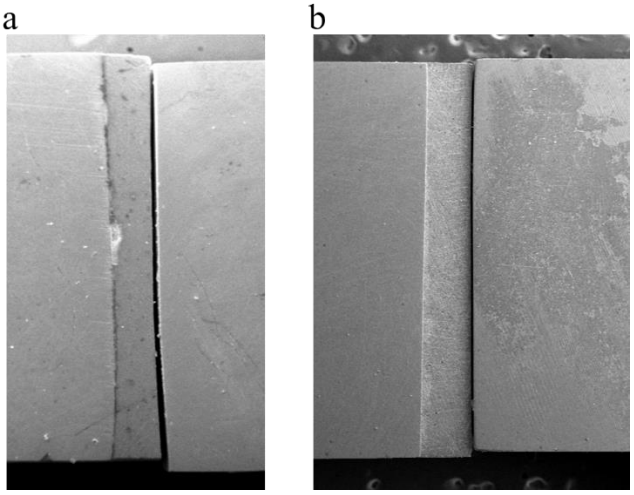

Figure 4.23 Adhesive alone (A).

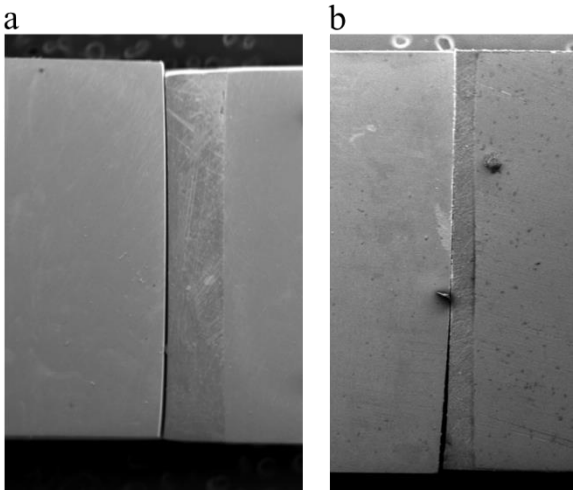

Figure 4.24 Etching + Adhesive (E+A).

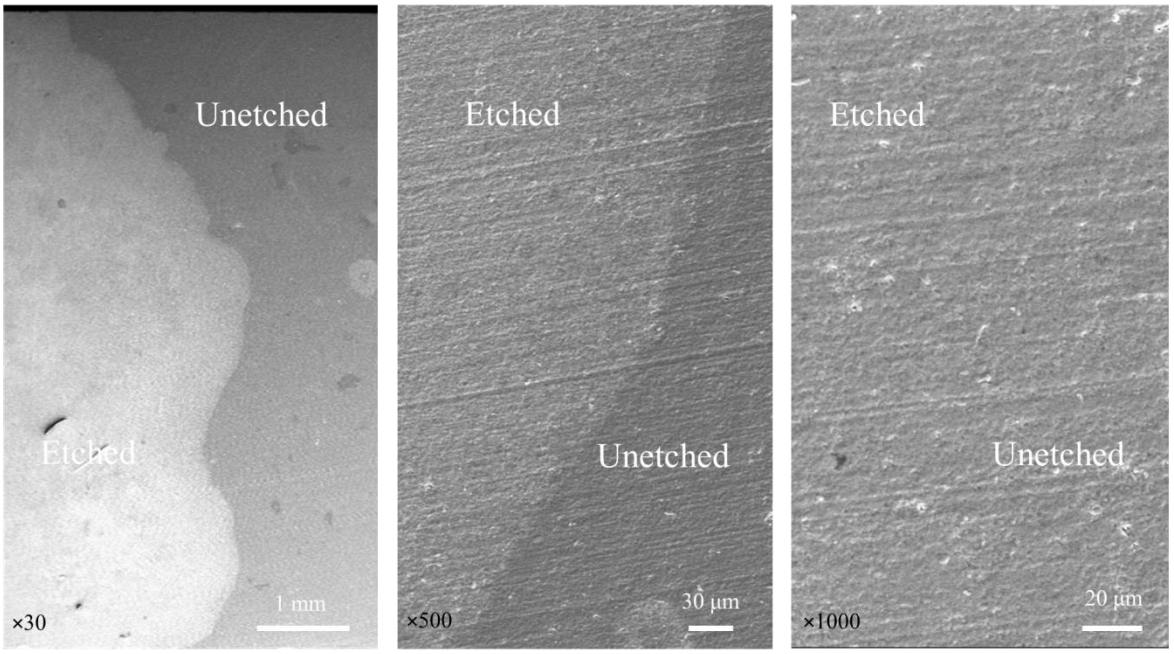

Figure 4.25 SEM images of the surface of a zirconia beam etched using a slurry of potassium hydrogen fluoride, showing the boundary between the treated and untreated areas. The cause of the contrast at low magnification cannot be seen at high magnification, *i.e.*, the etching effect was minimal to be resoluted at high magnification.

4.3.2 EDS analysis

4.3.2.1 Glass ionomer *vs* Zinc polycarboxylate

EDS provides information on the elemental composition of the test material surface. The analysis was performed over an area of a few square micrometres, however, the penetration depth of the beam was estimated to be around 1 - 2 μm. Three measurements were taken for each specimen and the average was calculated.

EDS examination of the fracture sites then suggested a bonding mechanism and the type of bond failure in each case. EDS analysis of particle elemental mass concentration (mass%) showed that the bonded area showed the presence of a thin layer of ZCC on the surface of the SS, indicating a cohesive cement failure. For GIC_F the bonded area showed very little or no residual cement, suggesting an interfacial failure (Figure 4.6 and Table 4.14). GIC_A also demonstrated the presence of a less regular and thin coating on the surface of SS compared with ZCC, indicating a mixed mode of failure (Figure 4.6 and Table 4.14).

Table 4.14 EDS results for the smooth surface stainless steel after fracture of bonding to GIC_F, GIC_A and ZCC.

	mass %			
Cement / Element	SS	GIC_F	GIC_A	ZCC
C	16.0	14.0	19.5	19.6
Al	0.9	0.4	5.9	0.2
Si	0.8	0.5	6.8	0.2
Cr	18.3	18.2	4.8	10.7
Mn	1.1	1.2	0.4	0.7
Fe	68.8	68.8	17.0	8.5
Ni	7.7	7.6	1.7	4.1
O			24.9	13.7
F			10.5	1.8
Mg				0.4
Na			1.2	
Ca			7.0	
P			0.5	
Zn				7.6
Sn				3.1

5. Discussion

5.1 General discussion

The symmetrical four-point flexure test was identified to be an uncomplicated and successful means of interfacial bond strength testing. The test has technique versatility enabling it to be used with a range of 'adhesive' or other retentive systems (apart from those that couldn't be tested) employed in the dental field, with necessary adjustments implemented as needed. The test (without comparison to currently used tests) was able to differentiate significantly between the various systems examined indicating acceptable discriminatory power. The high coefficient of variation of some groups can be attributed to the relatively low interfacial bond strength values.

Preparation of the top surface (tension surface) against the acetate strip produced a mirror-like smooth original specimen surface which was not subjected to further alteration. Surface defects have more detrimental influence on the measured flexural strength (corrected) (FS*) compared with internal defects [90]. Surface defects on the tension side of the beam are especially important because they are in the region of maximum stress [11]. A split-mould was used to facilitate specimen retrieval, minimizing stresses exerted and thus the risk of premature fracture, especially when testing adhesive joints [81]. The knife-edge design (Figure 3.3b) allowed better flow of excess material and enhanced consistent geometry of the specimens at the edges [81]. To allow overfilling of the mould with less chances of air entrapment and to increase the adaptability to the mould shape, both ends were open for unrestricted flow and with a flared section in the SS mould for handling [81].

In the preparation of the beams, the application of load through hand pressure yielded relatively less control over the beams dimensions compared with the application of constant load. This was primarily because it would appear that not enough time was allowed for full relaxation and adaptation of the material. An alternative approach was then used: after filling the rectangular slot of the mould with excess RBC, covered with an acetate strip and glass slide, it was placed under a constant load using a metal block on the microscope glass slide for around 10 min. The glass slide was thus gently pressed down until contact was made with the knife edges of the mould, the open ends of the mould enabled longitudinal full flow and relaxation of the material and thus better adaptation to the slot. The use of this constant load approach led to significant improvements in both the FS* and the coefficient of variation (CoV) (Table 4.4), giving an example of the importance of possible overlooked details in experiment setting.

The use of a log transformation is often necessary with strength data [75]. The goal of this is to create sampling distribution that is reasonably symmetrical, which in turn provides satisfactory grounds for the assumptions underlying statistical tests to be met [92]. Normally distributed data would increase the confidence in tests based on small sample size [92], as was the case in some groups in the current experiment where we had five specimens in each. In addition, the transformation also tends to stabilize the variance across test groups when their means differ appreciably.

Employing support span-to-depth ratio greater than 16:1 can result in increased deflections and appreciable departure from simple beam theory [76, 77]. When the resultant deflection is in excess of 10% of the support span, a correction factor should be included in the flexural strength formula (Equation 2, Section 3) [76].

5.2 Flexural strength (FS)

5.2.1 Monolithic bars

5.2.1.1 High viscosity RBCs

The corrected flexural strength (FS*) trend shown here was for FB > TEC > BB_{hp} (FB: Filtek One Bulk-Fill, TEC: Tetric Evoceram, BB: Beautifil Bulk,) (Table 4.1). The method was able to discriminate the differences well *i.e.,* there was less overlapping figures between the three groups. A similar trend of significantly higher FS* for FB compared with BB has been reported [93, 94]. Although BB had a notably higher volume fraction filler than FB (Table 3.1), the only appreciable difference is the surface "pre-reacted glass ionomer" and this may be responsible for the difference.

The flexural strength of monolithic dental composites is typically determined in three-point bend (3pb), as is used in ISO 4049 [30]. Classical beam theory is based on the assumption that the geometry of the specimen is unaffected when loaded, *i.e.*, no deformation [78]. However, the deflection depends on the modulus of elasticity and therefore may be considerable before fracture occurs, thus the departure from the classical beam theory can be appreciable [77]. It follows that a specimen with less deflection at fracture is preferable [77], although some corrections can be applied (*e.g.* Equation 2, Section 3.2). The deflection in the

four-point bend (4pb) (arrangement is different from that of 3pb, and requires a different correction [76, 77]. The deflection at the centre in 3pb is given by:

$$y = \frac{FL^3}{48EI_z} \quad [1]$$

while that for 4pb is obtained from:

$$y = \frac{Fc(3L^2-4c^2)}{48EI_z} \quad [2]$$

where F is the total load, L is the overall length between the outer supports, and *c* is the distance of each load application point from the nearest support, E is the elastic modulus, and I_z is the second moment of area [11]. The deflection calculated for 4pb, when c = L/4, is thus found to be 0.69 that of the 3pb deflection. In this way 4pb is relatively more suitable to characterize static flexural properties of monolithic specimens in the laboratory, and possibly more reliable results can be obtained.

Oddly, Chitchumnong *et al.* [77], reported that when the FS* of poly(methylmethacrylate) (PMMA) was measured in 4pb a greater deflection was recorded compared with that in 3pb. They did not explain how the maximum deflection was determined, and may have taken it directly from XH movement, but even so this is an odd (or possibly wrong) result.

5.2.1.2 Low viscosity (Filtek flowable bulk-fill) (FF)

The 50 mm specimens were far too flexible to fracture in the same way as the high viscosity RBCs. The corrected flexural strength (FS*) of FF was considerably higher than that of conventional and bulk-fill RBCs. The specimen size may have influenced the measured FS*, as shorter span beams have been associated with higher strength values [20]. However, similar trends of relatively higher FS* of FF compared with conventional and bulk-fill RBCs have been reported [82, 93, 95-97]. Without considering the organic matrix composition, filler volume was reported [82] to be the most influential on the measured FS* up to a maximum of 60%, but further increase in filler volume was suggested to be detrimental due to the higher number of defects introduced [82]. However, fillers standardization is difficult to achieve, and several RBCs products with > 60% filler volume are among the best in the dental market, *e.g.*, Z250. FF specimens took considerably longer times under load before fracture because of the possible greater deflection at a fixed crosshead speed (XHS). Fracture generally occurs when

no further damage can accumulate inside the specimen, *i.e.,* strong specimens have been under load for longer times compared with weaker ones [16]. A further detailed experiment involving a real-time monitoring of the amount of deflection versus experienced load may provide some information on the viscoelastic processes during the propagation of damage to fracture. A clearer understanding of system behaviour under static loading may be developed through a rigorous analysis of the static load, stress, and deflection data [98]. In the present experiment, FF had shorter span length compared with the high viscosity RBC*, i.e.,* 28 *vs.* 50 mm, so the comparison groups were not uniform in length.

With the exception of high occlusal stress-bearing areas, current RBCs have mechanical properties to survive challenges in all areas of the mouth [83]. Lack of data concerning the minimum acceptable clinical strength, and the fact that strength is a conditional property, has contributed to the wide range of mechanical properties of commercial RBCs [30]. Mechanical behaviour in the failure of filled resins (FRs) is influenced by the microstructure, which is dictated by the various combinations of the main components:

1. Organic resin matrix (high- and low-viscosity monomers and their percentages, activator-initiator systems, inhibitors).
2. Inorganic filler (composition, size, shape, volume fraction, density) [41].
3. Coupling agent [41] (matrix constraint is dependent on the degree of interfacial coupling between the filler and the resin matrix) [11].

Investigating these factors systematically presents a number of challenges and the interactions between them are even more difficult to elucidate. Ultimately, systematic investigations, whilst in principle are absolutely necessary, in practice there may be severe limitations to what can be achieved for these effects. Given the fact that very few materials have been studied here, it is not possible to offer an explanation in any detail for the results that have been obtained. However, it remains feasible the present method could (with sufficient effort) yield useful insights.

5.2.1.3 Hand pressed *vs.* constant load (Beautifil bulk-fill) (BB)

Forces generated by the fingertips reflect the complex nature of the structural arrangement of the human finger [99]. Without a proper control over the fingertip forces, the shaping of RBC paste into the mould slot may not be consistent. It was quite challenging to

control high fingertip pressure on a rigid object for 60 s. In contrast, a constant load applied to the specimen using a dead weight for 10 min represents a simple and attractive alternative. The FS* of specimens prepared under constant load were around 1.5 times higher compared with hand-pressed specimens. Of greater significance was the proportionate decrease in CoV (from 14.94 to 3.71%) with increasing FS* reflecting the reduction in process defects through allowing uniform resin flow and complete relaxation.

5.2.2 Monolithic *vs.* repair (Filtek One bulk-fill) (FB)

The aim here was to investigate the chemical bond contribution to the repair bond strength of Filtek One bulk-fill (FB) specimens of which had been repaired by adding fresh RBC to the repair joint and to compare this with the monolithic flexural strength. The monolithic group had a flexural bond strength of 76.24 ± 3.02 MPa while the initial repair group had a value of 22.06 ± 3.47 MPa. Upon examination of fractured specimens under light microscopy, it was noted that the repair material overlapped the fracture line (Figure 3.9a). This meant that more surface area was involved in the repair site, leading to significantly higher bond strength values compared with the butt-joint specimens. In order to rectify this, the subsequent group was gently ground using 1000 grit abrasive paper under continuous water flow and frequently examined under a light microscope. The corrected group (butt joint) had a flexural strength of 10.85 ± 3.57 MPa. The slight overlap in the interfacial joint design had significantly influenced the results of the test and, therefore, joint geometry must be strictly controlled in subsequent experiments.

5.2.3 Bond to dentine coupons

The aim here was also to investigate chemical bond potential to dentine coupons of various ‘adhesive’ systems. This was attempted through bonding to flat dentine surfaces.

5.2.3.1 Experimental design

Given that there are many factors known to be involved in the efficacy of bonding, various experimental designs can be used.

In a single-factor experiment, one independent variable is tested to observe the influence on the dependent variable. For example, the influence of grinding with 120-grit abrasive paper on the bond strength of RBC to dentine.

The factorial design, when employed, involved two or three independent variables, with each having two levels, *e.g.*, etching and no etching. Using this design allowed effective controls for the main treatments, *i.e.*, etching, primer, adhesive. In two- and three-factor experiments, the investigation of both the main effects and the interaction between the different kinds of treatment can be examined. For example, the separate effects of primer, adhesive and phosphoric acid etching on the bond strength of RBC to dentine.

5.2.3.2 Conventional cements

i. Zinc phosphate cement (ZPC)

The retention of zinc phosphate cement system is generally supposed to be based entirely on mechanical key [11]. However, the liquid of the cement system contains phosphoric acid, sufficient to dissolve the inorganic part of the tooth structure and thus enabling some degree of interlocking [11]. Even after a deliberate separate acid etching step or 120-grit abrasive paper roughening, specimens did not develop adequate interfacial strength to be tested (after 60 min). The present results support the view that ZPC has no chemical bond potential for tooth structure and works as a gap filling cement benefiting from uneven and unparallel surfaces to enhance retention, best viewed as effective against shear displacement. A further point is that the mode of failure experienced in 4pb (tensile) is not expected to be relevant to ZPC as a luting agent, where tension is not an important aspect of loading, and therefore the mode of loading has to be adjusted for such a material to obtain mimicry of the clinical scenario [15]. If failure is likely to be caused by shear stresses, then the test employed should produce shear forces, however, current shear set-ups greatly underestimate shear stresses at failure due to their non-uniform distribution (Section 2.4.2) [49].

ii. Zinc polycarboxylate cement (ZCC)

As shown earlier, zinc polycarboxylate cement placed on smooth dentine adhered well (after 60 min) enough to survive the handling for the test, with the fracture being cohesive

(Table 4.7). ZCC offers the possibility of true chemical bonding (as well as mechanical key) as opposed to the mechanical retention only of ZPC [11]. That chemical bonding is established between the calcium ions on the tooth surface forming coordination bonds with the oxygen atoms of the polycarboxylate ions. Zinc polycarboxylate cement system established the basis of adhesive dentistry [11], but there is still the likelihood of some acid etching of dentinal tissue before the acid become neutralized in the cement network, thus enhancing the strength of the interface [11]. However, the bond to SS (Figure 4.7), where such an etching effect is non-existent, has clearly demonstrated the chemical bond potential of ZCC.

iii. Glass ionomer cement (GIC)

On the basis of their chemistry, it is expected that glass ionomer cement systems have the inherent ability to bond chemically to tooth enamel and dentine [100]. The interfacial bond of three conventional GIC products to sound human dentine after 24 h immersion in water has been reported as not weak: using a microtensile bond strength test, Yip *et al.* [101] reported a significantly higher interfacial strength than had been previously reported for larger-scale tests. They further claimed that other reports underestimate the interfacial strength since failures were cohesive, thus implying a higher interfacial bond strength [101]. The same interpretation was also suggested by Soderholm [10] where the relatively lower fracture toughness values of GIC censored interfacial bond values through cohesive fractures. Yip *et al.* suggested that the non-trimming technique might enable a more uniform stress field for microtensile tests, allowing the stress to be directed along the interfacial joint resulting in fewer GIC cohesive failures [101]. The relative homogeneity of the interfacial stress field of the non-trimming technique was suggested because of the increased incidence of interfacial failures [101]. However, the distribution of failure modes was observed using light microscopy and the 'higher' incidence of interfacial failure was between 43.1 and 56.3% and the incidence of pretest failure was 17.0 – 18.8%. Pretest failures were also included in the failure mode assessment [101]. The non-trimming method was initially claimed to have the potential to measure low bond strength values because it produce less stress on the adhesive joint during specimen preparation [59], however, such a claim was not satisfied in the case of Yip *et al.* due to the increased pretest failures [101].

a. $GIC_{\mathbf{F}}$ (Fuji II)

Quite unexpectedly, GIC_F was not able to bond to dentine, SS or AA, even after surface roughening (after 24 h, at ~90% RH, ~18 - 19 ºC). The cause of such a finding is obscure, but contradicts the general assumption that GIC has a general chemical bond potential to tooth tissue. Minimal interaction of GIC_F to smooth SS was clearly demonstrated (Figure 4.7), in comparing it with ZCC and GIC_A (after 60 min, ~18 - 19 ºC). This result needs further investigation, but clearly the formulation of this product needs to be considered as the cause since the effect applied across all three substrates.

b. GIC_A (Aquacem)

GIC_A performed better than GIC_F and established an interfacial joint that could be tested to obtain quantitative data. However, the bond strength to dentine (0.17 MPa) was still very weak, and the results were obtained after 24 h (at ~90% RH, ~18 - 19 ºC) from the start of mixing. GIC_A showed a less homogeneous residuum on SS (Figure 4.7), suggesting a less intense chemical interaction compared with that with ZCC (after 60 min, ~18 -19 ºC). Again, the need for further study is evident.

iv. Calcium silicate cement (CS) (Biodentine) (BD)

Biodentine has been reported to form an interfacial zone with dentine that favours mineral permeation and so forming a high mineral-content zone [102] leading to marginal sealing and subsequent pulp protection [103]. However, the present results at one wk do not support that suggestion: even on a rough dentine surface BD could not establish a bond (at ~90% RH and ~18 -19 ºC). A further detailed long-term experiment is needed to ascertain the possibilities in longer term. However, it is to be noted that in chemical terms there is no obvious expectation of a chemical bond, whatever may happen due to reaction with tissue fluid.

5.2.3.3 Total-etch bonding systems

The quantitative contributions of the various steps of the three-step total-etch system to interfacial bond strength was investigated. The three×three experimental design has allowed this dissection of the contributions, a design principle that ought to be applied more generally where there are several steps to a process.

i. Three-step total-etch bonding system (Adper Scotchbond Multi-purpose)

For the three-way analysis of variance, although the data passed the normality test (Shapiro-Wilk) ($p = 0.145$), they failed the equal variance test (Brown-Forsythe) ($p < 0.05$). Accordingly, the data were transformed by taking logarithms (common logarithms, base 10) and the analysis repeated. Both equal variance ($p = 0.068$) and normality ($p = 0.139$) tests were then passed. Using the log transformed data, etching, primer and adhesive each gave highly significant ($p < 10^{-6}$) treatment effects, *i.e.*, all three factors contribute significantly to the development of the strength of the union. However, there is also a statistically-significant interaction between them pairwise ($p < 10^{-5}$), and also in the three-way interaction ($p \sim 0.036$). This indicates that the effect of each depends on the others such that the effects are not purely additive. Essentially this means that a full interpretation is not possible, but some key points can be made.

As expected, when RBC was applied directly to smooth surface specimens without prior treatment (N group) the lowest corrected flexural strength (FS*) value was obtained (1.38 ± 0.56 MPa), with a CoV of 40.96%. When the smooth surface was acid etched (E group) and RBC was applied directly to that surface, the flexural strength substantially improved (9.39 ± 1.78 MPa), highlighting the importance of surface roughening and mechanical key even without using a 'flowable' adhesive. When the adhesive was applied directly on smooth surface before adding the RBC a lesser improvement was recorded (5.06 ± 0.73 MPa), suggesting some form of chemical bonding to dentine surface was indeed present, although it is conceivable that its lower viscosity allowed greater penetration of the little roughness and partially open tubules (Figure 4.18 c and d).

The primer used was Adper Scotchbond multi-purpose primer (ASP), which is composed of a copolymer of acrylic and itaconic acids in aqueous solution (10 ~ 20%) and HEMA (35 ~ 45%). Such solutions containing polycarboxylic acids must themselves etch, and also produce a surface topography different from that produced by phosphoric acid treatment [104]. Due to its low molecular weight and relative hydrophilicity, HEMA is suggested to improve the wetting of and diffusion into the dentine structure, thus promoting interfacial coupling [105]. Here, when the primer alone was applied directly to the smooth surface of dentine before the RBC (P group), the FS* (9.73 ± 0.88 MPa) was similar to that of the Etch group (9.39 ± 1.78 MPa), suggesting a combination of chemical and mechanical means of retention. The same trend of flexural strength improvement with dentine etching continued

with the Etch + Adhesive group (12.8 ± 1.53 MPa) and Primer + Adhesive group (17.16 ± 3.03 MPa), but perhaps suggesting a better etching pattern with the primer (*t*-test: $p = 6.38 \times 10^{-3}$).

From these results for a three-step total-etch system, the combinations of Etch + Primer + Adhesive and Etch + Primer were the most effective surface treatments for dentine (20.84 ± 4.7 and 21.03 ± 2.63 MPa, respectively), results that are not distinguishable (*t*-test: p = 0.86).

We may also say that Etch + Primer had a further advantage for achieving immediate bond strength because of its relatively fewer steps compared with Etch + Primer + Adhesive. However, reports of the effect of bonding agent thickness on the interfacial bond strength to dentine have been inconsistent. While the double-layer application approach was found to improve the early bond strength of universal adhesives, it negatively affected the bonding quality of two-step self-etching adhesives [106]. The early tensile bond strength values (within 10 min) of Silux Plus and Z100 to flat dentine surfaces treated with Single Bond three times were not statistically different from the control treated once [107]. Lee *et al.* found that the microtensile bond strength of the thick adhesive layer on the internal angle of the cavity was significantly higher than that of the thin adhesive layer at the cavity margin and also half-way on the cavity wall. They reported an increased interfacial strength upon increased thickness for up to six coats [108]. Results from Hashimoto *et al.* have also indicated an increased microtensile bond strength to dentine with each coating up to four coats [109]. Such effects could also be studied using the present method, perhaps with greater reliability, but this would also be a further trial of the validity of the method.

The role of the adhesive, as a hydrophobic coat forming a protective layer over the primer, needs to be further investigated in light of the above. So-called "water trees", formed immediately during the bonding process, were suggested as a contributing factor to the lack of durability and enhancement of the degradation of resin-dentine bonds [110]. Tay *et al.* [111] used an experimental acetone-based water-free two-step total-etch and applied two coats of the adhesive to acid-treated dentine, followed by immersion in an artificial saliva (AS) for twelve months. They observed a gradual and significant increase in nanoleakage[5] that extended from the hybrid-layer adhesive interface towards the hybrid zone. Okuda *et al.* [112] reported a

[5] The term 'nanoleakage' was introduced in the dental literature by Sano [7] to describe the penetration of tracer ions into the hybrid layer following acid etching of dentine. Nanoleakage is said to be distinct from microleakage as it describes the penetration of oral and pulpal fluids through porosities created by the incomplete infiltration of resin monomers around collagen fibrils.

gradual increase in hydrolytic degradation in the hybrid zone over nine months of immersion in water. These authors used regression analysis and found a gradual decrease in microtensile bond strength to dentine with increased penetration of silver, and reported a higher correlation at longer time intervals than shorter ones. Water nanoleakage becomes of minor clinical consequence when an adequately thick adhesive is present [110]. One-step self-etch adhesive are claimed to be rendered more hydrophobic by covering it with more coats of adhesive resin and thus minimising water movement and consequent structural damage. Such damage of the polymer network of the adhesive would be expected to facilitate water diffusion [110]. Since the present experiment involved immediate bond testing (without water storage), the suggested protective effect of the adhesive could not be verified, and therefore, long-term immersion tests are clearly needed to verify the effectiveness of the so-called "protective" hydrophobic layer.

ii. Two-step total-etch bonding system (Adper Scotchbond Multi-purpose XT 1)

With the adhesive applied to the smooth dentine surface the flexural bond strength (corrected) (FS*) was 4.99 ± 0.96 MPa. When the dentine surface was roughened using 120-grit abrasive paper the value was significantly improved to 10.83 ± 2.17 MPa (*t*-test: $p = 0.67 \times 10^{-5}$) (Appendix 6, Tables 1, 2, and 3). However, the highest FS* values were obtained when the dentine surface was acid-etched prior to the adhesive (20.06 ± 2.31 MPa). While it is seemingly necessarily true that a rough surface topography will improve the measured joint strength compared with that to a smooth surface, because different pretreatments produce different retention figures it is crucial to determine the most appropriate topography for the best outcome [9]. It is clear from the results here that the mechanical interlocking obtained through roughening using 120-grit abrasive paper is less suitable than that obtained with the phosphoric acid etching. That is to say, each substrate (adherend) has to be specifically pretreated to generate a distinct surface roughness for the best results.

5.2.4 Zirconia

The combination of mechanical and chemical pretreatments have been reported to be particularly crucial to achieve durable bonding to ZrO_2 [113]. In their meta-analytic review, Inokoshi *et al.* [113] reported that the combination of Al_2O_3 gritblasting and MDP-containing resin cements achieved the best outcome. Such an outcome was said to be justified based on the known chemical interaction potential of MDP with ZrO_2 [114-116]. However, a

quantitative assessment of the chemical bond contribution of resin cements to ZrO_2 is yet to be explored. It may be noted that gritblasting zirconia may be associated with phase transformation in partially-stabilized zirconia (PSZ) that may compromise the long-term outcome of any bond [117].

Pretreatment with KHF_2 did not improve the 'adhesion' to ZrO_2. The observed mode of failure at the cement ZrO_2 interface (Figure 4.23 and 4.24) suggests limited chemical bond contribution. However, such an interpretation – based solely on mode of failure – might be (to some extent) subjective, and further EDS verification is required. A detailed investigation is needed to clarify further the chemical bond potential involving an adequate sample size when measuring interfacial strength, thorough EDS analysis, detection of compounds which provide evidence for the formation of a chemical bond, and aging of the specimen.

5.3 Fractography

Şanlı *et al.* [75] highlighted that using light microscopy to classify fractures into adhesive, cohesive, and mixed based on arbitrary criteria to be of little significance. Upon further examination of fracture surfaces, using an environmental scanning electron microscope and energy dispersive spectroscopy, remnants of cements and primers were detected, indicating some degree of cohesive failure [75]. The identification of the fracture origin is particularly important because this allowed the possibility of understanding the causes and sites of crack initiation. The origin of fracture provides important details concerning the possible cause of fracture [39]. For example, did the fracture initiation coincide with the maximum horizontal stress direction at the tension surface? Fracture origin always occurs at a stress concentration inherent in the specimen design [118], assuming that flaws introduced during fabrication are minimal or less influential.

One of the essential elements of this present study was to develop a laboratory test of the efficacy of dentine 'adhesion' that replicates the mode of failure and thus the underlying stress states observed in clinically-failed restorations.

5.3.1 Scanning electron microscopy (SEM)

The aim now was therefore to study fracture surfaces and identify failure origins. The fracture surfaces were initially examined using light microscopy and SEM was then used to

characterize classic fracture landmarks. The fractographic analysis was straightforward and relatively easy to interpret. Hackle lines radiating from a fracture mirror indicated the crack propagation direction. Failure location was assessed in using the fractographic landmarks mentioned earlier (Figure 4.14). The debonding of interfaces (that were strong enough to be tested) always initiated at the various joint interfaces and the crack growth direction was always from bottom (tension) to top surface. Furthermore, the fracture process seen here is suggested to echo the failure process that occurs intraorally [75, 91] and thus is seen to provide relevant and valuable quantitative information about intrinsic adhesion, suggesting valuable insights generated by the factorial test design.

5.3.2 Energy-Dispersive Spectroscopy (EDS)

EDS is a useful tool that can be employed to assess the elemental composition of a fracture surface and thus aids in confirmation of chemical bonding [9]. Prior to bonding, smooth surface stainless steel was analysed to provide a substrate control. After interfacial joint preparation and fracture, EDS indicated a significant modification of the substrate fracture surface due to presence of a continuous surface layer of ZCC, thereby showing some degree intimate contact, *i.e.,* failure was through cohesive fracture within the ZCC. $GIC_{\mathbf{A}}$ produced a less continuous remnant surface layer, indicating relatively less effective chemical bonding compared with ZCC (Figure 4.7). $GIC_{\mathbf{F}}$ showed very little or no potential of chemical bonding. This can be clearly seen from the results in Figure 4.7.

5.4 Mode of failure

Griffith explained that the theoretical strength of a material could not be approached due to inherent flaws [16]. However, identification and analysis of the main processes and the structural defects responsible for service failures is vital [32]. Development of a simple model that presents a possible scenario for service failure can help define the information needed to improve service lifetime [32]. Gale and Darvell demonstrated progressive bond failure, suggesting that a peel mode of failure is general and to be expected [12], *i.e.,* stress concentration is mainly at an edge so that the bulk of the interfacial joint is minimally stressed, and crack progression initiated from that edge site [119].

In analysing the fracture mechanism of three whole-crown *in vivo* failures, Quinn *et al.* [90] pointed out that compression curls are indicative that the final fracture had a flexural component. The way in which the load is applied during a test has to mimic that of the service conditions for failure interpretation to be meaningful [16]. Thompson *et al.* [120] characterized the surface fracture of 19 (10 Dicor, 9 Cerestore) all-ceramic crowns that had failed clinically. They verified that each of the Dicor crowns had the failure initiated along the internal surface. For the Cerestore crowns the failure began at the porcelain-core interface or cohesively inside the core substance [120]. They concluded that the locus of failure is primarily dictated by the locations and sizes of defects rather than by specimen thickness, which accords with the Griffith concept. Kelly [32] remarked that fracture toughness is better correlated with clinical behaviour, and that the fracture toughness of the substructure influences the clinical lifetimes of ceramic restorations. Despite the significantly higher fracture toughness of the ceramic restorations tested (Procera ~4.3, InCeram Alumina ~4.5, Bruxir ~6.5 $MPa.m^{1/2}$), Empress 2 (~2.6 $MPa.m^{1/2}$) had the lowest annual failure rate, suggesting that other factors were also involved [32]. Further development of higher toughness ceramics is not expected to improve clinical serviceability [16, 32]. That is to say, at this level of fracture toughness, efforts should be directed towards identification of failure origins, seeking the underlying causes and how to rectify them. Kelly also suggested that the improved clinical performance of Empress 2 (despite lower fracture toughness values) may be attributed to its amenability to etching and subsequently improving the interfacial bond strength [32]. Such a concept may of course be tested with the present method. Two types of crack propagation through brittle materials can be identified; stable and unstable [9]. Stable crack propagation involves a macrocrack formation and slow growth from the failure locus, and the fracture surfaces are relatively featureless due to low levels of stored energy consumed [9]. Unstable crack propagates intermittently and has a rough surface with a characteristic saw-tooth shape, *i.e.*, alternating crack growth and arrest [9]. The breakage in static tests is sudden, unstable, uncontrollable, and catastrophic [90], leading to erratic patterns on the fracture surface and suggesting failure origin characterization as a rational goal at this level.

5.5 Key aspects

The four-point bend (4pb) test has been employed here to assess the influence of various retention systems on the flexural strength of the union, that is, in effect testing in tensile peel. A detailed technique was developed, and the method differentiated between groups and subgroups, showing discriminatory power, better indeed than appears to have been achieved with other methods. As mentioned earlier, the use of the log transformation is to stabilize the variance, as is often necessary for strength data, and thus for helping to meet the assumptions of inferential statistics [75].

Experimental design has two main levels, initially involving the identification of the most influential independent variables, then the identified factors are optimised for a better outcome [121]. Quantitative factorial design is a systematic strategy often determines a promising direction of further research [122]. Factorial designs are classical screening methods narrowing the future research focus towards the most important variables [121]. Factorial designs might also be beneficial in properly obtaining control samples, *i.e.,* no treatment *versus* treatment at every level. A test set up should be compared to a stable and reproducible behaviour [15]. Successful replication of the significant findings depends largely on the background knowledge being reflected in the technique and avoiding critical mistakes [123], for example the establishment of a correct joint geometry which is not properly appreciated despite its importance. The development of a highly-reproducible specimen preparation method is challenging [15], and it becomes more critical at the level of the controls. A common practice in the dental field concerning control samples is to compare with the current 'best-performing' products, where the same specimen preparation defects may have influenced the outcome [15]. While there is some value in this, for comparisons across reports, it is insufficient in general to understand a system fully. Experiments employing factorial designs have two or three factors (which are the etch, primer, and adhesive in the present context) which are either present or absent, exploring the idea of possibilities and allowing multiple questions to be asked in a well-controlled and systematic manner [124].

Adhesion to dentine remains difficult despite decades of research. Pretreatment of dentine or the primer employed are important factors that influence the maintenance of the integrity of the adhesive interface formed with the various kinds of restoration materials [9]. Adhesive materials interact with dentine in a variety of ways: mechanically, chemically, or both [33]. However, the relative merit of such ways has not been ascertained by quantitative examination. Test methods commonly used to measure intrinsic adhesion have serious

difficulties in the implementation of the theoretical assumptions [16]. Besides, the experimental designs typically used in the dental literature are less efficient in highlighting the quantitative differences between multiple independent variables. This has led to confusion in that literature regarding the applicability of the adhesion mechanisms in various dental contexts. Thus, there is a definite need for information concerning the magnitude and mechanism of action of such forces acting across an interface. Such data is vital to monitor objectively the progress of development of dentine bonding agents.

The primary objective of the present work was to identify a specimen geometry and loading conditions that could achieve a consistent mode of failure, and thus reflecting a reliable and reproducible experiment. Development of a specimen of appropriate size scale is important to match the amount of energy stored elastically paying for the fracture [16] but also to avoid the excessive variability of smaller specimens due to natural dentine structure. Such a method is also important for the relevant biological samples, *i.e.*, human teeth, that are difficult to obtain and thus minimise waste.

The adhesive joint ability to continue to function for long periods in the intraoral environment remains a prerequisite for effective stress transfer, but it is by no means clear that this has in fact been attained. Occlusal loading and hydrolytic attack of susceptible sites of resin polymers are possibly the most relevant challenges. The rate of hydrolytic attack is relatively greater if the temperature is increased or the joint is being loaded [9]. However, the rate of strength loss due hydrolytic attack is significantly greater than that in the presence of applied load alone [9]. As mentioned earlier, Gale and Darvell (5) suggested progressive loss of adhesion in peeling mode, however, the rate of loss of chemical *versus* mechanical means of retention should be carefully investigated. Generally, upon immersion in water, mechanical retention is expected to last longer compared with chemical bonding because this latter is more susceptible to hydrolytic attack. However, some hydraulic cements, *e.g.*, GIC, are also expected to improve their mechanical and adhesive bond properties upon water immersion.

Truly adhesive materials would offer many benefits, perhaps the most significant of which is the conservation of tooth structure and minimization of the operative procedure [9]. For many years, the three-step total-etch system has been considered the ‘gold standard’ for bonding RBCs to tooth structure [125]. Clinical experiments, including some over 12 years, as well as long-term artificial ageing laboratory studies, have provided evidence of effective dentine bonding [125]. Roughening of the dentine surface increases the surface area and thus

enhances retention through mechanical and chemical (when feasible) means. Mechanical retention is facilitated through penetration of resin and formation of resin tags within the etched region, while adsorption is achieved through chemical bonding to both the inorganic and organic components of tooth structure [33]. Mechanical keying probably remains the dominant and most important mechanism of union [11]. For example, mechanical abrasion was reported to improve the interfacial strength to various substrates [9]. However, the resultant surface topography is relatively not suitable for establishing mechanical interlocking against tensile stress normal to that surface. Club-headed nodular structures (Figure 5.1 a) in the bonding material (from re-entrant surfaces) (Figure 5.1 b) are by far the best surface topography for mechanical interlocking of the adhesive on the surface of the adherend [9]. Abrasion also cleans the surface of dentine and subsequently enhances the wetting by bonding agents, if all debris removed. It has also been suggested that the improved joint strength is due to changes in stress distribution favouring plastic deformation [9].

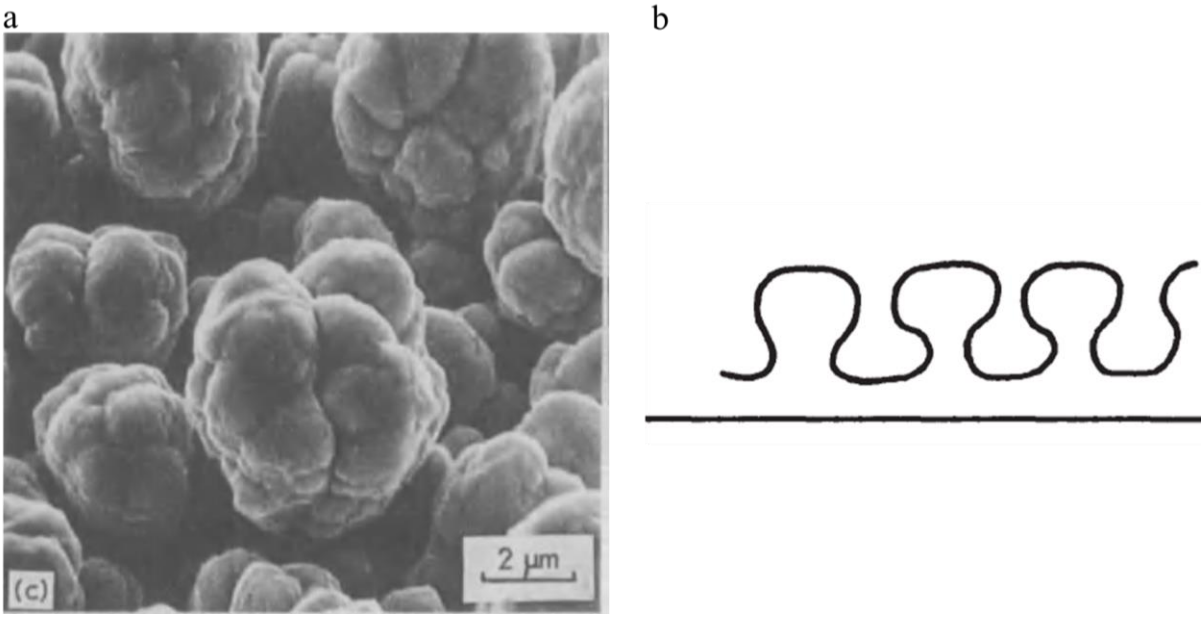

Figure 5.1 **(a)** Club-headed nodules on electroformed nickel foil. **(b)** Club-headed nodular structures. Adapted from '*Adhesion and Adhesives'* [9] with permission from Professor Anthony Kinloch.

Post-operative sensitivity (POS) remains an issue with RBC in posterior teeth especially in Class II[6] (Cl II) and mesio-occluso-distal (MOD) restorations [126]. POS could disappear within 24 h or up to 90 d, subsequently requiring restorations replacement [126]. Conventional GIC liners, frequently placed as a means of reducing the incidence of postoperative sensitivity, are believed to bond adhesively better to dentine [101] providing marginal seal for the isolation of dentinal tubules. Hence, such a seal is expected to reduce microleakage and bacterial penetration (or their byproducts) thus minimizing hydrodynamic stimuli and pain provocation. In a systematic review of pertinent clinical studies, Schenkel *et al.* [127], assessed the effects of cavity liners under RBCs (Cl I and Cl II) and questioned the treatment as the supporting evidence was inconsistent and the benefits only shown at some, but not all, time points. It was concluded that GI liners under RBCs in posterior teeth had no influence in reducing POS [128-134]. Strober *et al.* [133], further suggested that the elimination of resin-modified GI lining under RBC fillings would result in an annual saving of around US$82.8 million in the United States alone. The discrepancy between *in vitro* experiments and clinical studies concerning the adhesive potential of GI systems may suggest that the laboratory test methods used are not reflecting real world behaviour.

The study of fracture surfaces is an important means to enhance the understanding of the mechanical properties of a system [90], that is, fractography is a systematic approach to the identification of failure origins [90], with the potential of identifying underlying causes. Defect characterization and verification is a crucial method in minimizing the occurrence of structural weaknesses and thereby of improving mechanical properties [90]. It is clear that SEM combined with EDS may be quite helpful in the analysis of fracture surfaces. Generally, SEM can be used to examine adherend bonding surfaces after being roughened to assess the retentive potential, *i.e.,* identification and characterization of various surface topographies for mechanical interlocking [9]. Then, the composite interfacial zone can be further examined (via longitudinal cross-sections) before fracture to assess the depth of penetration of the adhesive and the subsequent mechanical interlocking to the surface topography [9]. The third and the most important step is to assess whether mechanical interlocking does occur in a relevant mode of loading, and its contribution to the strength of the joint [9]. EDS can be used as a complementary tool to investigate further details of fractured joints, *e.g.*, the effect of the atmospheric oxygen-affected layer, contaminants, hydrolytic degradation, and various

[6] A Class II cavity is a type of dental cavity that occurs in the proximal surfaces (sides) of posterior teeth (premolars and molars) [33].

precipitates after surface pretreatments on the ‘adhesive’ bond strength [9]. However, without a valid interfacial bond test with adequate discriminatory power, the correct identification of the weakest link under the relevant mode of failure, and subsequent interpretation of the fracture surface analysis, will be of limited value.

5.6 Summary of the principal results

- The symmetrical four-point bend test was found to be a convenient and successful method for both monolithic beams and interfacial joints. The test set-up employs a relevant mode of loading with a subsequent failure pattern initiating at the tooth-filling interface, and at a relevant specimen size. The method has the potential to be applied to a wide range of ‘adhesive’ and ‘retentive’ systems employed in the dental field, enabling the exploration of clinical practice guidelines with relatively greater authority, *e.g.*, concentration of etching gel, etching time, GIC bond to tooth substance, and so on.

- The role of the adhesive step of three-step total-etch system in the development of immediate bond strength has been questioned. Further research will be needed to verify the role and behaviour of the adhesive in the long term.

- The correction factor should be applied consistently for ‘thin’ beams for better approximation of maximum stress.

5.7 Future work

This project focused mainly on the development and optimization of a test system with discriminatory power, and most experiments were performed to demonstrate that the method is workable and effective. Many different adaptations to some adhesive systems were left unaddressed due to lack of time. Future work would involve a deeper analysis of particular adhesion mechanisms and attempts to understand the difficulty in establishing the theoretical expectations of various systems. The following ideas could be tested:

- Determine whether or not the adhesive layer has a protective role in maintaining the bond to dentine during water storage (at 37 °C).
- Perhaps the most important feature of GIC is its potential to bond chemically to the tooth substance without the need for any additional treatment or adhesive. However, the discrepancy between *in vitro* and *in vivo* studies suggests that the laboratory experimental set up is quite different from the clinical scenario. The dual objective of obtaining values for mechanical properties and establishing the existence of a chemical bond to tooth substance has confounded the experimental set up. That is to say that if GIC successfully established the bond to tooth structure, then it can be successfully used as a liner providing necessary protection against caries attack. Detailed information on the conditions necessary to optimize the chemical bond could be achieved with the current method, *e.g.,* etching time *vs.* concentration, whether to wash the conditioner or not, minimum time required, water immersion, powder-liquid ratio, *etc*.
- Metal-bonded ceramics: fabrication of cobalt-chromium beams, for example, with a porcelain coupon interposed in the symmetrical four-point bend set up might be a sensible way to evaluate the effect of various surface treatments on the bond of porcelain to non-precious alloys.
- There is a lack of systematic evidence concerning the use of hydrofluoric acid to etch the internal surface of ceramic restorations and phosphoric acid to etch the tooth (enamel and dentine). The symmetrical four-point bend test can be used to search systematically the effect of concentration and etching time, employing controls and replicates as necessary, and avoiding the usual arbitrary randomness of a very small number of such conditions.
- The analysis of SEM to interpret etching patterns should be standardized for clarity. For example, in the present work on zirconia the SEM work showed that KHF_2

(potassium hydrogen fluoride) did not produce a detectable etch figure, however, in another study using the same etching protocol SEM images were interpreted as an evidence of good adhesion. Inconsistency in bond strength findings was attributed to the lack of a standardized bond strength testing protocol. However, it would seem sensible to study the relationship to micromorphological findings. The aim here will be to suggest clear objective criteria that can be quantified and independently verified, avoiding interpretations merely based on the strength of the bond obtained.

6. Effect of cross-head speed on the bond strength of dental resin to tooth structure – a review and re-analysis

6.1 Introduction

The phenomenon of viscoelasticity may be considered as the combination of an instantaneous elastic behaviour, a time-dependent reversible (retarded) deformation, and irreversible flow [11]. When subjected to external forces, all organic polymers – with no exception – show various degrees of viscoelasticity [135]. Across the glass transition (T_g) polymers show a substantial change in chain-segment diffusivity and subsequent deformation. T_g is not a sharply-defined temperature as would apply for a first-order event; it is a more gradual yet reversible transition in properties occurring over a narrow range – it is a second-order outcome, dependent on diffusive processes. The response to an applied stress is therefore dependent on the relative ease of chain segment rearrangement, and consequently all mechanical properties are affected. Reptative movements of chain segments are affected by those stresses and steric hindrance both internally and between adjacent molecules [11]. As the size of side groups increases it becomes progressively more difficult for bond rotation around the backbone chain, that is, the activation energy is raised, and thus also for chain segment movement. Branching and cross-linking exaggerate the effect. Polymers with side chains have (local) crystallization inhibited, thus contributing to the formation of amorphous regions, but also those side chains will act as plasticizers, decreasing T_g, up to a certain point [11]. Because these processes are diffusive time is important, hence the retarded and flow components of the rheology depend on the timescale of observation, and thus by implication the rate of loading affects the outcome: diffusion implies stress relaxation. It follows also that mechanical properties depend profoundly on temperature with respect to the T_g as this affects the availability of the activation energy for diffusion.

The resin matrix for dental composites or filled resins (FRs) is no exception, its behaviour being sensitive to the rate of loading or, equivalently, it has strain rate-dependent properties. Increasing strain rate is equivalent to using a shorter duration test, *i.e.*, a specimen is under load for shorter time to reach failure, say. On the principle that, for relevance of outcome, test conditions must mimic those of service [15], it is implicit that the cross-head (XH) (or equivalent) speed (XHS) of any machine used in the testing of such rate-sensitive materials should be guided by the rates of strain experienced in practice, for example, corresponding to the rate of loading through tooth occlusion during chewing [136]. Indeed, Eliades *et al.* [136] have questioned the clinical relevance of bond strength tests conducted at commonly employed XHSs (0.1 ~ 10 mm/min), claiming that a rate of 2000 mm/min would be relevant. However, while this might be true of jaw movements it is difficult to see how this

relates to contact displacement for a dental device or material, when proprioception intervenes adjusting the magnitude, direction, and rate of occlusal forces, and thus the XHS that might be used in simulation. The point of relevance is nevertheless well taken and must remain open. Armstrong *et al*. [18] noted that such high velocities are generally inaccessible in practice, *i.e.*, in the usual kind of laboratory setting. Investigation of XHS effects is indeed warranted. It also follows that testing should be at temperature relevant to that of service in the mouth, as well as the materials being equilibrated with water at the tonicity of saliva (usually), for better relevance.

Water sorption also has a profound effect on the mechanical properties of FRs because it acts as a plasticizer, increasing effective free volume and reducing the efficacy of entanglements [137]. Since that sorption is diffusive, equilibration takes time, and specimens might not be uniform in properties throughout their thickness [138], the surface being affected initially and the changes slowly reflected in bulk properties [137]. While a microhybrid filled resin (FR) upon immersion in water for 90 d lost ~28% of the initial flexural strength (at 0.75 mm/min) [139], Musanje *et al.* [81] reported a slight increase in flexural strength at 9 months' immersion in artificial saliva (at 0.50 mm/min). With systematically-controlled differences in degree of conversion, filler volume fraction and proportion of silane-treated filler in experimental FRs, Ferracane *et al.* [140] reported that long-term aging (2 y) in water had little influence on flexural strength (at 0.254 mm/min). However, in order to dissect the effect of XHS in such results, and examine possible interactions with other confounding factors (such as degree of conversion, age, temperature, exposure to water), a systematic experimental design involving adequate controls and replicates is essential to extract the maximum information about the components of variation and exclude the effects of arbitrary choices by the experimenter.

Studies of the effect of crosshead-speed (XHS) on mechanical properties and on the bond strength to enamel and dentine of FRs are in fact rather few, but they show inconsistent and contradictory results. The aim now was to re-analyse all available observations to go beyond mere correlations, attempting to establish a model cause and effect relation, in order to clarify and emphasize the confounding effect of XHS on strength measurements, and what might be done to avoid those effects, and thus obtain clinically-relevant information. A literature search was conducted using Scopus, PubMed, ScienceDirect and Google Scholar databases. Every potentially-relevant study found through the search was examined.

6.2 Static mechanical strength

In a so-called 'static' mechanical test for strength, the intention first is to find the load at which failure occurs. This can only be done by gradually increasing the load until collapse occurs, but this means that a choice of deformation rate [essentially crosshead speed (XHS)][7] must be made for practicality – the test needs to be conducted in a reasonable time. However, knowing that polymers are strain rate-sensitive means that we know in advance that all mechanical properties will be more or less affected by the choice of strain rate. The problem is then one of selection. Tests carried out at different temperatures add a further layer of complication. That is to say, intraoral temperature (and its fluctuations) only complicates matters in terms of extrapolation to service from the results of laboratory experiments performed at other than such a temperature and thus the interpretation of results. When placed intraorally, polymers are subjected to high water activity, when sorption changes their properties as mentioned above, notably T_g and modulus of elasticity [16]. There is therefore an obvious necessity for standardization of the exposure time that is required for water equilibration at a chosen temperature (*e.g.*, 35 or 37 °C) to decrease ambiguity, avoid guesswork and improve relevance [15]. This means that there is really only one question to be answered: what is the strain rate-sensitivity of the system under the normal service conditions of temperature and water-sorption status? Apart from the value of understanding a polymer's intrinsic behaviour, a start can then be made on an assessment of the expected behaviour under service conditions where load and strain rate are likely to be highly variable. In addition, standardized conditions may help in comparisons between products, quite apart from being essential in standards compliance testing.

The use of just one XHS is typical in the dental literature; for example 0.05 [141], 0.5 [142-147], 1 [148-153], 2 , 5 [154-159] and 10 mm/min [160, 161]. However, this choice has been entirely arbitrary, relying on previous examples, convenience or misguided application of an ISO standard [162].

Strain-rate sensitivity, or its common proxy, cross-head speed sensitivity (XHSS) thus needs to be assessed in the face of the size of the scatter that is inevitable in all such testing. Taking as the simplest case the comparison of the effect at just two rates, essentially a *t*-test, this means choosing a range of rates that will give a sufficient 'lever', but coupled with a sample size large enough to reduce the error of the estimate of the mean property value of interest to

[7] It is recognized that load-controlled testing is also possible, but no examples in the present context are known. Even so, consequent strain rate is a monotonic increasing function of load rate and the arguments remain relevant.

be small in relation to the difference in those means at the two extremes. Since polymer properties are essentially dependent on the rates of diffusive processes as mentioned above – *i.e.*, for chain segments and side-groups – and XHS is a rate of change (and the proxy for strain rate), it is proper and expected that XHSS is a function of log(XHS) (equivalently, the geometric mean is the relevant approach to rate data, which is tantamount to using the arithmetic mean of log data) [163]. Effectively, we may write that the *t*-statistic will have the following form:

$$t = \frac{dy}{d\log_{10}(s)} \times \frac{\log_{10}(s_2) - \log_{10}(s_1)}{se(\bar{y}_2 - \bar{y}_1)}$$

where *y* is the property value, and *s* is XHS ('*se*' means standard error). Similarly, if the trend of behaviour is to be studied at multiple rates, linear regression in terms of log(*s*) is required.

No polymer deformation can be expected to be strictly affine (except in the limit of diamond), thus some plastic (*i.e.*, irrecoverable) deformation must occur under any load big enough to cause chain segment movement (or direct ordinary thermal motions). In hard glasses, *i.e.*, well below the T_g, such loads may be relatively high – or the duration of application long.

Over the range of crosshead speeds of 0.01 ~ 10.0 mm/min there has been reported (from Analysis of Variance, AoV) to be no effect on microtensile bond strength [164-166]. Armstrong *et al.* [18] suggested that FRs exhibit viscoelasticity at very low or high testing speeds so as to comply with the general behaviour of viscoelastic materials, even though such a selective limitation does not exist: it must apply, always. Yamaguchi *et al.* [164] concluded that the small size of 'microtensile' test specimens may have allowed a plane-stress condition during testing, that is, due to the relative thinness of the specimens (bonded area of ~1 mm^2), all the stresses are acting on the same plane, although how this was thought it could change the rheological behaviour is unclear. Generally, when work is done over a small range of XHSs, failure to detect the viscoelastic behaviour of FRs is both common and expected, especially given the usual scatter in results and typically small sample sizes. A more practical approach would be to include a wider scale of XHSs; this would be of clinical relevance as well. Besides, conclusions that deviate from the elementary polymer science expectations should be made with great care.

6.3 System compliance and specimen displacement

Most material test systems measure cross-head or actuator displacement and this can be used as a measure of specimen deformation. However, the displacement output recorded by the system is actually the sum of the system compliance and the specimen deformation. That is to say, stiffness measurements directly obtained from the XH movement need to be corrected to take into account the stiffness of the load string as well as the flexure jig [167]. Test speed is the rate of relative movement between the plane of the specimen supports and the load point. As the loading force increases, it is not only the specimen that will be strained, but the rest of the load string will also experience some deformation as well, most especially the load cell [88] – this cannot be recorded without separate instrumentation (displacement transducer) or being calculated from the load cell's compliance at the current or failure load. Even then the compliance of the test jig itself may be appreciable. Thus, when a specimen's displacement is small through being stiff, machine compliance can be a significant portion of the total XH displacement, that is, the load cell compliance will dominate. In contrast, in the case of a three-point bend (3-pb) test of materials with low modulus of elasticity (E), the displacement of the point of contact with the beam can be far greater than the load cell displacement, especially for thin beams. But still, in order to determine the actual displacement of the specimen load point, the machine compliance must be subtracted from the total displacement of the cross-head [88]. Since each machine system and the loading jig or grip arrangements have their specific compliances, generalizations cannot be made; explicit determinations are necessary. Retrospective calculation is not possible in the absence of full detail.

6.4 Regression Analysis *versus* Analysis of Variance

Analysis of variance (AoV) and regression analysis have several similarities, in fact regression analysis is a form of AoV; both focus on variation between population samples and use sums of squares to describe the deviation from the mean. However, there are fundamental distinctions that must be highlighted. The purpose of (ordinary) AoV is to determine whether there are any statistically-significant differences between the means of samples from two or more independent (*i.e.,* unrelated) populations [168]. The purpose of regression is rather different: to determine whether a systematic trend exists in the data. It can therefore be used to produce a formula which can be used to predict the dependent variable given the value of the independent variable [168]. When AoV is used to analyse the relationship between XHS

and mechanical properties of FRs a consistent significant relationship over the (typically narrow) range of XHSs used is hard to achieve [169, 170]. This is directly because of the limited range of XHSs tested and the fact that tests are not usually conducted at a temperature in the vicinity of T_g of the FR (tests are commonly carried out at room temperature which is necessarily higher than the temperature of the environment in which the curing occurred, *i.e.*, intraoral temperature is higher than room temperature). This creates confusion regarding the effect of XHSs on those mechanical properties; in turn this produces unsafe conclusions regarding recommended XHS ranges to be used as standards [136, 171-173].

The principles and the advocated practices of such tests must be carefully examined before data analysis to avoid erroneous findings and faulty clinical interpretations. More or less all of the presently reviewed papers used AoV and *t*-tests (*i.e.*, AoV on two samples) to examine the differences between FRs in relation to XHS, that is, all except [174-177], despite the given known relationship between XHS and observed mechanical properties of FRs [163]. In order to establish such a relation, regression analysis depends on the order of the data sets – the abscissa (the independent variable) is necessarily scalar, and that information is taken into account. Thus, regression analysis incorporates the natural ordering of groups, and the values of their location on the abscissa, so as to calculate the slope, and thus constitutive equations can be developed. AoV does not take natural order into account; improper use thus ignores (indeed, discards) highly-important information – which information is at root the whole point of the exercise.

The log transformation can be used to stabilize the variance of data and reduce the spread [178]; this is often necessary for strength data [75]. In the process of data analysis, transformation is a basic mathematical technique replacing a variable by a function of that variable, often done better to meet or approach the assumptions of normality and variance homogeneity, and thus better support the analytical methods to be used. Log and other transformations are thus used to reduce skewness and equalize dispersion, but do not change the rank order of the values. Even though transformed data are employed in an analysis, conclusions can still be made on the regular scale [179].

Other errors are possible. Oshida & Miyazaki [177] using tensile bond strength (log bond strength and log XHS), claimed that there was no XHS effect when the test was conducted below 1.0 mm/min, but for XHS >1.0 mm/min there was an increasing strain rate effect. In addition, despite the regression being reported as non-significant (NS), they also (and thus quite

improperly) reported increasing values of flexural strength and modulus of elasticity (MoE) with increasing XHS (0.1, 0.5, 1.0, 5.0, and 10.0 mm/min) for the material Z100 [177]. However, when now the same data was subjected to regression analysis (see below) a highly-significant slope was found for all properties. A possible explanation for this discrepancy is that they used only the means of the tensile bond strength and E, not individual values, thereby greatly reducing the degrees of freedom for the statistical test (3 *vs*. 48, 34, and 34). However, no analysis details were given. Hooi *et al.* [175] and Hooi *et al*. [176] may also have used just the means in their analysis of the biaxial flexural strength, which thus affected their reported value of r^2.

Takemori *et al*. [169] reported that XHS did not affect the tensile bond strength. They employed four XHSs (0.5, 1.0, 3.0, and 5.0 mm/min), taking 5.0 mm/min for the control group in three separate *t*-tests (a very weak approach to the analysis). Eliades *et al.* [136], Munoz *et al.* [180], Shooter *et al.* [181] and Kumar *et al.* [182] did not detect (all from AoV) any significant difference between the FRs studied. It is to be expected as a matter of principle that differing FR formulations behave differently in different situations or test conditions – identity is vanishingly unlikely. The task then is to quantify the magnitude of differences, and not merely to look for a significant result: it is not a statistical problem as such. Thus, in most work we already know that there must be a net effect, or a difference in properties, because the matrix is polymeric and that therefore testing for a significant difference in a weak experiment is pointless. The question is always: is it big enough to matter? In principle, limits can be put on a value by a NS result, but of course because they cross zero (on the natural scale) it is not of much help (using log-transformed data gives a different interpretation). The problem of large scatter simply reflects badly on either the design of the specimen or the execution of the bonding (for example), or the material curing, or all of these; even so some scatter is inevitable. Sample size thus plays a vital role in identifying the distinctions between FRs or conditions: discriminatory power depends on it. Absence of detection does not mean absence of effect.

6.5 Importance of sample size

Experimental studies evaluating the effect of test machine cross-head speed (XHS) on bond strength have yielded contradictory results. Some might say that this is not entirely unexpected due to the large number of publications. Although the observed differences noted could be true findings rather than random errors (although there are no grounds for believing that polymer behaviour could run counter to general expectations), the inconsistency is

probably and commonly to be attributed to sampling variability because small sample size has a great influence on the statistics of the outcome [183]. Certainly, small sample size is a common feature of papers in the field. Another possible explanation may lie in the fact that no two authors have used the exact same approach. A standardized and reproducible test regime is necessary if comparisons of materials and procedures between reports is to be of any value.

Tamura *et al.* [170] reported (from AoV) that an increase in crosshead speed (0.1, 0.5, 1.0, 5.0 and 10.0 mm/min) was associated with an increase in average shear bond strength to dentine. The exact opposite effect was reported by Bishara *et al.* [184] (from a *t*-test) and Eliades *et al.* [136]: increases in crosshead speed from 0.5 to 5.0 mm/min and from 1 to 200 mm/min, respectively, were associated with significant decreases in shear bond strength. Hara *et al.* [172] showed (from AoV) statistically-higher shear bond strengths for specimens loaded at 1.0 and 5.0 mm/min compared with those at 0.5 and 0.75 mm/min. Lindemuth and Hagge [171] reported (from AoV) that, with enamel, no significant differences were noted in shear bond strength with increasing XHS, however, with dentine, rates of 0.5, 1.0 and 5.0 mm/min were associated with significantly higher shear bond strengths than at 0.1 and 10.0 mm/min. Shalkey and Burgess [185] examined the shear strength of acrylic rods at a range of XHSs (0.5, 1.0, 5.0, 10, 20 and 50 mm/min) and reported (from AoV) that only at 100 and 200 mm/min was the shear strength significantly different. Others have reported that XHS had minimal influence on shear bond strength [173, 186, 187].

Oshida and Miyazaki [177] reported that at XHSs of 0.1, 0.5 and 1.0 mm/min there was no influence on the tensile bond strength to dentine, while at 5 and 10 mm/min there was a significant increasing difference. Other studies have not found significant differences due to XHS in tensile test results [164-166]. It is confusing when inconsistent findings are encountered, clouding theoretical expectations. Such a general finding suggests that more fundamental work is needed. Even so, it is already clear that many analyses are suspect.

6.6 Materials and Methods

The reports examined and available details of the work done are given in Table 6.1.

Extracted data were tabulated in a worksheet (SigmaPlot, v. 15; Systat Software, San José CA, USA). Only Oshida and Miyazaki [177] provided full data sets so the regression analysis was standard. For all others, where only means, standard deviations and sample sizes were given reconstruction was necessary. This utilized a user-defined ‘transform’ (*i.e.*,

calculation) (in SigmaPlot) to obtain the necessary sums and sums of squares to obtain a regression model and related statistics (Appendix 10), taking log(XHS) as the independent variable, as indicated above as being appropriate.

Likewise, the figure of merit for the range of XHSs used was found in terms of the log values (log speed range, LSR) from upper (U) and lower (L) values:

$$\mathrm{LSR} = \log(\mathrm{XHS_U}) - \log(\mathrm{XHS_L}) = \log(\mathrm{XHS_U}/\mathrm{XHS_L})$$

Because of the variation in systems and procedures, direct comparability between results is not possible. To obtain other figures of merit for comparison of studies therefore requires a normalization procedure. Given that log(XHS) is the independent variable, the estimate of the constant term in the regression, b_0, which is the ordinate value at XHS = 1 mm/min, was taken as a convenient reference point. Thus, relative residual noise was calculated from the residual variance, $s^2_{y.x,}$ as the scaled standard residual deviation, SSRD:

$$\mathrm{SSRD} = \frac{\sqrt{s^2_{y.x}}}{b_0}$$

Likewise, the relative effect size, RES, (*i.e.* proportional change per decade) was obtained by dividing the slope by b_0:

$$\mathrm{RES} = \frac{b_1}{b_0}$$

The standard error (se) of the RES is similarly obtained:

$$\mathrm{se(RES)} = \frac{se(b_1)}{b_0}$$

Sufficient sample size is a pre-requisite to address adequately a research question. The magnitude of the difference to be detected defines the discriminatory power needed. The smaller the difference to be explored, the greater the discriminatory power is needed [183]. Accordingly, sample size, N, is to be considered as a further figure of merit.

These figures of merit address the questions of the quality of the design and execution of the work, as distinct from the coefficient of determination (r^2), which is only a measure of the quality of the fit of the model to the data.

6.7 Results

The results of the regression analysis are shown graphically in Figures 6.1 – 6.9 and detailed in Tables 6.1 – 6.5, where the figures of merit are also given.

Table 6.1 Studies of the effect of XHS on test values for FRs, showing reported details. DW: distilled water; DiW: deionized water; NS: not stated. Enamel and dentine were human unless otherwise stated.

Ref	Substrate	Bonding agent	Property measured	Temp / °C	Sample size	Test type	XHS / $mm.min^{-1}$	Medium	Statistical analysis
[166]	Z250	Single Bond, Clearfil SE	adhesion, dentine	37	5	microtensile	0.1, 0.5, 1, 2, 4	DiW	2×AoV, Tukey
[171]	Prima TPH	Prime & bond Dentsply	adhesion, enamel dentine	37	10	shear (chisel)	0.1, 0.5, 1, 5, 10	100 %RH	1×AoV, post-hoc t-test
[173]	Ortho Brackets	Transbond XT	adhesion, bovine enamel	NS	30	shear (wire loop)	0.1, 0.5, 1, 5	NS	1×AoV
[172]	Z100	Single bond	adhesion, bovine dentine	37	30	shear (knife edge chisel)	0.5, 0.75, 1, 5	NS	1×AoV, Tukey
[136]	Ortho brackets	Concise, Transbond	adhesion, enamel	37	20	shear	1, 200	DW	2×AoV, Tukey
[165]	Z100	Clearfil SE	adhesion, dentine	37	NS	microtensile	0.01, 0.1, 1	0.5% chloramine	2×AoV, Tukey
[170]	Clearfil Apex	Clearfil SE, Clearfil tri-S	adhesion, bovine dentine	37	10	shear knife-edge	0.1, 0.5, 1, 5, 10	DiW	2×AoV, Tukey
[169]	Silux Plus	Clearfil New Bond	adhesion, dentine	NS	10	tensile	0.5, 1, 3, 5	tap water	t-test
[186]	Z250	Adper Single Bond	crunch-the-crown	37	10	compression	0.5, 1, 2.5, 5, 10	DW	1×AoV, Tukey
[164]	Clearfil Apex	Single Bond. Clearfil SE	adhesion, bovine dentine	37	10	microtensile	0.1, 0.5, 1, 5, 10	“water”	2×AoV
[184]	Ortho Brackets	Transbond XT	adhesion, enamel	NS	40	shear	0.5, 5	NS	t-test
[185]	Acrylic resin	--	bulk property	NS	10	shear	0.5, 1, 5, 10, 20, 50, 100, 200	NS	AoV, Tukey B post-hoc
[177]	Z100	Scotchbond Multi-Purpose	adhesion, bovine dentine	37	10	tensile	0.1, 0.5, 1, 5, 10	DiW	NS
[187]	Solidex Shofu	--	bulk property		12	shear (piston device)	0.5, 1, 1.5, 2	NS	1×AoV
[181]	Ortho Brackets	Ortho Solo, Enlight adhesive	adhesion, enamel	NS	25	shear (sharp chisel)	0.5, 1, 2, 5	NS	1×AoV
[188]	P50	Scotchbond MP	adhesion, dentine	37	10	shear (blunt knife chisel)	0.5, 1.2	“water”	NS
[180]	Z250	Adper Single Bond, XP Bond	adhesion, dentine	37	5	microshear	0.5, 1, 5	“water”	2×AoV, Tukey
[176]	soda-lime glass	--	bulk property	NS	24	biaxial flexure	0.01, 0.1, 1, 10	dry storage	GLM
[174]	GrandioSo, Filtek Supreme XTE, Venus Diamond, Venus Flow, SureFil SDR Flow	--	bulk property	37	15	compressive and flexural	1, 3, 5	DW	1×AoV, Bonferroni
[175]	soda-lime-glass	--	bulk property	NS	24	biaxial flexure	0.01, 0.1, 1, 10	desiccator	GLM
[189]	Experimental unfilled resins and FRs	--	bulk property	37	90	biaxial flexure	0.1, 1, 10	dry storage (NS), DW	1×AoV, Bonferroni
[182]	Z100, Z250, Filtek Supreme XT, Filtek Supreme Translucent	--	bulk property	37	30	biaxial flexure	0.01, 0.1, 1, 10	dry/wet (DW)	1×AoV, Bonferroni

6.7.1 Bond strength

6.7.1.1 Tensile tests

The statistical re-analysis results are given in Table 6.2 and Figure 6.1, for the two studies of this kind. Data from Oshida and Miyazaki [177] (Figure 6.1 a-c) showed a significant relation for increasing stress at failure with increasing XHS, *i.e.*, positive effect, while that from Takemori *et al*. [169] was not significant. This latter result may be attributed to the low XHS range (LSR = 1) and to a lesser extent to the large scatter of the results [169] (relative residual noise = 0.26).

Table 6.2 Results of re-analysis of the literature on tensile tests.

	Bonding agent	r^2	$b_0 \pm s(b_0)$	$b_1 \pm s(b_1)$	F	P	N	SSRD	RES ± se	LSR	Test temp / °C
Oshida and Miyazaki [177]	Scotchbond MP	0.138939	8.821717 ± 0.571614	2.214946 ± 0.795879	7.745180	7.67901×10^{-3}	50	0.455357	0.251079 ± 0.090218	2	RT?
	Z100 (Flexural)	0.133999	124.15250 ± 2.130813	8.084507 ± 2.966810	7.427189	8.93872×10^{-3}	50	0.120612	0.065125 ± 0.023896		
	Z100 (MoE)	0.543178	15.328880 ± 0.056290	0.592099 ± 0.078375	57.073860	1.04345×10^{-9}	50	0.025806	$0.038626 \pm 5.112875 \times 10^{-3}$		
Takemori *et al*. [169]	Clearfil New Bond	0.022369	17.715910 ± 0.845660	1.715910 ± 1.882940	0.869454	0.356993	40	0.263662	0.099105 ± 0.106285	1	RT?

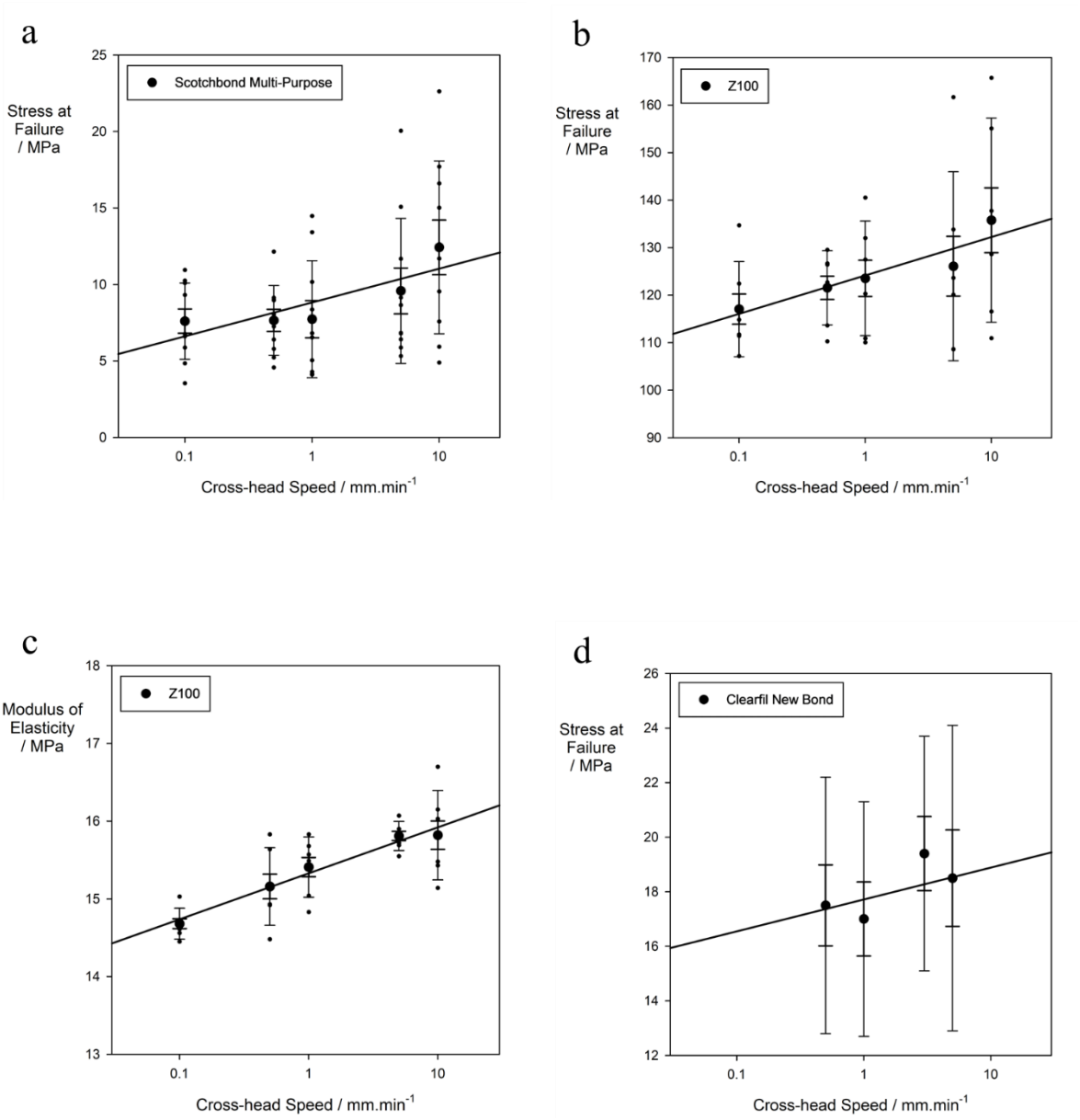

Figure 6.1 Mechanical properties trends in the re-analysis datasets (tensile tests). a: [177], b: [177], c: [177], d: [169].

6.7.1.2 Microtensile tests

These results are given in Table 6.3 and Figure 6.2, for the three studies of this kind. In principle, the effect of XHSs on bond strength should not be distinguishable by modest change in scale, unless a considerably larger sample size is used. Poitevin *et al.* [165] (Figure 6.2 a), Yamaguchi *et al.* [164] (Figure 6.2 b), and Reis *et al*. [166] (Figure 6.2 c) all showed a non-significant statistical relation, and the trends displayed were inconsistent. Poitevin *et al.* had a very large scatter (Figure 6.2 a) and small sample size (N = 30). Yamaguchi *et al.* and Reis *et al.* (Figure 6.2 b and c) also had large scatter (Table 6.3).

No overall conclusion can be drawn except that large scatter militates against a clear outcome and quantification of the scale of the effect. An increase in both the range of XHSs employed and sample size would be required, given the scatter found, to resolve this enquiry.

Table 6.3 Results of re-analysis of the literature on 'microtensile' tests

	Bonding agent	r^2	$b_0 \pm s(b_0)$	$b_1 \pm s(b_1)$	F	P	N	SSRD	RES ± se	LSR	Test temp / °C
Poitevin *et al.* [165]	Clearfil SE	0.003654	34.916667 ± 0.250	5.329295 ± 4.128054	0.102694	0.751004	30	0.481724	$6.969612 \times 10^{-3} \pm 0.098331$	3	RT?
Yamaguchi *et al.* [164]	Clearfil SE bond	0.014643	36.775800 ± 1.257939	-1.504489 ± 2.002046	0.564716	0.456996	40	0.170122	-0.049382 ± 0.051514	1.3	RT?
	Single bond	0.023612	46.528 ± 1.505996	-2.297663 ±2.396837	0.918959	0.343808	40	0.179783	-0.040910 ± 0.054439		
Reis *et al.* [166]	Single Bond	0.010502	44.981800 ± 0.604213	-1.174799 ± 1.129123	1.082543	0.300589	104	0.136348	0.026117 ± 0.025102	1.6	RT?
	Clearfil SE	0.032997	31.350670 ± 0.896203	3.211031 ± 1.628306	3.888812	0.051031	116	0.304772	0.102423 ± 0.051938		

.

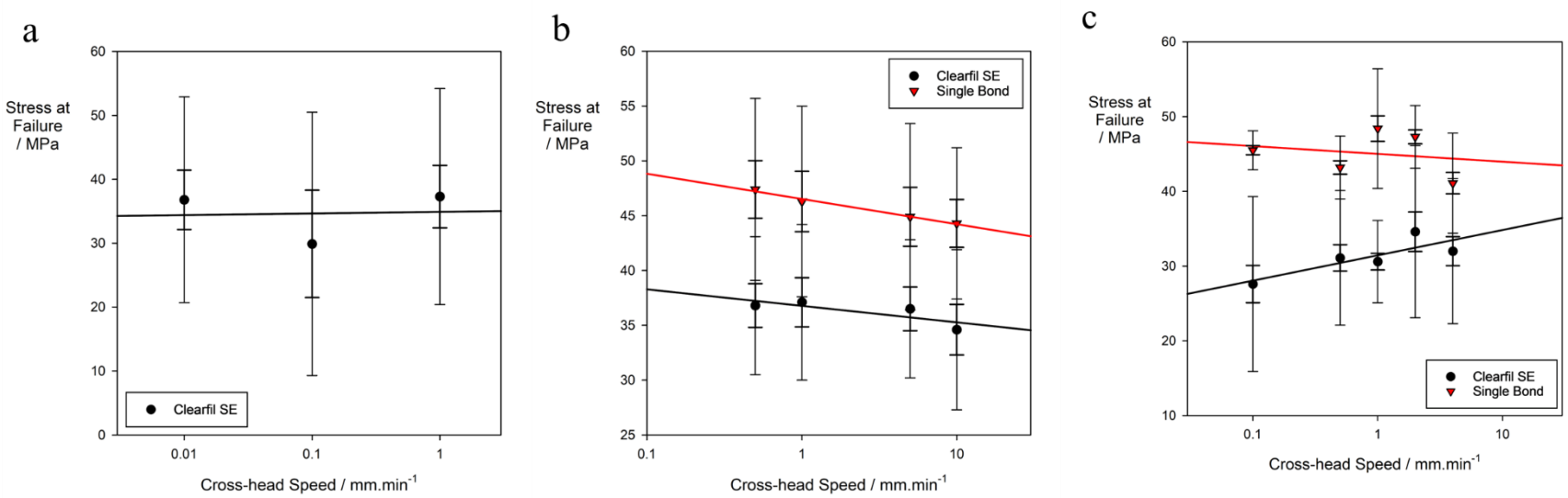

Figure 6.2 Mechanical properties trends in the re-analysis datasets (microtensile tests). a: [165], b: [164], c: [166].

6.7.1.3 Shear tests

The results of the re-analysis are given in Table 6.4, for the twelve studies of this kind. The embodiment of the idea of mode II failure (in-plane shear) in currently-used so-called shear tests has serious defects of stress concentration and levering. Sultan *et al.* [17] reported that interfacial stresses at failure under traditional 'shear' testing, did not scale with the size of the bonding area but did scale with the contact stresses, and thus the force per load area approach is simply wrong [17]. In fact, they are not shear tests at all. Such tests are therefore erroneous and irrelevant and should be abandoned [32]. Nevertheless, whatever the interpretation, strain rate effects should be discernible because the systems are polymeric.

The data from Bishara *et al.* [184] (Figure 6.3 a), Lindemuth & Hagge [171] (Figure 6.3 b), and Naves *et al.* [186] (Figure 6.3 c) showed a significant negative effect. In contrast, the data from Hara *et al.* [172] (Figure 6.4 a), Tamura *et al.* [170] (Figure 6.4 b), Munoz *et al.* [180] (XP bond, chisel) (Figure 6.4 c), Klocke *et al.* [173] (censored data) (Figure 6.4 d) showed the opposite trend, *i.e.*, a significant positive effect. For the data from Shooter *et al.* [181] (Figure 6.5 a), Abreu *et al.* [187] (Figure 6.5 b), Versluis *et al.* [188] (Figure 6.5 c), and the remainder from Munoz *et al.* [180] (Figure 6.4 c), the slopes were non-significant.

The data from Shalkey & Burgess [185] (Figure 6.6 a), despite employing a very good range of XHS and sample size, with low data scatter, the data do not show a single trend. This can be attributed to a mechanical effect, *i.e.*, time constant damping at higher XHSs (see below, 6.8). They used an Instron model 1125. This model had a strip chart recorder and pen response time of 0.5 s from 5 to 95% of full range [190], and reported (from AoV) a significantly lower value for "shear strength" at 100 and 200 mm/min XHS compared with values at lower XHSs. However, by censoring – analyzing the data above and below the apparent behaviour switch separately – very different conclusions are reached. That is, two trends were noted; a gradual increasing strength up to ~40 mm/min after which a steep decline in strength to 200 mm/min.

A similar finding was reported by Eliades *et al.* [136] (Figure 6.6 b) at 200 mm/min XHS compared with 1 mm/min, the delay of the pen recorder seems likely but further analysis is precluded by the lack of intermediate values, reflecting a poorly-designed experiment. They used only two XHSs over a wide range meaning that no meaningful trend investigation is possible now (*i.e.*, by censoring), underlining the need for multiple values for an independent variable whereby behaviour may be better investigated. They also had large data scatter and low sample size.

The uncensored data from Klocke *et al.* [173] (Figure 6.4 d) also appear to demonstrate the time constant effect starting at XHS < 10 mm/min, hence the censoring applied for the result presented above. Such effects of time constant damping at high XHSs were verified by Musanje and Darvell [163] when testing at XHSs ≥ 10 mm/min was done without signal filters being applied in the load cell amplifier. At relatively low speeds signal filters reduce the noise in the plot, however, at high speeds a sudden drop in the recorded load was noted [163]. They demonstrated this in measuring flexural strength and E for a range of FRs at temperatures between 0 and 37 °C. Test machine manufacturers generally employ filters to minimize the noise that may mask wanted signals. A filter with high frequency bandwidth (high-pass filter) will pass much of the wanted signal, however, unnecessary noise and spikes will pass too, and *vice versa, i.e.,* there are tradeoffs [191].

Table 6.4 Results of re-analysis of the literature on shear tests.

	Bonding agent		r^2	$b_0 \pm s(b_0)$	b1 ± s(b1)	F	P	N	SSRD	RES ± se	LSR	Test temp / °C
Shooter *et al.* [181]	Ortho Solo		0.009001	9.335310 ± 0.457917	-1.040056 ± 1.113837	0.871907	0.352770	98	0.433974	-0.111411 ± 0.119314	1	RT?
Bishara *et al.* [184]	Transbond		0.276924	10.634640 ± 0.733523	-5.200000 ± 1.363085	14.553280	4.87076×10^{-4}	40	0.405322	-0.488968 ± 0.128174	1	RT?
Lindemuth & Hagge [171]	Transbond		0.111833	15.754207 ± 0.367833	-1.259078 ± 0.512148	6.043861	0.017614	50	0.164080	-0.079920 ± 0.032509	2	RT?
Naves *et al.* [186]	Adper Single Bond		0.288516	688.500900 ± 28.086914	-210.20586 ± 47.645547	19.464578	5.7757×10^{-5}	50	0.228733	-0.305309 ± 0.069202	1.3	RT?
Shalkey & Burgess [185]	Acrylic rods		0.386213	38.481167 ± 0.822814	-4.147541 ± 0.592024	49.079869	7.68312×10^{-10}	80	0.119111	-0.107781 ± 0.015385	2.6	RT?
	Censored low		0.018094	36.654629 ± 0.537570	0.624999 ± 0.664542	0.884532	0.351673	50	0.077238	0.017051 ± 0.018130		
	Censored high		0.807243	72.420705 ± 4.045842	-21.742019 ± 2.007816	117.260591	1.61336×10^{-11}	30	0.037324	-0.300218 ± 0.027724		
Eliades *et al.* [136]	Transbond		0.609024	66.400000 ± 5.369586	-17.474783 ± 3.300	28.038618	4.9233×10^{-5}	20	0.214357	-0.258284 ± 0.041661	2.3	RT?
	Concise		0.681053	70.400000 ± 4.772101	-18.183161 ± 2.933	38.435644	7.5071×10^{-6}	20	0.255725	-0.263174 ± 0.049701		
Abreu *et al.* [187]	Solidex		0.010271	67.884872 ± 2.178250	6.533600 ± 9.456225	0.477386	0.493081	48	0.218211	0.096245 ± 0.139298	0.6	RT?
Hara *et al.* [172]	Single Bond		0.054305	13.607673 ± 0.515119	3.477299 ± 1.335846	6.775966	0.010425	120	0.408134	0.255540 ± 0.098169	1	RT?
Tamura *et al.* [170]	Clearfil SE		0.350342	42.891203 ± 0.441295	3.126064 ± 0.614432	25.885019	5.97545×10^{-6}	50	0.072304	0.072884 ± 0.014325	2	RT?
			0.637319	20.778840 ± 0.335220	4.286577 ± 0.465739	84.347587	3.8077×10^{-12}	50	0.113373	0.206295 ± 0.022462		
	Clearfil tri-s		0.588083	31.729772 ± 0.403592	4.651809 ± 0.561936	68.528384	8.39216×10^{-11}	50	0.089388	0.146607 ± 0.017710		
			0.578068	16.608327 ± 0.280063	3.162194 ± 0.389942	65.762422	1.50575×10^{-10}	50	0.118504	0.190398 ± 0.023479		
Versluis *et al.* [188]	Sctochbond MP		0.150558	17.037709 ± 0.875064	7.101316 ± 3.975742	3.190372	0.090930	20	0.198389	0.416800 ±0.233350	0.38	RT?
Munoz *et al.* [180]	Single Bond 2	wire	0.001740	23.483854 ± 1.111851	-0.380863 ± 2.530470	0.022654	0.882672	15	0.174812	-0.016218 ± 0.107754	1	RT?
		chisel	0.038770	29.811118 ± 1.321484	2.177832 ± 3.007575	0.524344	0.481823	15	0.163673	0.073054 ± 0.100888		
	XP Bond	wire	0.073257	21.607441 ± 0.738131	1.702961 ± 1.679918	1.027622	0.329214	15	0.126132	0.078814 ± 0.077747		
		chisel	0.448716	33.647171 ± 1.207878	8.942273 ± 2.749019	10.581332	6.2930×10^{-3}	15	0.132547	0.265766 ± 0.081701		
Klocke *et al.* [173]	Transbond		0.007951	228.080910 ± 3.856414	5.9688986 ± 6.137594	0.945783	0.332784	120	0.179826	0.026170 ± 0.026910	1.7	RT?
	Censored		0.044987	237.330010 ± 6.421148	21.682837 ± 10.649685	4.145326	0.044757	90	0.178320	0.091362 ± 0.044873		

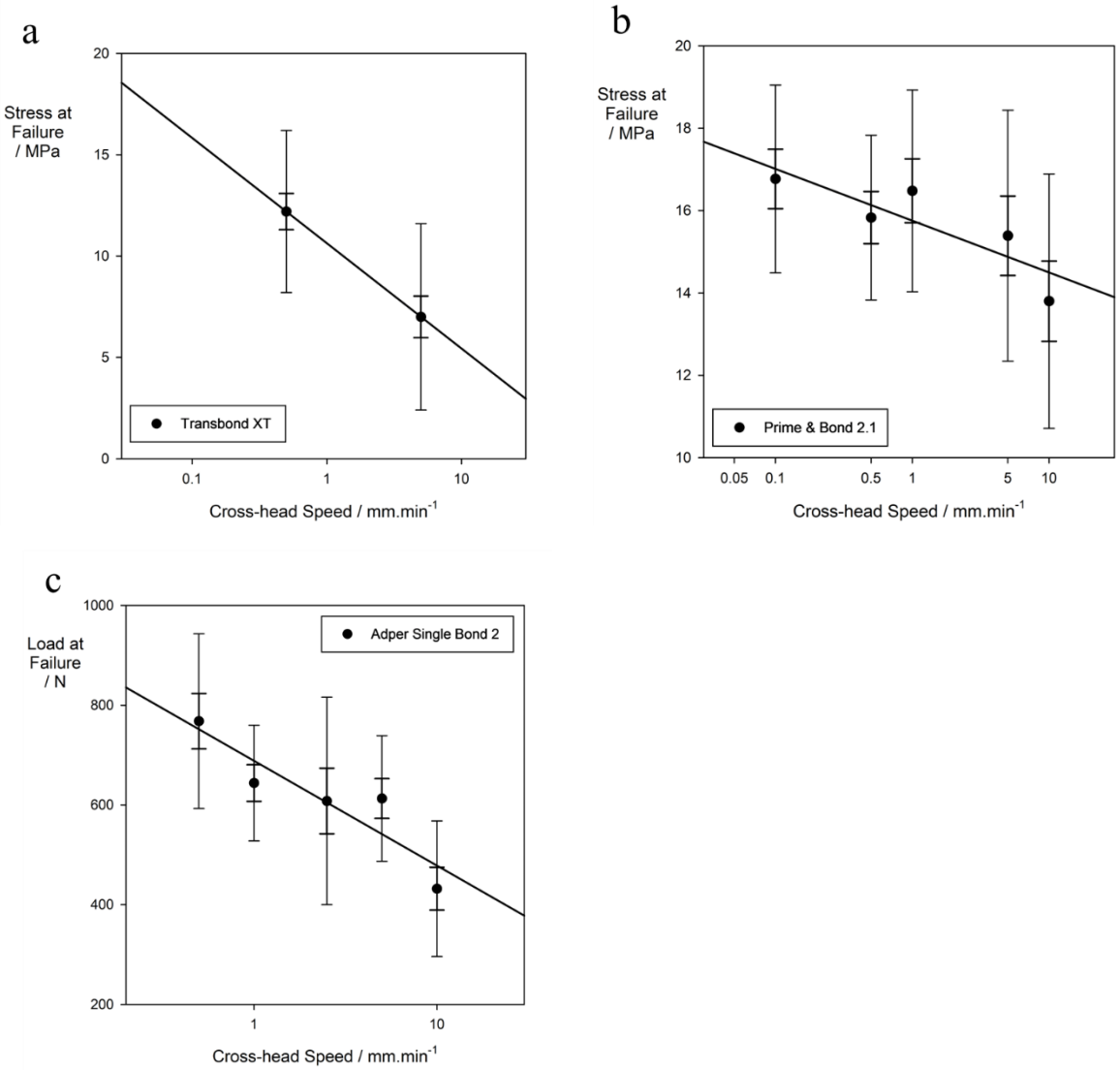

Figure 6.3 Mechanical properties trends in the re-analysis datasets (shear tests). a: [184], b: [171], c:[186].

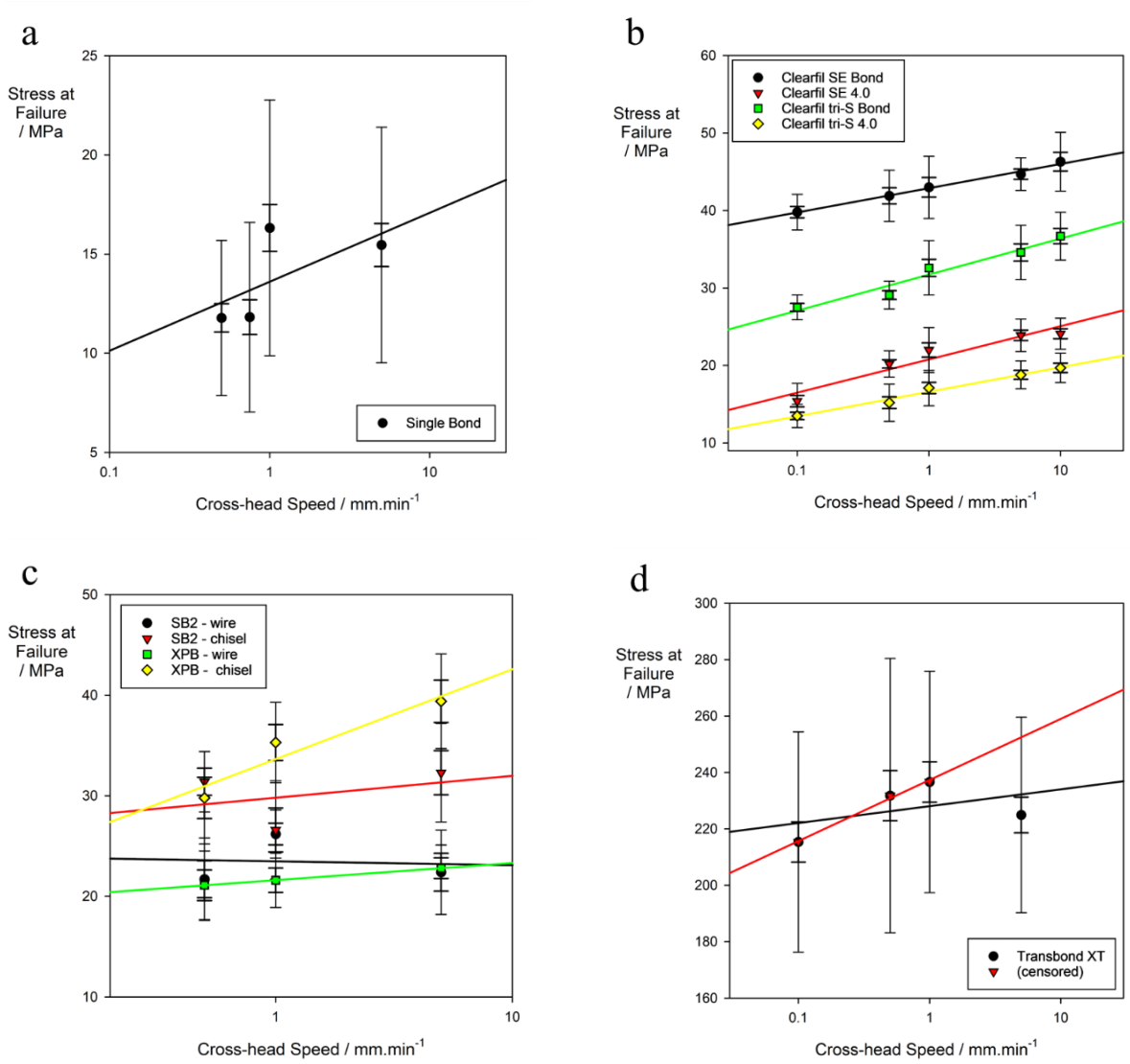

Figure 6.4 Mechanical properties trends in the re-analysis datasets (shear tests). a: [172], b: [170], c: [180], d: [173].

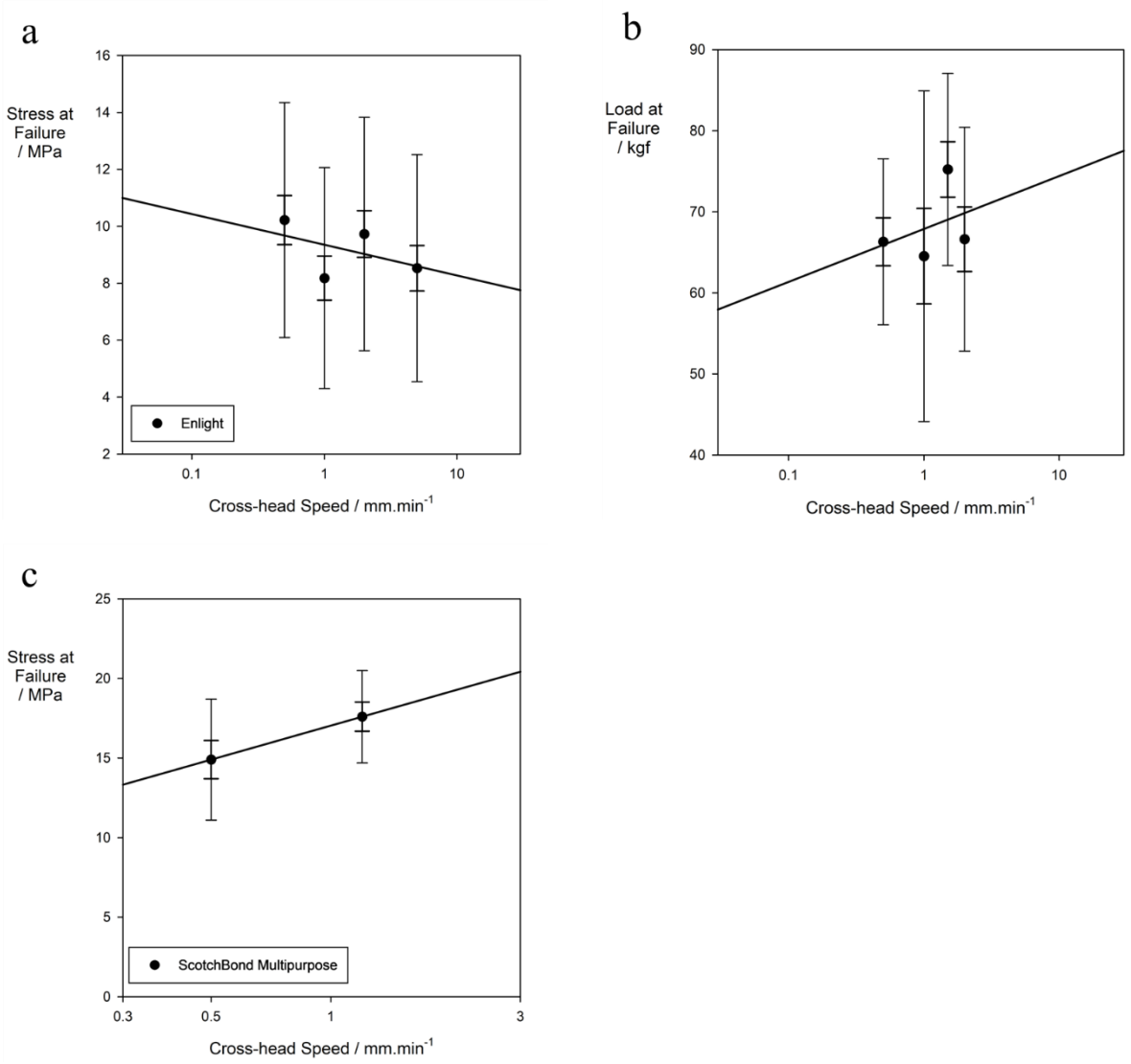

Figure 6.5 Mechanical properties trends in the re-analysis datasets (shear tests). a:[181], b: [187], c: [188], and Figure 6.4 c.

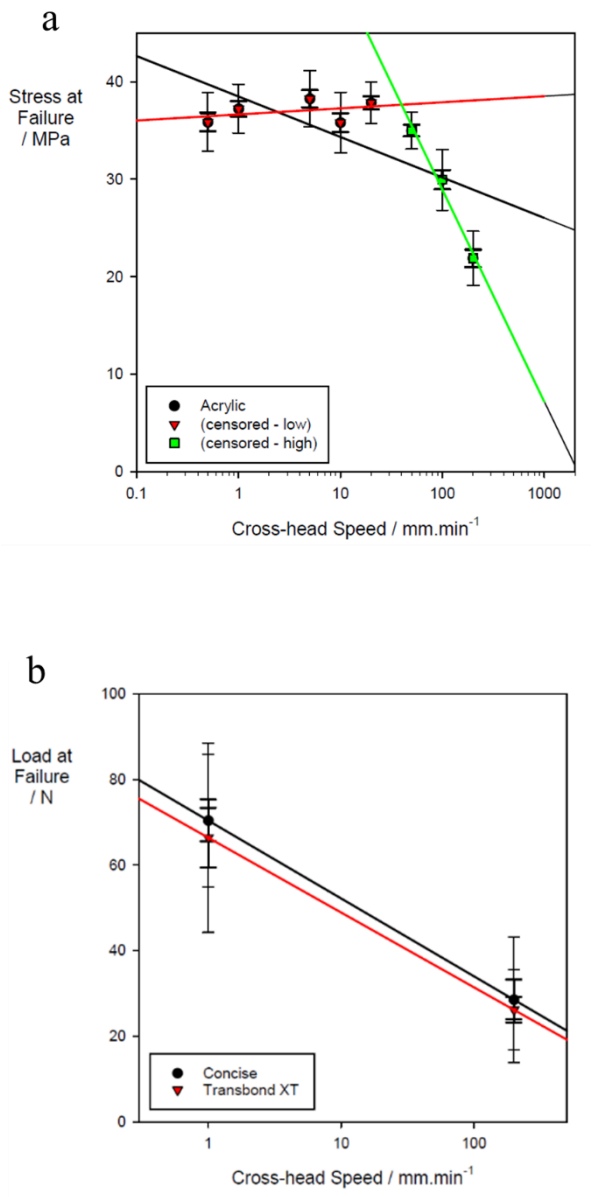

Figure 6.6 Mechanical properties trends in the re-analysis datasets (shear tests). a:[185], b:[136].

6.7.1.4 Biaxial flexural tests

The statistical re-analysis results for all seven flexural studies as well as the one compression study are given in Table 5.

For the data from Hooi *et al.* [176] data (Figure 6.7 a), Kumar *et al.* [182] (Figure 6.7 b-e) and Kumar & Shortall [189] (Figure 6.7 f) had a positive trend and mostly highly significantly so. The exceptions, Kumar & Shortall (13 wk wet) where p ~0.05, and Kumar *et al.* (61) (Z250 at 52 wk, p ~0.1) might be attributable to sampling variation (as with the few weaker effects), but more data are always required in marginal cases and where inconsistencies are present such as in these cases.

6.7.1.5 Three-point flexure and compression

Finally, the 3pb and compression and tests data from Elsafty *et al.* [174] (Figure 6.8, a and b) all have a non-significant result while only two materials gave a significant positive effect for flexural strength. The absence of detected effect is certainly due to the low range of XHS, *i.e.*, LSR = 0.7, and small sample sizes.

Table 6.5 Results of re-analysis of the literature on flexural tests

	Bonding agent	r^2	$b_0 \pm s(b_0)$	$b_1 \pm s(b_1)$	F	P	N	SSRD	RES ± se	LSR	Test temp / °C
Hooi *et al.* [176]	Uncoated	0.608089	75.090000 ± 0.986744	9.730000 ± 0.805673	145.85050	7.92808×10^{-21}	96	0.117535	0.129678 ± 0.010729	3	RT?
	5 N	0.440320	115.45000 ± 1.837202	12.900000 ± 1.500069	73.953180	1.7375×10^{-13}	96	0.142334	0.111737 ± 0.012993		
	30 N	0.639560	114.64000 ± 1.780957	18.780000 ± 1.454145	166.79220	1.51331×10^{-22}	96	0.138951	0.163817 ± 0.012684		
Kumar and Shortall [189]	1 wk dry	0.059355	128.00000 ± 1.559226	4.500000 ± 1.909654	5.552843	0.020671	90	0.117535	0.129578± 0.010729	2	RT?
	1 wk wet	0.126270	91.666670 ± 1.831645	8.00000 ± 2.243298	12.717620	5.884860×10^{-4}	90	0.142334	0.111737 ± 0.012993		
	13 wk wet	0.042732	101.00000 ± 1.853811	4.50000 ± 2.270446	3.928283	0.050651	90	0.138951	0.1638 ±0 .012684		
Kumar *et al.* (dry) [182]	Z100	0.065463	162.10000 ± 2.002181	4.70000 ± 1.634774	8.265713	4.79423×10^{-4}	120	0.123515	0.028994 ± 0.010085	3	RT?
	Z250	0.034928	170.60000 ± 2.192804	3.70000 ± 1.790417	4.270660	0.040964	120	0.128535	0.021688 ± 0.010495		
	Filtek Supreme Body	0.182060	155.00000 ± 1.911828	8.00000 ± 1.561001	26.264780	1.17644×10^{-6}	120	0.123344	0.051613 ± 0.010071		
	Filtek Supreme translucent	0.090255	164.90000 ± 1.897166	5.30000 ± 1.549029	11.706650	8.56378×10^{-4}	120	0.115049	0.032141 ± 0.009494		
Kumar *et al.* (1 wk) [182]	Z100	0.042309	134.70000 ± 2.092015	3.90000 ± 1.708123	5.213040	0.024208	120	0.155309	0.028953 ± 0.012681	3	RT?
	Z250	0.205756	142.10000 ± 2.148709	9.70000 ± 1.754413	30.568890	1.96195×10^{-7}	120	0.151211	0.068262 ± 0.012346		
	Filtek Supreme Body	0.142539	114.60000 ± 1.7144495	6.20000 ± 1.399879	19.615640	2.12897×10^{-5}	120	0.149607	0.054101 ± 0.012215		
	Filtek Supreme translucent	0.156395	135.70000 ± 2.461449	9.40000 ± 2.009764	21.875880	7.80641×10^{-6}	120	0.181389	0.069270 ± 0.014810		
Kumar *et al.* (13 wk) [182]	Z100	0.087031	132.30000 ± 2.227543	6.10000 ± 1.818781	11.248600	1.07183×10^{-3}	120	0.168371	0.046107 ± 0.013747	3	RT?
	Z250	0.190414	136.90000 ± 2.045831	8.80000 ± 1.670414	27.753460	6.28809×10^{-7}	120	0.149440	0.064280± 0.012202		
	Filtek Supreme Body	0.288254	116.50000 ± 1.417326	8.00000 ± 1.157242	47.789400	2.59332×10^{-10}	120	0.121659	0.068670 ± 0.009933		
	Filtek Supreme translucent	0.168012	132.00000 ± 2.132616	8.500 ± 1.741274	23.828890	3.3338×10^{-6}	120	0.161562	0.064394 ± 0.013191		
Kumar *et al.* (52 wk) [182]	Z100	0.046662	112.10000 ± 2.140410	4.20000 ± 1.747638	5.775583	0.017808	120	0.190938	0.037467 ± 0.015590	3	RT?
	Z250	0.023139	112.60000 ± 1.977929	2.70000 ± 1.614972	2.795100	0.097203	120	0.175660	0.023979 ± 0.014343		
	Filtek Supreme Body	0.178032	105.50000 ± 1.574694	6.50000 ± 1.285732	25.557930	1.58818×10^{-6}	120	0.149260	0.061611 ± 0.012187		
	Filtek Supreme translucent	0.228620	119.80000 ± 1.884687	9.10000 ± 1.538783	34.972610	3.33341×10^{-8}	120	0.157314	0.075960 ± 0.012845		
Elsafty *et al.* (FS) [174]	GrandioSo	0.179255	174.63970 ± 2.732011	9.421681 ± 5.591455	2.839273	0.115826	15	0.036162	0.053949 ± 0.032017	0.7	RT?
	Filtek Supreme XTE	0.157645	160. 63970 ± 2.951360	9.421681 ± 6.040383	2.432920	0.142816	15	0.042470	0.058651± 0.037602		
	Venus Diamond	0.239406	136.76830 ± 3.018017	12.494740 ± 6.176807	4.091912	0.064157	15	0.051010	0.091357 ± 0.045163		
	Venus Flow	0.613769	101.12180 ± 3.074334	28.598550± 6.292067	20.658620	5.49962×10^{-4}	15	0.070279	0.282813 ± 0.062223		
	SureFil SDR Flow	0.589691	83.527010 ± 3.308155	29.655970 ± 6.770616	18.683460	8.28143×10^{-4}	15	0.113426	0.529072 ± 0.229114		
Elsafty *et al.* (Compression) [174]	GrandioSo	0.025762	426.43720 ± 7.573659	9.088175 ± 15.500580	0.343761	0.567707	15	0.041055	0.021312 ± 0.036349	0.7	RT?
	Filtek Supreme XTE	0.033565	412.70400 ± 7.968393	10.958210 ±16.308460	0.451495	0.513391	15	0.044632	0.026552 ± 0.039516		
	Venus Diamond	0.054936	391.27950 ± 10.591230	18.843360 ± 21.676470	0.755683	0.400448	15	0.062571	0.048158 ± 0.055399		
	Venus Flow	0.098660	364.26980 ± 9.469711	23.119440 ± 19.381130	1.42973	0.254232	15	0.060094	0.063468 ± 0.053205		
	SureFil SDR Flow	0.122670	348.33410 ± 8.935529	24.655970 ± 18.287850	1.817687	0.200611	15	0.062023	0.119733 ± 0.125282		

.

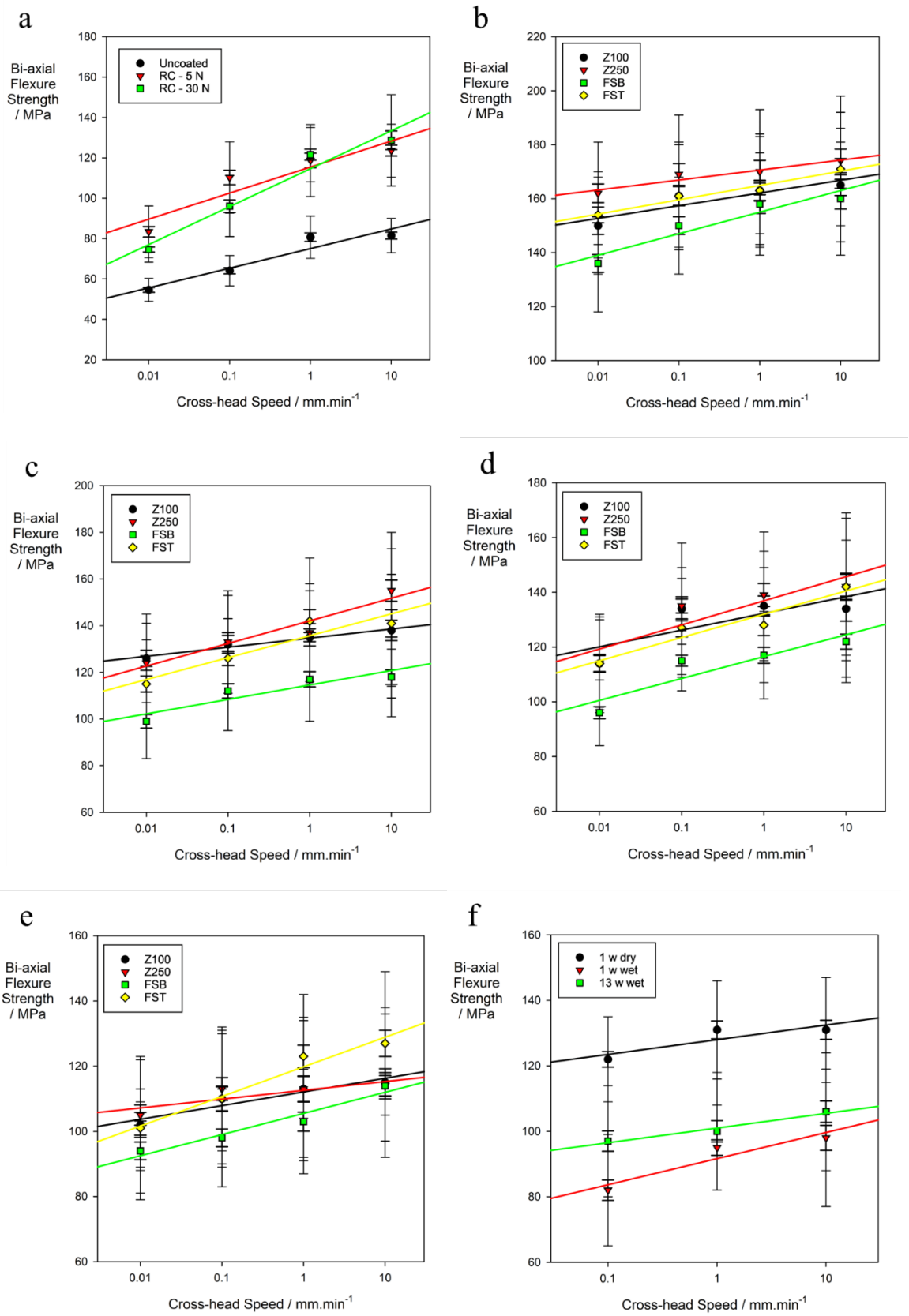

Figure 6.7 Results of re-analysis of the literature on biaxial flexure tests. a:[176], b: [182], c: [182], d: [182], e: [182], f: [189].

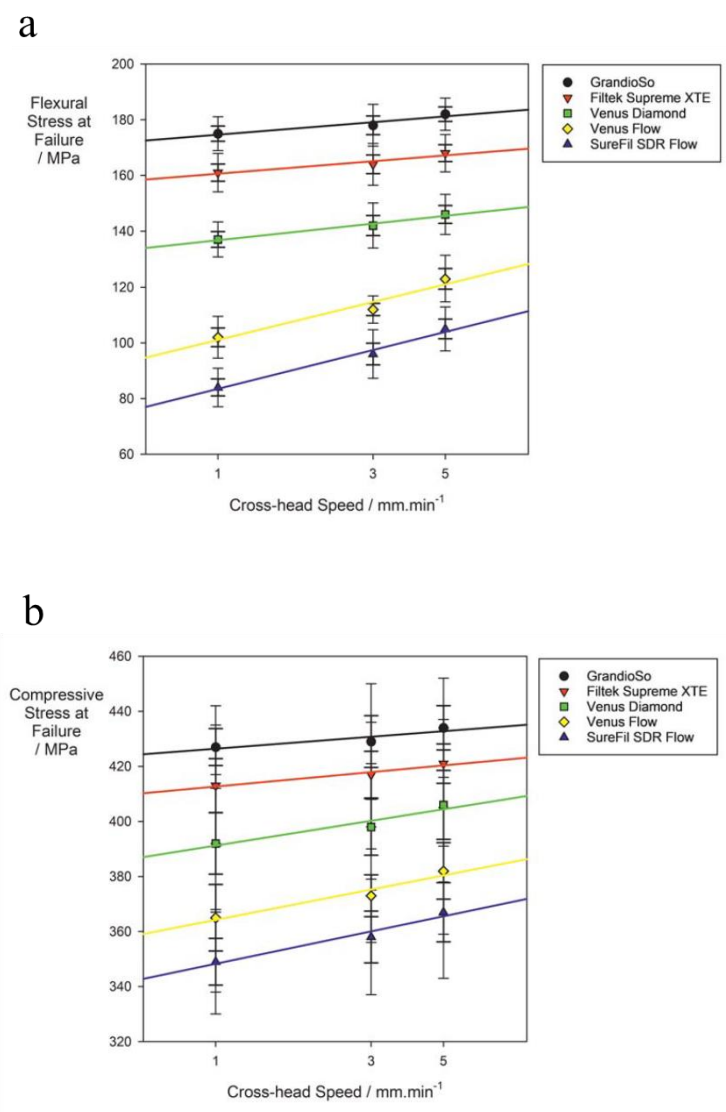

Figure 6.8 Mechanical properties trends in the re-analysis datasets (3pb, compression,). a: [174], b: [174].

6.7.2 Figures of merit

Figure 6.9 shows the three figures of merit; log speed range (LSR), sample number (N), scaled standard residual deviation (SSRD), calculated for each of the studies discussed above, and used to compare them in terms of their predictive ability and detection capability. LSR and N are controllable factors and clearly strongly influence the outcome, SSRD is the consequence (hence plotted against the *z*-axis).

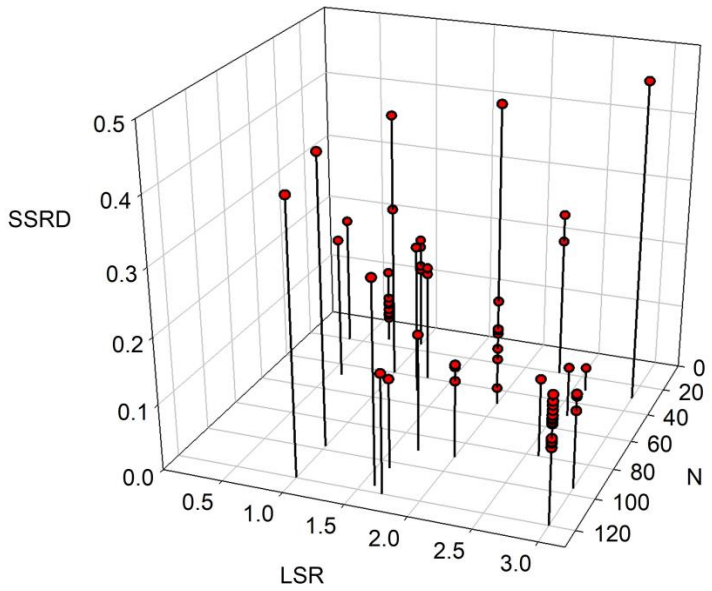

Figure 6.9 Graph of the figures of merit LSR, N, and SSRD. The best is towards the bottom, front, right. Most are seen to be rather inadequate.

6.8 Discussion

The question of whether XHS has an effect on the mechanical properties of dental resins or not is groundless: there are sound reasons for expecting it to be so. It is wrong-headed to test for the existence of an effect when it is known one must exist; the only question is how big the is effect and thus whether it matters.

A number of challenges have been identified. All electronic circuits have a time constant. That is, for a step change input the output is always (quasi-)exponential, settling asymptotically to the final value. Instantaneous, step change output is impossible. This applies to every step in an analogue signal path; indeed, even digital systems have such limitations. Ordinarily, because of noise in that signal, a low-pass filter is commonly used to smooth the output, further increasing the overall time constant and thus delaying the settling to the final value even further. For older systems where mechanical (pen) recorders were used, the effect can be much greater because of the limited pen drive motor speed and the inertia of the moving parts. Thus, the ability to record a maximum value in a dynamic system, *i.e.,* at the point of fracture, can be compromised, the effect being greater at higher XHS (*i.e.,* rates of change of load). Under such circumstances it is essentially impossible to record an accurate value for failure load: it is always low, and increasingly so the higher the XHS. It is therefore impossible to determine strain-rate sensitivity once the time constant for the input signal (equivalent to the reciprocal of XHS) approaches the output response time constant; for accurate results it must always be several times that value (thus for 1% accuracy one needs 5 times as long: $1 - e^{-5} = 0.993$). Failure to recognize this limitation in high-speed mechanical testing is a major defect. The implication is that time constants need to be determined.

Mechanical recorders continued to be part of test systems until computer programs were introduced which enabled better tracking minimizing the output delay. For example, Instron introduced Series IX software for Windows PCs in 1985, Merlin in 1993, and Bluehill in 2004 [192]. Such systems, of course, eliminate only the pen recorder, instrument noise must still be dealt with by filtration. Nevertheless, the likelihood of old machines continuing in use is high, and there is an almost complete absence of information on the recording systems used in publications in the present context.

The power of a statistical test is defined as its ability to detect and measure a statistically significant difference between groups, *i.e.*, the probability that a small *p*-value (say, < 0.05) will be obtained correctly. For example, a test of 80% power means that there is an 80% chance of ending up with $p < 0.05$ if there was a true difference to be detected [193]. Subsequently, any detected difference should be verified as whether it has a true practical impact in the context [193]. A study with inadequate statistical power increases the chance of missing a true effect and has increased risk of type II errors, *i.e.*, false negative [183]. It is also important that a sample be representative of its parent population, *i.e.*, be homogeneous, and avoid systematic bias. Generally, statistical power is a direct function of sample size. Larger sample sizes may more accurately represent the behaviour of that source population, and thus minimise the difference (on average) between the sample mean and the putative population mean [194]. However, the benefit of increased sample size must be weighed against the costs. The larger the sample the more reliable the results, but the more expensive and logistically challenging is the gathering of the data. It is a matter of finding the right balance between accuracy and the logistics in relation to the outcome.

Another way to increase the power of a study is to increase the effect size. This can be achieved through maximizing the differences between the chosen tested values of the independent variables [135] (*i.e.*, XHS here), assuming a monotonic effect (which, of course, is not guaranteed – using several intermediate values implicitly tests for regularity). The targeted difference between the individual test groups is determined *a priori* by the researcher, typically through a small-scale or pilot study under the exact same conditions to evaluate the feasibility of the project. The larger is the estimated difference, the smaller the required sample size can be [194]. In cases where budget, time and sample availability are constrained, researchers may attempt to make the measurement of a dependent variable as reliable as possible, but must in any event attempt to take measurements under as tightly-controlled conditions as possible [194].

Given the remarks made about displacement correction [76, 77], it is apparent that none of the reports considered in this chapter have reported any such correction. Given that the expectation of more brittle behaviour at higher strain rate implies less deflection at failure, it would appear that the calculated strain rate sensitivity would be affected by that omission. Accordingly, it would seem appropriate to apply such a correction as a matter of routine in all such work.

6.9 Simulation of the human masticatory cycle

Maximum bite force increases significantly with age up to adolescence. Average bite force is higher in males than females. A wide range of duration of maximum bite force has been reported [195]. Furthermore, masticatory muscles and periodontal tissue have an important role in controlling the bite force that may be used [70]. Tooth morphology will also contribute to the distribution of masticatory loads along bonded interfaces. 'Bonded' dental resins are used extensively in filling tooth cavities. Upon being subjected to masticatory forces, occlusal FR fillings are pressed inward into the tooth, *i.e.* causing it to be subjected to some compressive loading. This will be accompanied by expansion in directions perpendicular to the direction of compression, *i.e.*, Poisson strain, creating compression and shear stresses against the walls. It is difficult to determine exactly how those masticatory forces will be transferred to an adhesive joint and we cannot directly relate subsequent failures to tensile or shear stresses anywhere. This is further complicated by the fact that dental resins are strain-rate sensitive, *i.e.*, the values of properties measured are dependent on the XHS of the test, as discussed above.

In contrast to masticatory loading, stresses due to polymerization shrinkage and water sorption expansion may be expected to be small but of very long duration.

All this makes laboratory experimental replication of the velocity of the mandible during chewing using simple *in vivo* observations an extremely challenging matter. Crucially, it also suggests that a single representative XHS is not possible.

6.10 Concluding remarks

XHS has a significant influence on the observed mechanical properties of dental resins, thus comparisons of studies employing differing XHSs might lead to faulty conclusions. This is further blurred by the fact that service conditions (masticatory force, frequency, and distribution over tooth morphology) are extremely complex. A simple approach might be more pragmatic. It is important to ensure a consistent strain rate during testing. Constant XHS has been used to control the strain rate and may prove helpful if corrected by considering machine compliance [191]. However, the constant rate of loading in controlled load tests may generate relatively constant rates of change of stress. This might avoid the complicated strain rate effects of dental resins in displacement-controlled tests if the loading departs appreciably from linearity with time. Nevertheless, it can be said that while time-constant effects in the recording system must be avoided, large values for LSR and sample size are essential for the estimation of the size of the effect (and thus the RES as a figure of merit) with low standard error. Such criteria have rarely been met so far.

Due to the large number of medical research studies that have statistical errors, publication standards are considered low; the use of statistical methodology in medical journals has been subjected to great debate [196]. Subsequent future research will be struggling to restore the consistency in knowledge and resolve the problem. More restrictive rules are suggested to avoid interpretations based on statistical misuse as most mistakes are (presumably) inadvertent and arise from a lack of the necessary knowledge [196]. This is especially true for educational institutes where the exposure of students to such learning environment can leave them with inadequate basic research skills. Subsequently, the faulty interpretation of results may affect the attitude towards existing practice and contaminate good knowledge.

The present context has shown the frequency of poor analyses which have yielded weak or uninterpretable results, the lack of appreciation of the limitations of recording systems, the high scatter of results in such testing, and the generally low sample sizes, all of which have compromised the value of the work reported. Accordingly, it is not yet possible to provide a definitive statement of the magnitude of strain rate sensitivity as a generality, or with much confidence in a number of circumstances, although on balance it would appear that the physical expectation is met. There is clearly a need for improved studies.

7. Conclusions

7.1 Symmetrical four-point bend

From the above consideration of the literature, the mechanics of the various possible test approaches, the experience of applying four-point bending, and the data collected using it, the following observations may be made.

i. The symmetrical four-point bend represents a better approach, addressing the key drawbacks in traditional testing, *i.e.*, uniform bending avoiding spurious stress concentrations, a specimen size reflecting energy content and flaw population, correct joint geometry and bonding area, failure modes, *etc*. By improving test reliability and expanding the range of materials tested, this method can be seen to enable more detailed data collection, improving failure initiation modelling and replicating common clinical scenarios. We can efficiently characterize the retentive potential of different 'adhesive' systems currently employed with less variation in the measurements and more objective discrimination, *i.e.*, mechanical versus chemical. For example, we can also compare bond strengths to dentine affected by various contaminants acting as a mechanical barrier and the subsequent decontamination methods.

ii. The 4pb test set up also avoids problems from contact stress, and can employ a suitable span-depth ratio to minimize vertical shear stress. The effect of deformation of the beam from ideal geometry can be corrected for and this correction should be applied as a matter of routine.

iii. The 4pb test set up described here could be used in the ISO standard 4046 for flexural properties, with deflection correction, but also for adhesion testing in ISO 4046 for the various types of dental material on tooth tissue.

iv. Relevant clinical practice guidelines can be examined in a systematic and evidence-based approach. Generally experimental evidence should be translated into clinical practice. For example, there are no systematic laboratory studies to support the conditions used routinely for phosphoric acid etching (concentration and etching times) when applied to tooth substance. Exploring the full possible range of concentration and application time and the consequent effects on bond strength would allow treatment recommendations based on a rigorously-obtained data, *i.e.* the full response surface.

7.2 Strain rate

i. Strain rate has a significant influence on the measured interfacial strength and should be approached in a cause-and-effect relationship to avoid the inconsistency in findings and be able highlight the real differences between various RBCs.

ii. Constant cross-head speed has been used to control the strain rate and may prove useful if corrected by using the deformation experienced only by the specimens. However, constant load-rate tests are less sophisticated than displacement-controlled tests.

iii. It can be recommended that a displacement correction should be applied as a matter of routine in any study of strain rate sensitivity.

8. References

1. Smith CE. Cellular and chemical events during enamel maturation. Critical Reviews in Oral Biology & Medicine. 1998; 9(2):128-161.
2. Pan H, Zhao X, Darvell BW, Lu WW. Apatite-formation ability–predictor of "bioactivity"? Acta Biomaterialia. 2010; 6(11):4181-4188.
3. Marshall Jr GW, Marshall SJ, Kinney JH, Balooch M. The dentin substrate: structure and properties related to bonding. Journal of Dentistry. 1997; 25(6):441-458.
4. Marshall SJ, Bayne SC, Baier R, Tomsia AP, Marshall GW. A review of adhesion science. Dental Materials. 2010; 26(2):11-16.
5. Van Meerbeek B, De Munck J, Yoshida Y, Inoue S, Vargas M, Vijay P, Van Landuyt KL, Lambrechts P, Vanherle G. Buonocore Memorial Lecture. Adhesion to enamel and dentin: Current status and future challenges. Operative Dentistry. 2003; 28(3):215-235.
6. Bertassoni LE, Orgel JPR, Antipova O, Swain MV. The dentin organic matrix–limitations of restorative dentistry hidden on the nanometer scale. Acta Biomaterialia. 2012; 8(7):2419-2433.
7. Sano H. Microtensile testing, nanoleakage, and biodegradation of resin-dentin bonds. Journal of Dental Research. 2006; 85(1):11- 14.
8. Adapted from "collagen structure" and "extrinsic toughening mechanims in dentin" by BioRender.com, 2024. Retrieved from https://app.biorender.com/biorender-templates.
9. Kinloch AJ. Adhesion and Adhesives Science and Technology. 1st ed. London, United Kingdom: Chapman & Hall. 1987; 41-53, 56-96.
10. Soderholm K-JM. Review of the fracture toughness approach. Dental Materials. 2010; 26(2):63-77.
11. Darvell BW. Materials science for dentistry. 10th ed. Sawton, England: Woodhead publishing. 2018; 2-19, 745-769, 249-290, 517-519.
12. Gale MS, Darvell BW. Controlling dentine penetration in computer microleakage tracer mapping. Journal of Dentistry. 1997; 25(2):129-136.
13. Heintze SD. Systematic reviews: I. The correlation between laboratory tests on marginal quality and bond strength. II. The correlation between marginal quality and clinical outcome. Journal of Adhesive Dentistry. 2007; 9(1):77-106.

14. Söderholm K-JM. Critical evaluation of adhesive test methods used in dentistry. Journal of Adhesion Science and Technology. 2009; 23(7-8):973-990.
15. Darvell BW. Mechanical test relevance—A personal perspective on some methods and requirements. Frontiers in Dental Medicine. 2023; 3:1-13.
16. Darvell BW. Adhesion strength testing—time to fail or a waste of time? ournal of Adhesion Science and Technology. 2009; 23(7-8):935-944.
17. Sultan H, Kelly JR, Kazemi RB. Investigating failure behavior and origins under supposed "shear bond" loading. Dental Materials. 2015; 31(7):807-813.
18. Armstrong S, Geraldeli S, Maia R, Raposo L, Soares C, Yamagawa J. Adhesion to tooth structure: a critical review of "micro" bond strength test methods. Dental Materials. 2010; 26(2):50-62.
19. Griffith AA. The phenomena of rupture and flow in solids. Philosophical Transactions of the Royal Society A Mathematical, Physical and Engineering Sciences. 1920; 221:582-593.
20. Kelly JR. Perspectives on strength. Dental Materials. 1995; 11(2):103-110.
21. Mutluay MM, Yahyazadehfar M, Ryou H, Majd H, Do D, Arola D. Fatigue of the resin–dentin interface: A new approach for evaluating the durability of dentin bonds. Dental Materials. 2013; 29(4):437-449.
22. Tagami J, Nikaido T, Nakajima M, Shimada Y. Relationship between bond strength tests and other in vitro phenomena. Dental Materials. 2010; 26(2):94-99.
23. Spencer P, Ye Q, Park J, Topp EM, Misra A, Marangos O, Wang Y, Bohaty BS, Singh V, Sene F. Adhesive/dentin interface: the weak link in the composite restoration. Annals of Biomedical Engineering. 2010; 38(6):1989-2003.
24. De Munck J, Mine A, Poitevin A, Van Ende A, Cardoso MV, Van Landuyt KL, Peumans M, Van Meerbeek B. Meta-analytical review of parameters involved in dentin bonding. Journal of Dental Research. 2012; 91(4):351-357.
25. Rodolpho PADR, Donassollo TA, Cenci MS, Loguércio AD, Moraes RR, Bronkhorst EM, Opdam NJM, Demarco FF. 22-Year clinical evaluation of the performance of two posterior composites with different filler characteristics. Dental Materials. 2011; 27(10):955-963.
26. Liu Y, Tjäderhane L, Breschi L, Mazzoni A, Li N, Mao J, Pashley DH, Tay FR. Limitations in bonding to dentin and experimental strategies to prevent bond degradation. Journal of Dental Research. 2011; 90(8):953-968.

27. Carvalho RM, Manso AP, Geraldeli S, Tay FR, Pashley DH. Durability of bonds and clinical success of adhesive restorations. Dental Materials. 2012; 28(1):72-86.
28. Mjör IA, Dahl JE, Moorhead JE. Age of restorations at replacement in permanent teeth in general dental practice. Acta Odontologica Scandinavica. 2000; 58(3):97-101.
29. Bernardo M, Luis H, Martin MD, Leroux BG, Rue T, Leitão J, DeRouen TA. Survival and reasons for failure of amalgam versus composite posterior restorations placed in a randomized clinical trial. The Journal of the American Dental Association. 2007; 138(6):775-783.
30. Ilie N, Hilton TJ, Heintze SD, Hickel R, Watts D, Silikas N, Stansbury JW, Cadenaro M, Ferracane JL. Academy of dental materials guidance—Resin composites: Part I—Mechanical properties. Dental Materials. 2017; 33(8):880-894.
31. Leloup G, D'Hoore W, Bouter D, Degrange M, Vreven J. Meta-analytic review of factors involved in dentin adherence. Journal of Dental Research. 1998; 77:1605-1614.
32. Kelly JR. Future of dental biomaterials: Gazing into Bob's crystal ball. Journal of Prosthetic Dentistry. 2020; 125(1):1-7.
33. Ritter AV. Sturdevant's Art and Science of Operative Dentistry. 7th ed. New York, United States: Elsevier Health Sciences. 2019; 136-169.
34. Nakabayashi N, Kojima K, Masuhara E. The promotion of adhesion by the infiltration of monomers into tooth substrates. Journal of Biomedical Materials Research. 1982; 16(3):265-273.
35. Nakabayashi N, Nakamura M, Yasuda N. Hybrid layer as a dentin-bonding mechanism. Journal of Esthetic Restorative Dentistry. 1991; 3(4):133-138.
36. Misra A, Spencer P, Marangos O, Wang Y, Katz JL. Parametric study of the effect of phase anisotropy on the micromechanical behaviour of dentin–adhesive interfaces. Journal of the Royal Society Interface. 2005; 2(3):145-157.
37. Misra A, Spencer P, Marangos O, Wang Y, Katz JL. Micromechanical analysis of dentin/adhesive interface by the finite element method. Journal of Biomedical Materials Research Part B: Applied Biomaterials:. 2004; 70(1):56-65.
38. Singh V, Misra A, Marangos O, Park J, Ye Q, Kieweg SL, Spencer P. Fatigue life prediction of dentin–adhesive interface using micromechanical stress analysis. Dental Materials. 2011; 27(9):187-195.

39. Mecholsky Jr JJ. Fractography: determining the sites of fracture initiation. Dental Materials. 1995; 11(2):113-116.
40. Marshall Jr GW, Balooch M, Gallagher RR, Gansky SA, Marshall SJ. Mechanical properties of the dentinoenamel junction: AFM studies of nanohardness, elastic modulus, and fracture. Journal of Biomedical Materials Research. 2001; 54(1):87-95.
41. Van Noort R, Barbour M. Introduction to dental materials. 4th ed. St Louis, United States: Elsevier Health Sciences. 2014; 113-125.
42. Renzo MD, Ellis TH, Domingue A, Bertrand L, Sacher E, Stangel I. Chemical reactions between dentin and bonding agents. Journal of Adhesion. 1994; 47(1-3):115-121.
43. Rosenberg M, Bartl P, Leško J. Water-soluble methacrylate as an embedding medium for the preparation of ultrathin sections. Journal of Ultrastructure Research. 1960; 4(3-4):298-303.
44. DeHoff PH, Anusavice KJ, Wang Z. Three-dimensional finite element analysis of the shear bond test. Dental Materials. 1995; 11(2):126-131.
45. Van Meerbeek B, Peumans M, Poitevin A, Mine A, Van Ende A, Neves A, De Munck J. Relationship between bond-strength tests and clinical outcomes. Dental Materials. 2010; 26(2):100-121.
46. Shono Y, Ogawa T, Terashita M, Carvalho RM, Pashley EL, Pashley DH. Regional measurement of resin-dentin bonding as an array. Journal of Dental Research. 1999; 78(2):699-705.
47. McDonough WG, Antonucci JM, He J, Shimada Y, Chiang MYM, Schumacher GE, Schultheisz CR. A microshear test to measure bond strengths of dentin–polymer interfaces. Biomaterials. 2002; 23(17):3603-3608.
48. Burke FJT, Hussain A, Nolan L, Fleming GJP. Methods used in dentine bonding tests: An analysis of 102 investigations on bond strength. European Journal of Prosthodontics and Restorative Dentistry. 2008; 16(4):158-165.
49. Kelly JR, Benetti P, Rungruanganunt P, Della Bona A. The slippery slope–critical perspectives on in vitro research methodologies. Dental Materials. 2012; 28(1):41-51.
50. Scherrer SS, Cesar PF, Swain MV. Direct comparison of the bond strength results of the different test methods: a critical literature review. Dental Materials. 2010; 26(2):78-93.
51. Braga RR, Meira JBC, Boaro LCC, Xavier TA. Adhesion to tooth structure: a critical review of “macro” test methods. Dental Materials. 2010; 26(2):38-49.

52. Bažant ZP, Le J-L, Bazant MZ. Scaling of strength and lifetime probability distributions of quasibrittle structures based on atomistic fracture mechanics. Proceedings of the National Academy of Sciences. 2009; 106(28):11484-11489.
53. Ferracane JL, Lohbauer U, Palin WM. The mechanical behavior of the material-tissue and material-material interface in dental reconstructions. International Journal of Adhesion and Adhesives. 2016; 69:2-14.
54. Sultan H, Kelly JR, Kazemi R. Investigating failure behavior and origins under supposed "shear bond" loading. Dental materials. 2015; 31(7):807-813.
55. Fowler CS, Swartz ML, Moore BK, Rhodes BF. Influence of selected variables on adhesion testing. Dental Materials. 1992; 8(4):265-269.
56. Van Noort R, Noroozi S, Howard IC, Cardew G. A critique of bond strength measurements. Journal of Dentistry. 1989; 17(2):61-67.
57. Pashley DH, Sano H, Ciucchi B, Yoshiyama M, Carvalho RM. Adhesion testing of dentin bonding agents: a review. Dental Materials. 1995; 11(2):117-125.
58. Fusayama T, Nakamura M, Kurosaki N, Iwaku M. Non-pressure adhesion of a new adhesive restorative resin. Journal of Dental Research. 1979; 58(4):1364-1370.
59. Pashley DH, Carvalho RM, Sano H, Nakajima M, Yoshiyama M, Shono Y, Fernandes CA, Tay F. The microtensile bond test: a review. Journal of Adhesive Dentistry. 1999; 1(4):299-309.
60. Roylance D. Introduction to fracture mechanics. Cambridge, MA 02139: Massachusetts Institute of Technology; 2001.
61. Van Noort R, Noroozi S, Howard IC, Cardew G. A critique of bond strength measurements. Journal of dentistry. 1989; 17(2):5-7.
62. De la Macorra JC, San-Nicolás A. Method to compare μ-tensile bond strength of a self-etching adhesive and μ-cohesive strength of adjacent dentin. Dental Materials. 2005; 21(10):946-953.
63. Staninec M, Marshall GW, Hilton JF, Pashley DH, Gansky SA, Marshall SJ, Kinney JH. Ultimate tensile strength of dentin: Evidence for a damage mechanics approach to dentin failure. Journal of Biomedical Materials Research. 2002; 63(3):342-345.
64. Eckert GJ, Platt JA. A statistical evaluation of microtensile bond strength methodology for dental adhesives. Dental Materials. 2007; 23(3):385-391.

65. Purk JH, Dusevich V, Glaros A, Spencer P, Eick JD. In vivo versus in vitro microtensile bond strength of axial versus gingival cavity preparation walls in Class II resin-based composite restorations. Journal of the American Dental Association. 2004; 135(2):185-193.
66. Yang B, Ludwig K, Adelung R, Kern M. Micro-tensile bond strength of three luting resins to human regional dentin. Dental Materials. 2006; 22(1):45-56.
67. Matinlinna JP, Mittal KL. Adhesion aspects in dentistry. Boca Raton: CRC Press. 2009.
68. Ferracane JL, Dossett JM, Pelogia F, Macedo MRP, Hilton TJ. Navigating the dentin bond strength testing highway: lessons and recommendations. Journal of Adhesion Science and Technology. 2009; 23(7-8):1007-1022.
69. Gluckich J. Strain-energy size effect. California Institute of Technology, Pasadena, California, Division P; 1970. Report No.: 32-1438:1-39.
70. Koc D, Dogan A, Bek B. Bite force and influential factors on bite force measurements: a literature review. European Journal of Dentistry. 2010; 4(2):223-232.
71. Mandras RS, Retief DH, Russell CM. The effects of thermal and occlusal stresses on the microleakage of the Scotchbond 2 dentinal bonding system. Dental Materials. 1991; 7(1):63-67.
72. Gale MS, Darvell BW. Thermal cycling procedures for laboratory testing of dental restorations. Journal of Dentistry. 1999; 27(2):89-99.
73. Sauro S, Pashley DH. Strategies to stabilise dentine-bonded interfaces through remineralising operative approaches–State of The Art. International Journal of Adhesion and Adhesives. 2016; 69:39-57.
74. Sano H. Microtensile testing, nanoleakage, and biodegradation of resin-dentin bonds. Journal of dental research. 2006; 85(1):11-14.
75. Şanlı S, Çömlekoğlu MD, Çömlekoğlu E, Sonugelen M, Pamir T, Darvell BW. Influence of surface treatment on the resin-bonding of zirconia. Dental Materials. 2015; 31(6):657-668.
76. ASTM International - D6272-17 Standard Test Method for Flexural Properties of Unreinforced and Reinforced Plastics and Electrical Insulating Materials by Four-Point Bending, (July 2020).
77. Chitchumnong P, Brooks SC, Stafford GD. Comparison of three-and four-point flexural strength testing of denture-base polymers. Dental Materials. 1989; 5(1):2-5.
78. Timoshenko SP. Strength of materials, Part I. Elementary theory and problems. 2nd ed. New York, United States: D. Van Nostrand. 1940; 1-34.

79. Neelakantan P, John S, Anand S, Sureshbabu N, Subbarao C. Fluoride release from a new glass-ionomer cement. Operative Dentistry. 2011; 36(1):80-85.
80. Scientific Documentation IPS e.max CAD [Internet]. Ivoclar Vivadent, Schaan, Leichtenstein. 2009 (Accessed 10/08/2024). Available from: https://www.ivoclar.com/en_ca/downloadcenter/#dc=ca&lang=en.
81. Musanje L, Shu M, Darvell BW. Water sorption and mechanical behaviour of cosmetic direct restorative materials in artificial saliva. Dental Materials. 2001; 17(5):394-401.
82. Ilie N, Hickel R. Investigations on mechanical behaviour of dental composites. Clinical Oral Investigations. 2009; 13:427-438.
83. Ferracane JL. Resin composite—state of the art. Dental Materials. 2011; 27(1):29-38.
84. Hadis MA, Shortall AC, Palin WM. Competitive light absorbers in photoactive dental resin-based materials. Dental Materials. 2012; 28(8):831-841.
85. Ivoclar-Vivadent. IPS e.max ZirCAD labside -- Instructions for use. 2019 (Accessed 15/09/2024). Available from: https://content.pattersondental.com/items/PDFs/images/PDF_920288.pdf.
86. Juntavee N, Attashu S. Effect of different sintering process on flexural strength of translucency monolithic zirconia. Journal of Clinical and Experimental Dentistry. 2018; 10(8):821-830.
87. Ruyter EI, Vajeeston N, Knarvang T, Kvam K. A novel etching technique for surface treatment of zirconia ceramics to improve adhesion of resin-based luting cements. Acta Biomaterialia Odontologica Scandinavica. 2017; 3(1):36-46.
88. Instron-Corporation. Universal Testing Machine Compliance. 2019 (Accessed 15/09/2024). Available from: https://www.instron.com/-/media/literature-library/whitepapers/2010/12/compliance-correction.pdf.
89. MTS-Corporation. MTS Criterion and Exceed Accessories. 2024 (Accessed 15/9/2024). Available from: https://www.mts.com/-/media/materials/pdfs/brochures/mts-criterion-accessories-catalog.pdf?as=1.
90. Quinn GD. Fractography of ceramics and glasses. 2nd ed. Gaithersburg, Maryland, USA: National Institute of Standards and Technology. 2007; 1-10.
91. Scherrer SS, Quinn JB, Quinn GD, Kelly JR. Failure analysis of ceramic clinical cases using qualitative fractography. International Journal of Prosthodontics. 2006; 19(2):151-158.

92. West RM. Best practice in statistics: The use of log transformation. Annals of Clinical Biochemistry. 2022; 59(3):162-165.
93. Eweis AH, Yap AU, Yahya NA. Comparison of flexural properties of bulk-fill restorative/flowable composites and their conventional counterparts. Operative Dentistry. 2020; 45(1):41-51.
94. Ilie N, Bucuta S, Draenert M. Bulk-fill resin-based composites: an in vitro assessment of their mechanical performance. Operative Dentistry. 2013; 38(6):618-625.
95. Sumino N, Tsubota K, Takamizawa T, Shiratsuchi K, Miyazaki M, Latta MA. Comparison of the wear and flexural characteristics of flowable resin composites for posterior lesions. Acta Odontologica Scandinavica. 2013; 71(3-4):820-827.
96. Haugen HJ, Marovic D, Par M, Khai Le Thieu M, Reseland JE, Johnsen GF. Bulk fill composites have similar performance to conventional dental composites. International Journal of Molecular Sciences. 2020; 21(14):5136-5157.
97. Chung SM, Yap AUJ, Chandra SP, Lim CT. Flexural strength of dental composite restoratives: Comparison of biaxial and three-point bending test. Journal of Biomedical Materials Research Part B: Applied Biomaterials. 2004; 71(2):278-283.
98. Richardson HH. Static and dynamic load, stress, and deflection cycles in spur-gear systems: Massachusetts Institute of Technology; 1955 (Accessed 12/10/2024).
99. Hu D, Howard D, Ren L. Biomechanical analysis of the human finger extensor mechanism during isometric pressing. PloS One. 2014; 9(4):94533.
100. Berg JH, Croll TP. Glass ionomer restorative cement systems: an update. Pediatric Dentistry. 2015; 37(2):116-124.
101. Yip HK, Tay FR, Ngo HC, Smales RJ, Pashley DH. Bonding of contemporary glass ionomer cements to dentin. Dental Materials. 2001; 17(5):456-470.
102. Atmeh AR, Chong EZ, Richard G, Festy F, Watson TF. Dentin-cement interfacial interaction: calcium silicates and polyalkenoates. Journal of Dental Research. 2012; 91(5):454-459.
103. About I. Biodentine: from biochemical and bioactive properties to clinical applications. Giornale Italiano Di Endodonzia. 2016; 30(2):81-88.

104. Trevelin LT, Villanueva J, Zamperini CA, Mathew MT, Matos AB, Bedran-Russo AK. Investigation of five α-hydroxy acids for enamel and dentin etching: demineralization depth, resin adhesion and dentin enzymatic activity. Dental Materials. 2019; 35(6):900-908.
105. Nakabayashi N, Takarada K. Effect of HEMA on bonding to dentin. Dental Materials. 1992; 8(2):125-130.
106. Fujiwara S, Takamizawa T, Barkmeier WW, Tsujimoto A, Imai A, Watanabe H, Erickson RL, Latta MA, Nakatsuka T, Miyazaki M. Effect of double-layer application on bond quality of adhesive systems. Journal of the Mechanical Behavior of Biomedical Materials. 2018; 77:501-509.
107. Koike T, Hasegawa T, Itoh K, Yukitani W, Yamashita T, Wakumoto S, Hisamitsu H. Effect of multiple application of a dentin adhesive on contraction gap width of a resin-based composite. American Journal of Dentistry. 2002; 15(3):159-163.
108. Lee HE, Kim HC, Hur B, Park JK. The effect of adhesive thickness on microtensile bond strength to the cavity wall. Journal of Korean Academy of Conservative Dentistry. 2007; 32(1):9-18.
109. Hashimoto M, Sano H, Yoshida E, Hori M, Kaga M, Oguchi H, Pashley DH. Effects of multiple adhesive coatings on dentin bonding. Operative Dentistry. 2004; 29(4):416-423.
110. Tay FR, Pashley DH, Suh BI, Hiraishi N, Yiu CKY. Water treeing in simplified dentin adhesives-deja vu? Operative Dentistry. 2005; 30(5):561-579.
111. Tay FR, Hashimoto M, Pashley DH, Peters MC, Lai SCN, Yiu CKY, Cheong C. Aging affects two modes of nanoleakage expression in bonded dentin. Journal of Dental Research. 2003; 82(7):537-541.
112. Okuda M, Pereira PN, Nakajima M, Tagami J, Pashley DH. Long-term durability of resin dentin interface: nanoleakage vs microtensile bond strength. Operative Dentistry. 2002; 27(3):289-296.
113. Inokoshi M, De Munck J, Minakuchi S, Van Meerbeek B. Meta-analysis of bonding effectiveness to zirconia ceramics. Journal of Dental Research. 2014; 93(4):329-334.
114. Yoshida K, Tsuo Y, Atsuta M. Bonding of dual-cured resin cement to zirconia ceramic using phosphate acid ester monomer and zirconate coupler. Journal of Biomedical Materials Research Part B: Applied Biomaterials. 2006; 77(1):28-33.

115. Nagaoka N, Yoshihara K, Feitosa VP, Tamada Y, Irie M, Yoshida Y, Van Meerbeek B, Hayakawa S. Chemical interaction mechanism of 10-MDP with zirconia. Scientific Reports. 2017; 7(45563):1-7.
116. Chen L, Suh BI, Brown D, Chen X. Bonding of primed zirconia ceramics: evidence of chemical bonding and improved bond strengths. American Journal of Dentistry. 2012; 25(2):103-108.
117. Thammajaruk P, Inokoshi M, Chong S, Guazzato M. Bonding of composite cements to zirconia: A systematic review and meta-analysis of in vitro studies. Journal of the Mechanical Behavior of Biomedical Materials. 2018; 80:258-268.
118. Machida H. Technology of a traction drive CVT: Past, present and future. Tribology and Interface Engineering Series. 2005; 48:3-13.
119. Darvell BW. A glossary of terms for dental materials science. 12th ed: BW Darvell Bath UK. 2016.
120. Thompson JY, Anusavice KJ, Naman A, Morris HE. Fracture surface characterization of clinically failed all-ceramic crowns. Journal of Dental Research. 1994; 73(12):1824-1832.
121. Hanrahan G, Lu K. Application of factorial and response surface methodology in modern experimental design and optimization. Critical Reviews in Analytical Chemistry. 2006; 36(3-4):141-151.
122. Box GEP, Hunter JS, Hunter WG. Statistics for Experimenters. Wiley Series in Probability and Statistics. New Jersey: Wiley Hoboken, N. J.; 2005.
123. Landes D. The creation of knowledge and technique: Today's task and yesterday's experience. Daedalus. 1980:111-120.
124. Byar DP. Factorial and reciprocal control designs. Statistics in Medicine. 1990; 9(1-2):55-64.
125. Swift EJ. Options for dentin/enamel bonding: part IV. Journal of Esthetic Restorative Dentistry. 2010; 22(4):270-275.
126. Briso ALF, Mestrener SR, Delício G, Sundfeld RH, Bedran-Russo AK, de Alexandre RS, Ambrosano GMB. Clinical assessment of postoperative sensitivity in posterior composite restorations. Operative Dentistry. 2007; 32(5):421-426.
127. Schenkel AB, Veitz-Keenan A. Dental cavity liners for Class I and Class II resin-based composite restorations. Cochrane Database of Systematic Reviews. 2019; (3):1-34.

128. Burrow MF, Banomyong D, Harnirattisai C, Messer HH. Effect of glass-ionomer cement lining on postoperative sensitivity in occlusal cavities restored with resin composite—a randomized clinical trial. Operative Dentistry. 2009; 34(6):648-655.
129. Grogono AL, McInnes PM, Zinck JH, Weinberg R. Posterior composite and glass ionomer/composite laminate restorations: 2-year clinical results. American Journal of Dentistry. 1990; 3(4):147-152.
130. Akpata ES, Sadiq W. Post-operative sensitivity in glass-ionomer versus adhesive resin-lined posterior composites. American Journal of Dentistry. 2001; 14(1):34-38.
131. Sabbagh J, Fahd JC, McConnell RJ. Post-operative sensitivity and posterior composite resin restorations: a review. Dental Update. 2018; 45(3):207-213.
132. Banomyong D, Messer H. Two-year clinical study on postoperative pulpal complications arising from the absence of a glass-ionomer lining in deep occlusal resin-composite restorations. Journal of Investigative and Clinical Dentistry. 2013; 4(4):265-270.
133. Strober B, Veitz-Keenan A, Barna JA, Matthews AG, Vena D, Craig RG, Curro FA, Thompson VP. Effectiveness of a resin-modified glass ionomer liner in reducing hypersensitivity in posterior restorations: a study from the practitioners engaged in applied research and learning network. The Journal of the American Dental Association. 2013; 144(8):886-897.
134. Banomyong D, Harnirattisai C, Burrow MF. Posterior resin composite restorations with or without resin-modified, glass-ionomer cement lining: a 1-year randomized, clinical trial. Journal of Investigative and Clinical Dentistry. 2011; 2(1):63-69.
135. Shaw MT, MacKnight WJ. Introduction to Polymer Viscoelasticity. 4th ed. New Jersey, United States: John Wiley & Sons. 2018; 107-128.
136. Eliades. T KE, Zinelis S, Eliades, G. Effect of loading rate on bond strength. Journal of Orofacial Orthopedics. 2004; 65(4):336-342.
137. Ferracane JL. Hygroscopic and hydrolytic effects in dental polymer networks. Dental Materials. 2006; 22(3):211-222.
138. Asaoka K, Hirano S. Diffusion coefficient of water through dental composite resin. Biomaterials. 2003; 24(6):975-979.
139. Lohbauer U, Frankenberger R, Krämer N, Petschelt A. Time-dependent strength and fatigue resistance of dental direct restorative materials. Journal of Material Science: Materials in Medicine. 2003; 14(12):1047-1053.

140. Ferracane JL, Berge HX, Condon JR. In vitro aging of dental composites in water—effect of degree of conversion, filler volume, and filler/matrix coupling. Journal of Biomedical Materials Research 1998; 42(3):465-472.
141. Pongprueksa P, De Munck J, Inokoshi M, Van Meerbeek B. Polymerization efficiency affects interfacial fracture toughness of adhesives. Dental Materials. 2018; 34(4):684-692.
142. Michaud P-L, Brown M. Effect of universal adhesive etching modes on bond strength to dual-polymerizing composite resins. Journal of Prosthetic Dentistry. 2018; 119(4):657-662.
143. Eden GT, Craig RG, Peyton FA. Evaluation of a tensile test for direct filling resins. Journal of Dental Research. 1970; 49(2):428-834.
144. Bordin-Aykroyd S, Sefton J, Davies EH. In vitro bond strengths of three current dentin adhesives to primary and permanent teeth. Dental Materials. 1992; 8(2):74-78.
145. Elawsya ME, Elshhehawy TM, Zaghloul NM. Influence of various antioxidants on micro-shear bond strength of resin composite to bleached enamel. Journal of Esthetic and Restorative Dentistry. 2021; 33(2):371-379.
146. Amory C, Yvon J. Shear bond strength of a light-cured resin composite vs. dentin characteristics. Dental Materials. 1994; 10(3):203-209.
147. Peerling RH, Plasmans PM, Vrijhoef MM. Transverse resistance of composite resin restorations on dentin. Dental Materials. 1989; 5(1):27-30.
148. Fukushima T, Horibe T. A scanning electron microscopic investigation of bonding of methacryloyloxyalkyl hydrogen maleate to etched dentin. Journal Dental Research. 1990; 69(1):46-50.
149. Rechmann P, Bartolome N, Kinsel R, Vaderhobli R, Rechmann BMT. Bond strength of etch-and-rinse and self-etch adhesive systems to enamel and dentin irradiated with a novel CO 2 9.3 μm short-pulsed laser for dental restorative procedures. Lasers in Medical Science. 2017; 32(9):1981-1993.
150. Mazzoni A, Angeloni V, Comba A, Maravic T, Cadenaro M, Tezvergil-Mutluay A, Pashley DH, Tay FR, Breschi L. Cross-linking effect on dentin bond strength and MMPs activity. Dental Materials. 2018; 34(2):288-295.
151. Ting S, AFM A, Sun J, Kakuda S, Sidhu SK, Yoshida Y, Selimovic D, Sano H. Effect of different remaining dentin thickness and long term water storage on dentin bond strength. Dental Materials Journal. 2018:562-567.

152. Barbosa-Martins LF, de Sousa JP, de Castilho ARF, Puppin-Rontani J, Davies RPW, Puppin-Rontani RM. Enhancing bond strength on demineralized dentin by pre-treatment with selective remineralising agents. Journal of the Mechanical Behavior of Biomedical Materials. 2018; 81:214-221.
153. Bonstein T, Garlapo D, Donarummo Jr J, Bush PJ. Evaluation of varied repair protocols applied to aged composite resin. Journal of Adhesive Dentistry. 2005; 7(1):41-49.
154. McInnes-Ledoux P, Ledoux WR, Weinberg R. Bond strength of dentinal bonding agents to chemomechanically prepared dentin. Dental Materials. 1987; 3(6):331-336.
155. Hasegawa T, Manabe A, Itoh K, Wakumoto S. Bonding stability and shelf life of GLUMA. Dental Materials. 1989; 5(3):150-152.
156. Webb RE, Johnston AD. Dentin-bonding molar efficiency using N-phenylglycine, N-phenyl-beta-alanine, or N-methyl-N-phenylglycine. Journal of Dental Research. 1991; 70(3):211-214.
157. Perdigao J, Swift Jr EJ, Denehy GE, Wefel JS, Donly KJ. In vitro bond strengths and SEM evaluation of dentin bonding systems to different dentin substrates. Journal of Dental Research. 1994; 73(1):44-55.
158. Goodis HE, Marshall Jr GW, White JM, Gee L, Hornberger B, Marshall SJ. Storage effects on dentin permeability and shear bond strengths. Dental Materials. 1993; 9(2):79-84.
159. Aquilino SA, Williams VD. The effect of storage solutions and mounting media on the bond strenghts of a dentinal adhesive to dentin. Dental Materials. 1987; 3(3):131-134.
160. Gray SE, Burgess JO. An in vivo and in vitro comparison of two dentin bonding agents. Dental Materials. 1991; 7(3):161-165.
161. Senda A, Kamiya K, Gomi A, Kawaguchi T. In vitro and clinical evaluations of a dentin bonding system with a dentin primer. Operative Dentistry. 1995; 20:51-57.
162. Darvell BW. Misuse of ISO standards in dental materials research. Dental Materials. 2020; 36(12):1493-1494.
163. Musanje L, Darvell BW. Effects of strain rate and temperature on the mechanical properties of resin composites. Dental Materials. 2004; 20(8):750-765.
164. Yamaguchi K, Miyazaki M, Takamizawa T, Tsubota K, Rikuta A. Influence of crosshead speed on micro-tensile bond strength of two-step adhesive systems. Dental Materials. 2006; 22(5):420-425.

165. Poitevin A, De Munck J, Van Landuyt K, Coutinho E, Peumans M, Lambrechtse P, Van Meerbeek B. Critical analysis of the influence of different parameters on the microtensile bond strength of adhesives to dentin. Journal of Adhesive Dentistry. 2008; 10(1):7-16.
166. Reis A, de Oliveira B, José R, Loguercio AD. Influence of crosshead speed on resin-dentin microtensile bond strength. Journal of Adhesive Dentistry. 2004; 6(4):275-278.
167. Broughton W. Testing the mechanical, thermal and chemical properties of adhesives for marine environments. Amsterdam, Netherlands: Elsevier. 2012; 99-121.
168. Jawlik AA. Statistics from a to z: Confusing concepts clarified. New Jersey, United States: John Wiley & Sons. 2016; 11-27.
169. Takemori T, Chigira H, Itoh K, Hisamitsu H, Wakumoto S. Factors affecting tensile bond strength of composite to dentin. Dental Materials. 1993; 9(2):136-138.
170. Tamura Y, Tsubota K, Otsuka E, Endo H, Takubo C, Miyazaki M, Latta MA. Dentin bonding: Influence of bonded surface area and crosshead speed on bond strength. Dental Materials Journal. 2011; 30(2):206-211.
171. Lindemuth JS, Hagge MS. Effect of universal testing machine crosshead speed on the shear bond strength and bonding failure mode of composite resin to enamel and dentin. Military Medicine. 2000; 165(10):742-746.
172. Hara AT, Pimenta LAF, Rodrigues Jr AL. Influence of cross-head speed on resin-dentin shear bond strength. Dental Materials. 2001; 17(2):165-169.
173. Klocke A, Kahl-Nieke B. Influence of cross-head speed in orthodontic bond strength testing. Dental Materials. 2005; 21(2):139-144.
174. El-Safty SM. Effect of speed of loading on compressive strength and flexural strength of dental resin-composites. Egyptian Dental Journal. 2018; 64(1):625-633.
175. Hooi P, Addison O, Fleming GJP. Atmospheric moisture effects on the testing rate and cementation seating load following resin-strengthening of a soda lime glass analogue for dental porcelain. Journal of Dentistry. 2013; 41(12):1208-1213.
176. Hooi P, Addison O, Fleming GJP. Testing rate and cementation seating load effects on resin-strengthening of a dental porcelain analogue. Journal of Dentistry. 2013; 41(6):514-520.
177. Oshida Y, Miyazaki M. Dentin bonding system. Part II: Effect of crosshead speed. Biomedical Materials and Engineering. 1996; 6(2):87-100.

178. Curran-Everett D. Explorations in statistics: the log transformation. Advances in Physiology Education. 2018; 42(2):343-347.
179. Cox NJ. Transformations: an introduction: Boston College, Newton, Massachusetts; 2007 [Available from: http://fmwww.bc.edu/repec/bocode/t/transint.html.
180. Muñoz MA, Baggio R, Mendes YBE, Gomes GM, Luque-Martinez I, Loguercio AD, Reis A. The effect of the loading method and cross-head speed on resin–dentin microshear bond strength. International Journal of Adhesion and Adhesives. 2014; 50:136-141.
181. Shooter KJ, Griffin MP, Kerr B. The effect of changing crosshead speed on the shear bond strength of orthodontic bonding adhesive. Austeralian Orthodontic Journal. 2012; 28(1):44-50.
182. Kumar N, Zafar MS, Dahri WM, Khan MA, Khurshid Z, Najeeb S. Effects of deformation rate variation on biaxial flexural properties of dental resin composites. Journal of Taibah University Medical Sciences. 2018; 13(4):319-326.
183. Biau DJ, Kernéis S, Porcher R. Statistics in brief: the importance of sample size in the planning and interpretation of medical research. Clinical Orthopaedics and Related Research. 2008; 466(9):2282-2288.
184. Bishara SE, Soliman M, Laffoon J, Warren JJ. Effect of changing a test parameter on the shear bond strength of orthodontic brackets. The Angle Orthodontist. 2005; 75(5):832-835.
185. Shalkey DA, Burgess JO. Shear-strength of acrylic rods at varying crosshead speeds. Journal of Dental Research. 1995; 74(193):36.
186. Naves LZ, Silva GR, Correr-Sobrinho L, Costa AR, Valdivia ADCM, Soares CJ. Influence of crosshead speed on failure load and failure mode of restored maxillary premolars. Brazilian Oral Research. 2016; 30(1):3-8.
187. De Abreu CW, Duarte Filho G, Kojima AN, Jóias RM, Mesquita AMM. Evaluation of crosshead speed influence on shear bond strength test. Brazilian Dental Science. 2014; 17(3):50-53.
188. Versluis A, Tantbirojn D, Douglas WH. Why do shear bond tests pull out dentin? Journal of Dental Research. 1997; 76(6):1298-1307.
189. Kumar N, Shortall A. Performance of the experimental resins and dental nanocomposites at varying deformation rates. Journal of Investigative and Clinical Dentistry. 2014; 5(3):237-242.

190. Instron-Corporation. User instruction manual -- manual no M10-1125-1(C). 1979 (accessed 15/09/2024). Available from: https://www.nmt.edu/academics/mtls/faculty/mccoy/docs/instron/InstronManual_M10_1125_1_C.pdf.
191. Instron-Corporation. Technical note | Data acquisition: bandwidth, accuracy, and R&R. 2012 (Accessed 15/09/2024). Available from: https://www.instron.com/en/-/media/literature-library/whitepapers/2012/11/bandwidth-whitepaper.pdf.
192. Instron-Corporation. Bluehill Universal. (Accessed 15/09/2024). Available from: https://www.instron.com/en/products/materials-testing-software/bluehill-universal.
193. Altman DG. Statistics and ethics in medical research: III How large a sample? British medical journal. 1980; 281(6251):1336.
194. VanVoorhis CW, Morgan BL. Understanding power and rules of thumb for determining sample sizes. Tutorials in Quantitative Methods for Psychology. 2007; 3(2):43-50.
195. Roldán SI, Restrepo LG, Isaza JF, Vélez LG, Buschang PH. Are maximum bite forces of subjects 7 to 17 years of age related to malocclusion? The Angle Orthodontist. 2016; 86(3):456-461.
196. Strasak AM, Zaman Q, Marinell G, Pfeiffer KP, Ulmer H. The use of statistics in medical research: A comparison of The New England Journal of Medicine and Nature Medicine. The American Statistician. 2007; 61(1):47-55.

9. Appendices

Appendix 1: Irradiance and spectral output of the LED light curing unit.

The LED light source was checked with a fibre-coupled UV-Vis spectrophotometer (USB4000), using a 400 µm fibre and cosine corrector (CC3) (all Ocean Optics, London, England). Calibration against light source (DH2000) was using deuterium and halogen Lamps (Ocean Optics), with an integration time of 3×10^{-4} s (1 scan). Three measurements were taken with the LCU tip centred on the cosine corrector at 0 mm distance.. The integration limits were 400 - 500 nm with background noise removal (based on regions where there was no signal).

Irradiance recorded: 2468 ± 120 mW/cm² (mean, sd).

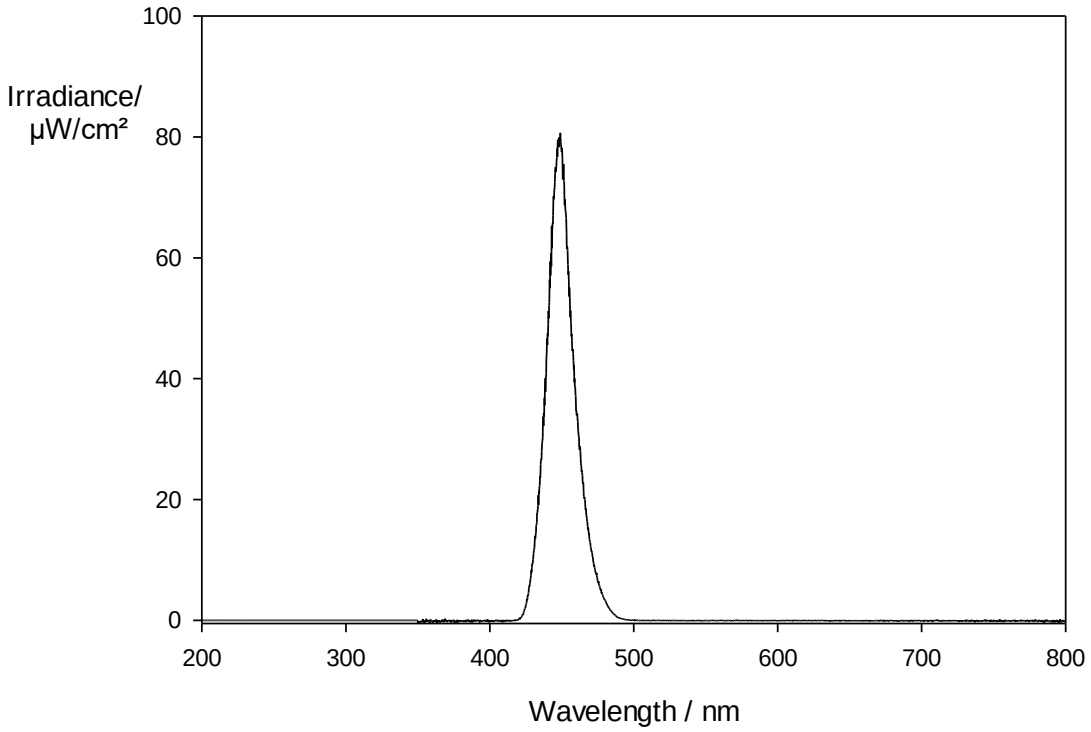

Fig A1 Spectrum of the light-curing unit used.

Appendix 2: Raw data for four-point bend testing of monolithic Filtek One (FB), Beautifil Bulk (BB) (hand-pressed [hb] and constant-load [cl]), Tetric Evoceram (TEC) and Filtek Flowable (FF) (50 and 28 mm specimens), showing the calculated simple (FS) and corrected (FS*) flexural strength, and the difference of these values.

Table 1 Monolithic FB.

	Width / mm	Height / mm	Load / N	Deflection / mm	FS / MPa	FS* / MPa	FS - FS* / MPa
1	4.89	1.95	50.11	2.89	80.85	77.74	3.11
2	4.91	2.00	49.42	2.53	75.49	72.88	2.60
3	4.87	2.02	50.94	1.99	76.90	74.80	2.11
4	4.89	1.85	40.71	3.15	72.97	70.07	2.90
5	4.94	2.00	47.69	2.80	72.40	69.64	2.76
6	4.89	1.99	47.08	2.57	72.94	70.39	2.54
7	4.91	1.98	48.58	2.86	75.71	72.79	2.92
8	4.91	2.01	53.56	2.99	81	77.68	3.32
9	4.88	2.04	53.13	2.50	78.48	75.75	2.73
10	4.88	2.08	53.96	2.34	76.67	74.13	2.54
11	4.88	1.99	48.47	2.48	75.24	72.71	2.53
12	4.87	1.93	48.63	2.30	80.42	77.99	2.43
13	4.88	2.01	54.39	2.37	82.76	80.07	2.69
14	4.90	1.93	47.97	2.49	78.85	76.26	2.58

Table 2 Monolithic BB_{hb}.

	Width / mm	Height / mm	Load / N	Deflection / mm	FS / MPa	FS* / MPa	FS - FS* / MPa
1	4.89	2.14	39.63	2.71	53.09	50.99	2.10
2	4.90	1.96	38.14	1.34	60.78	59.70	1.09
3	4.82	2.13	29.12	1.17	39.95	39.27	0.68
4	4.89	2.09	30.56	1.24	42.92	42.16	0.76
5	4.91	1.98	30.48	1.87	47.50	46.30	1.20
6	4.89	1.98	33.40	1.80	52.27	51	1.27
7	4.92	2.08	40.90	1.59	57.64	56.34	1.30
8	4.88	1.95	38.27	1.19	61.87	60.89	0.98
9	4.89	2.03	43.47	1.22	64.72	63.62	1.09
10	4.91	1.96	35.38	1.60	56.27	55.07	1.20
11	4.90	1.91	29.57	1.95	49.63	48.37	1.26

Table 3 Monolithic BB_{cl}.

	Width / mm	Height / mm	Load / N	Deflection / mm	FS / MPa	FS* / MPa	FS - FS* / MPa
1	4.89	1.78	41.27	2.23	79.91	77.75	2.16
2	4.88	1.96	47.23	1.43	75.58	74.14	1.44
3	4.86	2.00	53.39	1.57	82.39	80.63	1.76
4	4.88	2.00	52.21	1.39	80.24	78.72	1.52
5	4.87	1.97	48.20	1.54	76.51	74.93	1.58
6	4.89	2.06	50.18	1.20	72.55	71.32	1.22
7	4.90	2.00	52.40	1.44	80.20	78.63	1.58
8	4.88	1.80	39.27	1.19	74.51	73.42	1.09
9	4.89	1.98	50.00	1.48	78.24	76.68	1.56
10	4.91	2.05	53.46	1.35	77.73	76.26	1.47

Table 4 Monolithic TEC.

	Width / mm	Height / mm	Load / N	Deflection / mm	FS / MPa	FS* / MPa	FS - FS* / MPa
1	4.87	1.86	34.22	1.85	60.93	59.50	1.43
2	4.90	1.96	39.79	1.80	63.41	61.89	1.53
3	4.88	2.00	43.92	1.18	67.50	66.41	1.09
4	4.89	1.96	39.78	0.92	63.53	62.75	0.78
5	4.92	1.97	36.12	0.99	56.75	56.00	0.75
6	4.85	1.99	39.87	1.67	62.28	60.86	1.41
7	4.89	1.82	30.33	1.23	56.17	55.32	0.86
8	4.91	1.99	43.62	1.55	67.30	65.89	1.42
9	4.89	1.86	32.81	1.10	58.18	57.37	0.81

Table 5 Monolithic FF_{50}.

	Width / mm	Height / mm	Load / N	Deflection / mm	FS / MPa	FS* / MPa	FS - FS* / MPa
1	4.91	1.59	107.92	2.31	169.54	159.49	10.05
2	4.92	1.78	105.74	1.85	132.27	125.24	7.03
3	4.91	1.65	92.30	1.89	134.64	127.87	6.78
4	4.90	1.76	80.35	1.46	103.23	98.95	4.28
5	4.91	1.77	96.45	1.87	122.27	115.74	6.53
6	4.91	1.76	111.28	2.12	142.67	134.08	8.59
7	4.91	1.78	110.43	2.08	138.42	130.15	8.27
8	4.90	1.74	111.86	2.25	147.03	137.74	9.29
9	4.93	1.75	116.31	2.06	150.22	141.48	8.74
10	4.90	1.86	93.53	1.58	107.59	102.49	5.10

Table 6 Monolithic FF_{28}.

	Width / mm	Height / mm	Load / N	Deflection / mm	FS / MPa	FS* / MPa	FS - FS* / MPa
1	4.89	1.70	101.02	1.91	139.39	132.09	7.30
2	4.92	1.78	119.41	2.24	149.37	139.76	9.61
3	4.90	1.73	114.58	2.12	152.35	143.34	9.02
4	4.89	1.72	104.18	1.90	140.43	133.02	7.41
5	4.91	1.78	114.25	1.89	143.21	135.43	7.78
6	4.89	1.78	118.37	1.83	148.98	141.15	7.83
7	4.91	1.77	109.93	1.55	139.36	133.18	6.17
8	4.91	1.73	110.32	2.03	146.39	138.09	8.30
9	4.87	1.77	119.58	1.79	152.83	145.02	7.81
10	4.86	1.76	107.81	2.42	139.65	130.05	9.60
11	4.88	1.74	109.93	1.56	145.09	138.73	6.36

Appendix 3: Raw data for four-point testing of repaired Filtek One (FB) (monolithic, overlap, butt joint), showing the calculated simple (FS) and corrected (FS*) flexural strength, and the difference of these values.

Table 1 FB (overlap joint).

	Width / mm	Height / mm	Load / N	Deflection / mm	FS / MPa	FS* / MPa	FS - FS* / MPa
1	4.89	2.04	17.61	1.43	25.96	25.44	0.52
2	4.87	2.13	18.84	1.57	25.53	24.95	0.58
3	4.85	2.13	13.39	1.39	18.26	17.89	0.37
4	4.87	1.99	14.32	1.54	22.28	21.81	0.47
5	4.89	2.03	17.92	1.2	26.68	26.24	0.44
6	4.87	2.15	18.42	1.44	24.55	24.03	0.52
7	4.85	2.07	11.89	1.19	17.16	16.88	0.29
8	4.91	2.09	16.11	1.48	22.53	22.06	0.48

Table 2 FB (butt joint).

	Width / mm	Height / mm	Load / N	Deflection / mm	FS / MPa	FS* / MPa	FS - FS* / MPa
1	4.89	2.04	6.36	2.71	9.38	9.02	0.35
2	4.88	2.13	7.85	1.34	10.64	10.43	0.21
3	4.87	2.15	9.25	1.17	12.33	12.12	0.21
4	4.85	2.07	5.32	1.24	7.68	7.55	0.13
5	4.87	2.01	7.27	1.87	11.08	10.80	0.28
6	4.89	2.00	6.67	1.80	10.23	9.98	0.25
7	5.05	2.07	11.95	1.59	16.57	16.20	0.37
8	4.89	2.20	13.00	1.19	16.48	16.18	0.29
9	4.89	2.02	2.86	1.22	4.30	4.23	0.07
10	4.87	2.06	9.57	1.60	13.89	13.58	0.31
11	4.85	2.13	7.03	1.95	9.58	9.31	0.27

Appendix 4: Raw data for four-point bend testing of monolithic zinc phosphate cement (ZPC) and zinc polycarboxylate (ZCC), showing the calculated simple (FS) and corrected (FS*) flexural strength, and the difference of these values.

Table 1 Zinc phosphate cement (ZPC).

	Width / mm	Height / mm	Load / N	Deflection / mm	FS / MPa	FS* / MPa	FS - FS* / MPa
1	2.64	2.04	0.82	0.70	2.02	1.99	0.02
2	2.57	2.14	1.12	0.75	2.57	2.53	0.03
3	2.60	2.17	0.79	0.74	1.74	1.72	0.02
4	2.53	1.99	0.51	0.45	1.37	1.36	0.01
5	2.56	2.01	0.93	0.66	2.43	2.40	0.03

Table 2 Zinc polycarboxylate (ZCC).

ZCC	Width / mm	Height / mm	Load / N	Deflection / mm	FS / MPa	FS* / MPa	FS - FS* / MPa
1	2.74	1.99	1.68	0.14	4.18	4.17	0.01
2	2.70	2.13	2.04	1.23	4.50	4.40	0.10
3	2.67	2.09	2.01	0.82	4.65	4.59	0.07
4	2.66	2.01	2.06	0.88	5.18	5.10	0.08
5	2.69	2.08	1.56	0.94	3.62	3.56	0.06

Appendix 5: Raw data for four-point testing of adhesive bond strength of glass ionomer cement Aquacem (GIC_A), to smooth stainless steel (SS) and dentine coupons, showing the calculated simple (FS) and corrected (FS*) flexural strength, and the difference of these values.

Table 1 Glass ionomer cement Aquacem (GIC_A) on smooth stainless steel (SS).

	Width / mm	Height / mm	Load / N	Deflection / mm	FS / MPa	FS* / MPa	FS - FS* / MPa
1	2.59	1.98	0.11	0.65	0.29	0.29	0
2	2.58	2.15	0.20	0.77	0.45	0.45	0.01
3	2.63	2.05	0.17	0.56	0.42	0.41	0
4	2.67	2.03	0.19	0.87	0.47	0.46	0.01
5	2.59	2.02	0.09	0.43	0.23	0.23	0

Table 2 Glass ionomer cement Aquacem (GIC_A) on Dentine.

	Width / mm	Height / mm	Load / N	Deflection / mm	FS / MPa	FS* / MPa	FS - FS* / MPa
1	2.62	2.09	0.03	0.58	0.07	0.07	0
2	2.58	2.15	0.08	0.75	0.18	0.18	0
3	2.59	2.05	0.09	0.74	0.22	0.22	0
4	2.53	1.99	0.08	0.27	0.22	0.21	0
5	2.60	2.11	0.06	0.57	0.14	0.14	0

Appendix 6: Raw data for four-point band testing of adhesive bond strength of two-step total-etch resin cements (Adper Scotchbond 1 XT) (ASX) to dentine coupons, showing the calculated simple (FS) and corrected (FS*) flexural strength, and the difference of these values. Three groups were tested: Adhesive alone (A), Etching + Adhesive (E+A), 120 grit + Adhesive (G+A).

Table 1 Adhesive alone (A).

	Width / mm	Height / mm	Load / N	Deflection / mm	FS / MPa	FS* / MPa	FS - FS* / MPa
1	4.94	2.02	2.62	0.68	3.90	3.86	0.04
2	5.02	2.27	4.44	0.63	5.15	5.10	0.05
3	5.06	1.93	2.65	0.56	4.22	4.19	0.03
4	5.56	2.14	4.84	0.40	5.70	5.67	0.03
5	5.32	2.16	5.10	0.41	6.16	6.13	0.04

Table 2 Etching + Adhesive (E+A).

	Width / mm	Height / mm	Load / N	Deflection / mm	FS / MPa	FS* / MPa	FS - FS* / MPa
1	5.08	2.06	16.24	0.83	22.60	22.34	0.26
2	5.02	2.03	12.42	0.93	18.01	17.78	0.23
3	5.06	1.91	14.51	1	23.58	23.27	0.31
4	5.16	1.97	15.85	6.30	23.74	21.74	2.01
5	5.00	1.88	10.85	0.65	18.42	18.27	0.15
6	5.10	1.90	11.93	1.11	19.44	19.16	0.28

Table 3 120 grit + Adhesive (G+A).

	Width / mm	Height / mm	Load / N	Deflection / mm	FS / MPa	FS* / MPa	FS - FS* / MPa
1	5.06	1.92	6.57	0.83	10.57	10.45	0.11
2	5.06	1.94	6.18	0.27	9.74	9.70	0.03
3	5.13	1.98	8.23	0.39	12.28	12.21	0.06
4	5.17	2.18	11.27	0.37	13.76	13.69	0.08
5	5.00	1.98	5.34	0.57	8.17	8.11	0.06

Appendix 7: Raw data for four-point testing of adhesive bond strength of three-step total-etch resin cements (Adper Scotchbond Multipurpose) (ASX) to dentine coupons, showing the calculated simple (FS) and corrected (FS*) flexural strength, and the difference of these values. Eight groups were tested: No treatment (N), Primer alone (P), Adhesive alone (A), Etching alone (E), Etching + Primer (E+P), Etching + Adhesive (E+A), Primer + Adhesive (P+A),

Table 1 No treatment (N).

	Width / mm	Height / mm	Load / N	Deflection / mm	FS / MPa	FS* / MPa	FS - FS* / MPa
1	5.05	1.96	0.82	1.12	1.27	1.25	0.02
2	5.09	1.88	0.41	0.71	0.68	0.68	0.01
3	5.10	1.92	0.74	0.73	1.18	1.17	0.01
4	5.08	1.90	1.36	1.18	2.22	2.19	0.03
5	5.07	1.90	0.93	0.90	1.52	1.51	0.02

Table 2 Etching alone (E).

	Width / mm	Height / mm	Load / N	Deflection / mm	FS / MPa	FS* / MPa	FS - FS* / MPa
1	5.22	1.96	7.72	0.75	11.55	11.43	0.12
2	4.98	1.70	5.34	0.63	11.13	11.05	0.08
3	5.24	1.99	7.72	1.42	11.16	10.95	0.22
4	5.10	1.92	5.59	0.88	8.92	8.82	0.10
5	5.10	2.10	4.83	0.48	6.44	6.40	0.04
6	4.80	1.80	4.98	0.93	9.61	9.50	0.11
7	5.02	2.01	5.10	0.48	7.54	7.49	0.05
8	5.16	1.86	5.66	0.54	9.51	9.45	0.07

Table 3 Primer alone (P).

	Width / mm	Height / mm	Load / N	Deflection / mm	FS / MPa	FS* / MPa	FS - FS* / MPa
1	5.06	2.06	6.55	0.53	9.15	9.08	0.07
2	4.91	1.99	6.73	0.37	10.38	10.33	0.05
3	4.93	2.00	5.98	0.43	9.10	9.04	0.05
4	5.03	2.05	6.59	1.08	9.35	9.21	0.14
5	5.07	1.94	7.06	0.73	11.10	10.99	0.11

Table 4 Adhesive alone (A).

	Width / mm	Height / mm	Load / N	Deflection / mm	FS / MPa	FS* / MPa	FS - FS* / MPa
1	5.18	2.07	2.89	0.69	3.91	3.87	0.04
2	5.11	2.43	5.77	0.62	5.74	5.68	0.06
3	4.93	2.00	3.24	0.60	4.93	4.89	0.04
4	4.97	2.03	3.76	0.42	5.51	5.48	0.03
5	5.10	2.00	3.70	0.75	5.44	5.39	0.06

Table 5 Etching + Primer (E+P).

	Width / mm	Height / mm	Load / N	Deflection / mm	FS / MPa	FS* / MPa	FS - FS* / MPa
1	5.16	2.13	14.30	0.95	18.33	18.07	0.25
2	5.11	1.92	13.08	0.76	20.83	20.62	0.21
3	5.20	2.06	18.83	0.54	25.60	25.41	0.19
4	5.09	2.00	15.67	0.56	23.09	22.91	0.18
5	5.19	2.00	12.87	0.73	18.60	18.41	0.19
6	5.00	2.12	16.78	0.74	22.40	22.16	0.24
7	5.08	1.90	12.12	0.64	19.83	19.66	0.16

Table 6 Etching + Adhesive (E+A),

	Width / mm	Height / mm	Load / N	Deflection / mm	FS / MPa	FS* / MPa	FS - FS* / MPa
1	5.11	2.00	8.81	0.66	12.93	12.81	0.12
2	5.42	2.10	11.47	0.49	14.40	14.30	0.10
3	5.16	1.91	9.08	0.52	14.47	14.37	0.10
4	5.01	1.90	6.81	0.37	11.30	11.24	0.05
5	5.09	1.94	7.24	0.32	11.34	11.29	0.05

Table 7 Primer + Adhesive (P+A).

	Width / mm	Height / mm	Load / N	Deflection / mm	FS / MPa	FS* / MPa	FS - FS* / MPa
1	5.10	1.99	11.90	2.34	17.68	17.12	0.56
2	5.09	1.97	12.88	1.24	19.56	19.23	0.33
3	5.10	2.06	15.80	2.01	21.90	21.28	0.62
4	5.01	1.80	8.84	1.45	16.34	16.05	0.29
5	5.03	1.96	9.56	1.87	14.84	14.47	0.37
6	5.22	1.86	7.85	1.44	13.04	12.80	0.24
7	5.31	2.09	12.17	1.28	15.74	15.45	0.29
8	5.11	2.05	14.96	1.62	20.90	20.43	0.47
9	5.00	2.07	15.33	1.54	21.47	21	0.47
10	5.00	1.95	11.49	2.23	18.13	17.59	0.54
11	5.14	1.85	8.02	1.76	13.68	13.37	0.30

Table 8 Etching + Primer + Adhesive (E+P+A).

	Width / mm	Height / mm	Load / N	Deflection / mm	FS / MPa	FS* / MPa	FS - FS* / MPa
1	5.09	1.86	12.30	0.69	20.95	20.77	0.18
2	5.00	1.77	8.40	2.08	16.09	15.68	0.40
3	5.10	1.83	10.43	1.39	18.32	18.00	0.32
4	5.16	1.93	11.68	2.01	18.23	17.75	0.48
5	5.12	1.88	14.79	2.32	24.52	23.79	0.73
6	5.12	1.97	19.72	0.92	29.77	29.41	0.37
7	5.01	1.88	11.60	1.97	19.65	19.16	0.50
8	5.09	1.82	12.74	1.57	22.67	22.23	0.44
9	5.06	1.85	13.56	2.32	23.49	22.80	0.69
10	5.51	2.08	15.39	1.88	19.37	18.85	0.52

Appendix 8: Raw data for four-point testing of adhesive bond strength of self-adhesive resin cements (RelyX Unicem) (RX) to zirconia beams, showing the calculated simple (FS) and corrected (FS*) flexural strength, and the difference of these values. Eight groups were tested: No treatment (N) and Etching alone (E).

Table 1 Adhesive alone (A).

	Width / mm	Height / mm	Load / N	Deflection / mm	FS / MPa	FS* / MPa	FS - FS* / MPa
1	5.35	2.18	11.73	0.4	12.46	12.37	0.09
2	5.47	2.2	14.7	0.34	14.99	14.90	0.10
3	5.3	2.17	16.58	0.53	17.94	17.76	0.17
4	5.37	2.2	15.32	0.35	15.91	15.81	0.10
5	5.37	2.2	16.22	0.47	16.85	16.70	0.15

Table 2 Etching + Adhesive (E+A).

	Width / mm	Height / mm	Load / N	Deflection / mm	FS / MPa	FS* / MPa	FS - FS* / MPa
1	5.33	2.16	16.45	0.42	17.86	17.72	0.14
2	5.42	2.25	17.64	0.49	17.36	17.20	0.16
3	5.33	2.2	23.2	0.31	24.28	24.14	0.14
4	5.3	2.2	10.6	0.31	11.16	11.09	0.06
5	5.3	2.2	20.01	0.38	21.06	20.91	0.15

Appendix 9: A copy of the report generated by SigmaPlot 15 for the three-way analysis of variance (three-way AoV) of the log-transformed corrected flexural strength (logFS*) results for the four-point bend test of the adhesive bond strength of three-step total-etch resin cement (Adper Scotchbond Multipurpose) to dentine coupons.

Due to an apparent bug in the Sigmaplot programming for three-way AoV, while the main results are consistent, there are differences in some calculated values when the order of addition of the factors is changed (this has been reported). Accordingly, the analysis was repeated for all 6 permutations of the 3 factors, with the order shown in the section title. Only where the results differed from the first set are they shown in the subsequent sections. The overall conclusions are not affected.

1. Etch + Primer + Adhesive

Normality Test (Shapiro-Wilk): Passed (P = 0.139)
Equal Variance Test (Brown-Forsythe): Passed (P = 0.068)

Source of variation	DF	SS	MS	F	P
Adhesive	1	0.75	0.75	99.98	2.54×10^{-14}
Etch	1	2.25	2.25	300.82	$<0.1 \times 10^{-14}$
Primer	1	3.10	3.10	413.68	$<0.1 \times 10^{-14}$
Adhesive × Etch	1	0.40	0.40	52.95	2.77×10^{-9}
Adhesive × Primer	1	0.20	0.20	26.86	4.32×10^{-6}
Etch × Primer	1	0.57	0.57	76.52	1.67×10^{-11}
Adhesive × Etch × Primer	1	0.03	0.03	4.60	0.037
Residual	48	0.36	0.01		
Total	55	7.09	0.13		

There is a statistically significant interaction between Adhesive, Etch and Primer (P = 0.037). This indicates that the effect of one factor is not consistent at all combinations of the two other factors; and, therefore, an unambiguous interpretation of the main effects is not possible.

All Pairwise Multiple Comparison Procedures (Holm-Sidak method):
Overall significance level = 0.05

Comparisons for factor: Etch

Comparison	Diff of Means	t	P
1 *vs.* 0	0.42	17.34	$<0.1\times 10^{-14}$

Comparisons for factor: Primer

Comparison	Diff of Means	t	P
1 *vs.* 0	0.49	20.34	$<0.1 \times 10^{-14}$

Comparisons for factor: Adhesive

Comparison	Diff of Means	t	P
1 *vs.* 0	0.24	1.0	2.54×10^{-14}

Three Way Interaction Term Analysis:

Evaluated Etch × Primer across levels of Adhesive:

The effect of the Etch × Primer interaction depends on what level of Adhesive is present.

There is a significant Etch × Primer interaction at level 0 of Adhesive. ($P = 3.54 \times 10^{-6}$)

There is a significant Etch × Primer interaction at level 1 of Adhesive. ($P = 0.024$)

Simple, Simple Main Effects at level 0 of Adhesive:

The difference in the mean values among the different levels of Etch evaluated within level 0 of Primer and level 0 of Adhesive is greater than would be expected by chance. There is a statistically significant difference ($P = <0.1\times 10^{-14}$).

Comparisons for factor: Etch within 0-0

Comparison	Diff of Means	t	P
1 *vs.* 0	0.86	17.47	$<0.1 \times 10^{-14}$

The difference in the mean values among the different levels of Etch evaluated within level 1 of Primer and level 0 of Adhesive is greater than would be expected by chance. There is a statistically significant difference ($P = 3.29 \times 10^{-8}$).

Comparisons for factor: Etch within 1-0

Comparison	Diff of Means	t	P
1 *vs.* 0	0.33	6.58	3.29×10^{-8}

The difference in the mean values among the different levels of Primer evaluated within level 0 of Etch and level 0 of Adhesive is greater than would be expected by chance. There is a statistically significant difference ($P = <0.1\times 10^{-14}$).

Comparisons for factor: Primer within 0-0

Comparison	Diff of Means	t	P
1 *vs.* 0	0.88	16.15	$<0.1 \times 10^{-14}$

The difference in the mean values among the different levels of Primer evaluated within level 1 of Etch and level 0 of Adhesive is greater than would be expected by chance. There is a statistically significant difference ($P = 2.83 \times 10^{-10}$).

Comparisons for factor: Primer within 1-0

Comparison	Diff of Means	t	P
1 *vs.* 0	0.36	7.93	2.83×10^{-10}

Simple, Simple Main Effects at level 1 of Adhesive:

The difference in the mean values among the different levels of Etch evaluated within level 0 of Primer and level 1 of Adhesive is greater than would be expected by chance. There is a statistically significant difference ($P = 1.84 \times 10^{-9}$).

Comparisons for factor: Etch within 0-1

Comparison	Diff of Means	t	P
1 *vs.* 0	0.50	7.39	1.84×10^{-9}

The difference in the mean values among the different levels of Etch evaluated within level 1 of Primer and level 1 of Adhesive is not great enough to exclude the possibility that the difference is just due to random sampling variability. There is not a statistically significant difference ($P = 0.031$).

The difference in the mean values among the different levels of Primer evaluated within level 0 of Etch and level 1 of Adhesive is greater than would be expected by chance. There is a statistically significant difference ($P = 0.4 \times 10^{-14}$).

Comparisons for factor: Primer within 0-1

Comparison	Diff of Means	t	P
1 *vs.* 0	0.53	11.32	0.4×10^{-14}

The difference in the mean values among the different levels of Primer evaluated within level 1 of Etch and level 1 of Adhesive is greater than would be expected by chance. There is a statistically significant difference ($P = 6.39 \times 10^{-5}$).

Comparisons for factor: Primer within 1-1

Comparison	Diff of Means	t	P
1 *vs.* 0	0.21	4.38	6.39×10^{-5}

Least square means for Etch:

Group	Mean	SEM
0	0.72	0.02
1	1.21	0.02

Least square means for Primer:

Group	Mean	SEM
0	0.72	0.02
1	1.21	0.02

Least square means for Adhesive:

Group	Mean	SEM
0	0.84	0.02
1	1.09	0.02

Least square means for Etch × Primer:

Group	Mean	SEM
0 × 0	0.40	0.03
0 × 1	1.11	0.02
1 × 0	1.03	0.02
1 × 1	1.32	0.02

Least square means for Etch × Adhesive:

Group	Mean	SEM
0 × 0	0.54	0.03
0 × 1	1.14	0.02
1 × 0	0.96	0.02
1 × 1	1.21	0.02

Least square means for Primer × Adhesive:

Group	Mean	SEM
0 × 0	0.53	0.02
0 × 1	1.15	0.03
1 × 0	0.90	0.03
1 × 1	1.27	0.02

Least square means for Adhesive × Etch × Primer:

Group	Mean	SEM
0 × 0 × 0	0.10	0.04
0 × 0 × 1	0.99	0.04
0 × 1 × 0	0.96	0.03
0 × 1 × 1	1.32	0.03
1 × 0 × 0	0.70	0.04
1 × 0 × 1	1.23	0.03
1 × 1 × 0	1.10	0.04
1 × 1 × 1	1.31	0.03

2. Etch + Adhesive + Primer

Simple, Simple Main Effects at level 0 of Primer:

The difference in the mean values among the different levels of Etch evaluated within level 1 of Adhesive and level 0 of Primer is greater than would be expected by chance. There is a statistically significant difference ($P = 1.84\times 10^{-9}$).

Comparisons for factor: Etch within 1-0

Comparison	Diff of Means	t	P
1 *vs.* 0	0.40	7.39	1.84×10^{-9}

The difference in the mean values among the different levels of Adhesive evaluated within level 1 of Etch and level 0 of Primer is greater than would be expected by chance. There is a statistically significant difference (P = 0.007).

Comparisons for factor: Adhesive within 1-0

Comparison	Diff of Means	t	P
1 *vs.* 0	0.14	2.83	0.007

Simple, Simple Main Effects at level 1 of Primer:

The difference in the mean values among the different levels of Etch evaluated within level 0 of Adhesive and level 1 of Primer is greater than would be expected by chance. There is a statistically significant difference ($P = 3.29 \times 10^{-8}$).

Comparisons for factor: Etch within 0-1

Comparison	Diff of Means	t	P
1 *vs.* 0	0.33	6.58	3.29×10^{-8}

The difference in the mean values among the different levels of Adhesive evaluated within level 0 of Etch and level 1 of Primer is greater than would be expected by chance. There is a statistically significant difference ($P = 4.46 \times 10^{-6}$).

Comparisons for factor: Adhesive within 0-1

Comparison	Diff of Means	t	P
1 *vs.* 0	0.24	5.17	4.46×10^{-6}

The difference in the mean values among the different levels of Adhesive evaluated within level 1 of Etch and level 1 of Primer is not great enough to exclude the possibility that the difference is just due to random sampling variability. There is not a statistically significant difference (P = 0.859).

3. Primer + Etch + Adhesive

All Pairwise Multiple Comparison Procedures (Holm-Sidak method):

Overall significance level = 0.05

Three Way Interaction Term Analysis:

Evaluated Primer × Etch across levels of Adhesive:

The effect of the Primer × Etch interaction depends on what level of Adhesive is present.

There is a significant Primer × Etch interaction at level 0 of Adhesive. ($P = 7.65 \times 10^{-8}$).

There is a significant Primer × Etch interaction at level 1 of Adhesive. ($P = 1.42 \times 10^{-4}$).

4. Primer + Adhesive + Etch

Three Way Interaction Term Analysis:

Evaluated Primer × Adhesive across levels of Etch:

The effect of the Primer × Adhesive interaction depends on what level of Etch is present.

There is a significant Primer × Adhesive interaction at level 0 of Etch. ($P = 7.65 \times 10^{-8}$)

There is a significant Primer × Adhesive interaction at level 1 of Etch. ($P = 1.4 \times 10^{-4}$)

Simple, Simple Main Effects at level 0 of Etch:

The difference in the mean values among the different levels of Primer evaluated within level 1 of Adhesive and level 0 of Etch is greater than would be expected by chance. There is a statistically significant difference ($P = 0.4 \times 10^{-14}$).

Comparisons for factor: Primer within 1-0

Comparison	Diff of Means	t	P
1 *vs.* 0	0.53	11.32	0.4×10^{-14}

The difference in the mean values among the different levels of Adhesive evaluated within level 0 of Primer and level 0 of Etch is greater than would be expected by chance. There is a statistically significant difference ($P = 1.3 \times 10^{-14}$).

Comparisons for factor: Adhesive within 0-0

Comparison	Diff of Means	t	P
1 *vs.* 0	0.60	10.91	1.4×10^{-14}

The difference in the mean values among the different levels of Adhesive evaluated within level 1 of Primer and level 0 of Etch is greater than would be expected by chance. There is a statistically significant difference ($P = 4.46 \times 10^{-6}$).

Comparisons for factor: Adhesive within 1-0

Comparison	Diff of Means	t	P
1 *vs.* 0	0.24	5.17	4.46×10^{-6}

Simple, Simple Main Effects at level 1 of Etch:

The difference in the mean values among the different levels of Primer evaluated within level 0 of Adhesive and level 1 of Etch is greater than would be expected by chance. There is a statistically significant difference ($P = 2.83 \times 10^{-10}$).

Comparisons for factor: Primer within 0-1

Comparison	Diff of Means	t	P
1 *vs.* 0	0.36	7.93	2.83×10^{-10}

The difference in the mean values among the different levels of Adhesive evaluated within level 0 of Primer and level 1 of Etch is greater than would be expected by chance. There is a statistically significant difference (P = 0.007).

Comparisons for factor: Adhesive within 0-1

Comparison	Diff of Means	t	P
1 *vs.* 0	0.14	2.83	0.007

The difference in the mean values among the different levels of Adhesive evaluated within level 1 of Primer and level 1 of Etch is not great enough to exclude the possibility that the difference is just due to random sampling variability. There is not a statistically significant difference (P = 0.859).

5. Adhesive + Etch + Primer

Three Way Interaction Term Analysis:

Evaluated Adhesive × Etch across levels of Primer:

The effect of the Adhesive × Etch interaction depends on what level of Primer is present.

There is a significant Adhesive × Etch interaction at level 0 of Primer. ($P = 7.79 \times 10^{-10}$)

There is a significant Adhesive × Etch interaction at level 1 of Primer. ($P = 4.75 \times 10^{-6}$)

Simple, Simple Main Effects at level 0 of Primer:

The difference in the mean values among the different levels of Adhesive evaluated within level 0 of Etch and level 0 of Primer is greater than would be expected by chance. There is a statistically significant difference ($P = 1.3 \times 10^{-14}$).

Comparisons for factor: Adhesive within 0-0

Comparison	Diff of Means	T	P
1 *vs.* 0	0.60	10.91	1.4×10^{-14}

The difference in the mean values among the different levels of Adhesive evaluated within level 0 of Etch and level 0 of Primer is greater than would be expected by chance. There is a statistically significant difference ($P = 6.7 \times 10^{-3}$).

Comparisons for factor: Adhesive within 1-0

Comparison	Diff of Means	t	P
1 *vs.* 0	0.14	2.83	6.7×10^{-3}

Simple, Simple Main Effects at level 1 of Primer:

The difference in the mean values among the different levels of Adhesive evaluated within level 0 of Etch and level 1 of Primer is greater than would be expected by chance. There is a statistically significant difference ($P = 4.46 \times 10^{-6}$).

Comparisons for factor: Adhesive within 0-1

Comparison	Diff of Means	t	P
1 *vs.* 0	0.24	5.17	4.46×10^{-6}

The difference in the mean values among the different levels of Adhesive evaluated within level 1 of Etch and level 1 of Primer is not great enough to exclude the possibility that the difference is

just due to random sampling variability. There is not a statistically significant difference (P = 0.859).

6. Adhesive + Primer + Etch

Three Way Interaction Term Analysis:

Evaluated Adhesive × Primer across levels of Etch:

The effect of the Adhesive × Primer interaction depends on what level of Etch is present.

There is a significant Adhesive × Primer interaction at level 0 of Etch. ($P = 7.79 \times 10^{-10}$)

There is a significant Adhesive × Primer interaction at level 1 of Etch. ($P = 4.75 \times 10^{-6}$)

Simple, Simple Main Effects at level 0 of Etch:

The difference in the mean values among the different levels of Adhesive evaluated within level 0 of Primer and level 0 of Etch is greater than would be expected by chance. There is a statistically significant difference ($P = 1.4 \times 10^{-14}$).

Comparisons for factor: Adhesive within 0-0

Comparison	Diff of Means	t	P
1 *vs.* 0	0.60	10.91	1.4×10^{-14}

The difference in the mean values among the different levels of Adhesive evaluated within level 1 of Primer and level 0 of Etch is greater than would be expected by chance. There is a statistically significant difference ($P = 4.46 \times 10^{-6}$).

Comparisons for factor: Adhesive within 1-0

Comparison	Diff of Means	t	P
1 *vs.* 0	0.24	5.17	4.46×10^{-6}

The difference in the mean values among the different levels of Primer evaluated within level 1 of Adhesive and level 0 of Etch is greater than would be expected by chance. There is a statistically significant difference ($P = 0.4 \times 10^{-14}$).

Comparisons for factor: Primer within 1-0

Comparison	Diff of Means	t	P
1 *vs.* 0	0.53	11.32	0.4×10^{-14}

Simple, Simple Main Effects at level 1 of Etch:

The difference in the mean values among the different levels of Adhesive evaluated within level 0 of Primer and level 1 of Etch is greater than would be expected by chance. There is a statistically significant difference (P = 0.007).

Comparisons for factor: Adhesive within 0-1

Comparison	Diff of Means	t	P
1 *vs.* 0	0.14	2.83	0.007

The difference in the mean values among the different levels of Adhesive evaluated within level 1 of Primer and level 1 of Etch is not great enough to exclude the possibility that the difference is just due to random sampling variability. There is not a statistically significant difference (P = 0.859).

Appendix 10: Calculation for the re-analysis of available reports examining the effect of cross-head speed on mechanical test results

The sum and sums of squares required for the regression analysis were reconstructed from the published means, standard deviations and sample sizes using a Sigmaplot (v.15) transform employing the following identities, where L is the number of groups and g is the item index in the worksheet:

```
X       = Log(col(1,1,L))          ; XHS speed values
Y       = col(1+g,1,L)             ; property mean values
sy      = col(2+g,1,L)             ; property value standard deviations
n       = col(3+g,1,L)             ; group sample sizes
sy2     = sy^2                     ; property value variances
N       = total(n)

SumX    = total(X*n)               ; sums and sums of squares
SumY    = total(Y*n)
SumXY   = total(X*Y*n)
SumX2   = total(X^2*n)
SYi     = sy2 * (n-1)
Y2      = SYi + (Y*n)^2/n
SumY2   = total(Y2)

SY      = SumY2 - SumY^2/N         ; sums of squares deviations
SX      = SumX2 - (SumX)^2/N
SXY     = SumXY -  SumX*SumY/N

b1      = SXY/SX                   ; parameter estimates + stats
b0      = (SumY - b1 * SumX)/N
r2      = SXY^2/SX/SY
s2b1    = b1^2*(1/r2 - 1)/(N-2)    ; slope estimate variance
sb1     = Sqrt(s2b1)               ; standard error of the slope
sb0     = Sqrt(s2b1*SumX2/N)       ; standard error of the intercept
F       = r2/(1 - r2) * (N-2)      ; F-ratio
s2yx    = (SY - b1*SXY)/(N-2)      ; residuals variance
```

varprop	=	(1 - r2)*(N-1)/(N-2)	; proportion of variance not due to regression
residsd	=	SQRT(s2yx)	; residuals standard deviation
SSRD	=	SQRT(s2yx)/b0	; scaled standard residuals deviation
RES	=	b1/b0	; relative effect size
RESse	=	sb1/b0	; relative effect size standard error

The significance probability was calculated in Mathematica 12.2 (Wolfram Research, Champaign IL, USA) using the function:

$$\text{Probability}[x \geq F, x \approx \text{FRatioDistribution}[1, n-2]]$$